

Copyright

by

Joshua Kenneth Lonthair

2019

The Dissertation Committee for Joshua Kenneth Lonthair Certifies that this is the approved version of the following Dissertation:

**RESILIENCE TO AN ACID-BASE DISTURBANCE AND THE
DEVELOPMENT AND PLASTICITY OF ACID-BASE
REGULATORY PATHWAYS IN ESTUARINE TELEOSTS**

Committee:

Andrew J. Esbaugh, Supervisor

Deana L. Erdner

Peter Thomas

Martin Tresguerres

**RESILIENCE TO AN ACID-BASE DISTURBANCE AND THE
DEVELOPMENT AND PLASTICITY OF ACID-BASE
REGULATORY PATHWAYS IN ESTUARINE TELEOSTS**

by

Joshua Kenneth Lonthair

Dissertation

Presented to the Faculty of the Graduate School of
The University of Texas at Austin
in Partial Fulfillment
of the Requirements
for the Degree of

Doctor of Philosophy

The University of Texas at Austin

December 2019

Dedication

I dedicate this work to my parents, Alice and Jay Lonthair, who have taught me that anything worth having is worth fighting for. Thank you for being my sounding board throughout this process.

Acknowledgements

The most important person that I need to thank is my advisor, Andrew J. Esbaugh, who has provided support throughout the entirety of this work. The advice, encouragement, and knowledge has made me a better scientist, writer, and person. Thank you to my committee, Deana Erdner, Peter Thomas, and Martin Tresguerres, for their guidance, feedback, and general support throughout this work, it truly has made it better. To my lab mate's past and present, Kerri Ackerly, Elizabeth Allmon, Angelina Dichiera, Rasmus Ern, Jacob Johansen, Alexis Khursigara, Leighann Martin, and Benjamin Negrete Jr., thank you for support throughout this process, your collaboration and emotional support helped me beyond measure. To my FAMLites: Jeff Kaiser, Lee Fuiman, Cindy Faulk, Venus Mills, and Bea Limon, without you FAML would not have been the same place, and this work would have been impossible. Thank you to Bob Dickey, and all of the staff at UTMSI, everyone's dedication to the institute before and after Hurricane Harvey makes UTMSI truly an amazing institution and a great place to do science. I would like to especially thank Jamey Pelfrey, who has been the most amazing asset that I will miss, she is the person that I went to about anything and everything about the doctoral process, from getting health insurance, to paying tuition, and making sure that I was still sane. If it was not for you, I would have never gotten to this moment. To my parents, my sister, and my chosen family, I am so sincerely appreciative of all that you have done for me. You have always supported me throughout this crazy journey. Finally, I would truly like to thank all those members of the UTMSI student community past and present, the laughs and the memories are what I will probably cherish the most of this experience.

Abstract

Resilience to an Acid-Base Disturbance and the Development and Plasticity of Acid-Base Regulatory Pathways in Estuarine Teleosts

Joshua Kenneth Lonthair, Ph.D.

The University of Texas at Austin, 2019

Supervisor: Andrew J. Esbaugh

Since the industrial revolution marine environments have displayed marked increases in CO₂ levels. Changes in ocean chemistry – collectively termed ocean acidification (OA) – are predicted to have numerous effects on marine fish, including critical behavioral endpoints and survival, with the most severe impacts hypothesized to occur in the vulnerable early life stages. However, many regions around the globe routinely have CO₂ levels in excess of those predicted by climate change, including the estuaries in the Gulf of Mexico, which are essential habitat for many ecologically and commercially important fish species. We hypothesize that the species that inhabit these environments contain physiological traits that confer resilience to OA. Thus, it is imperative that we understand the resilience of these species as well as the underlying mechanisms that may inform on the adaptive capacity of fish in general.

The underlying physiological cause for many of the outcomes of OA is a systemic acid-base disturbance, which causes an elevated arterial $p\text{CO}_2$ and plasma $[\text{HCO}_3^-]$. Because embryos and early life stage fish lack gills and practice cutaneous gas exchange, acid-base disturbances could be exacerbated in these life stages. Furthermore, little is

known about the ontogeny, development, plasticity of acid-base regulatory mechanisms in early life stage marine fish, raising many questions about their ability to compensate for disturbance. Here we present work that shows tolerance of early life stage estuarine species to elevated CO₂ levels, including survival, standard length, and yolk size. However, we did observe significant heart rates in both studied estuarine species, and although we saw no immediate impacts, the long-term impacts of elevated heart rate are of keen interest. We also observed that alterations in acid-base regulatory machinery were the largely the result of development, rather than in response to exposure to an acid-base disturbance, including an acidosis and alkalosis. Although we did observe significant increases in NHE2 and VHA as the result of exposure to elevated CO₂ levels. Of interest is that H⁺ excretion was significant elevated in response to exposure to hypercapnia, and we hypothesize that this H⁺ excretion is the result of both the NHE and VHA pathway, from data obtained via the scanning ion-selective electrode technique (SIET) and pharmacological inhibition, but this must be further investigated.

Table of Contents

List of Tables	xiii
List of Figures	xiv
Chapter 1: General Introduction	1
Ocean Acidification	1
Current paradigms in Fish Acid-Base Physiology.....	3
Na ⁺ /H ⁺ exchanger (NHEs).....	5
V-type H ⁺ ATPase (VHA)	7
Key Points on Osmoregulatory Physiology.....	8
Overall Goals	10
Figures	11
Chapter 2: The early life stages of an estuarine fish, the red drum (<i>Sciaenops ocellatus</i>), are tolerant to high pCO ₂	12
Authors	12
Abstract.....	12
Introduction.....	13
Methods	16
Estuarine pCO ₂ monitoring.....	16
Rearing system.....	17
Embryonic incubation experiments	18
Behavior experiments	19
Statistical analysis.....	20
Results.....	21
Literature synthesis	21

Estuarine $p\text{CO}_2$ monitoring.....	21
Sensitivity experiments.....	22
Survival, heart rate, standard length, and yolk depletion rate.....	22
Behavior.....	22
Discussion.....	23
Acknowledgements.....	28
Tables.....	29
Figures.....	31
Chapter 3: Impacts of hypercapnia on the early life stages of the orange spotted grouper, <i>Epinephelus coioides</i>	37
Authors.....	37
Abstract.....	37
Introduction.....	38
Methods.....	41
Lethal and sublethal impacts.....	41
Acid-base mRNA Expression.....	43
Immunofluorescence methods.....	44
Statistical methods.....	45
Results.....	45
Sensitivity experiments.....	45
Lethal and sub-lethal impacts.....	45
Acid-base regulatory pathway plasticity.....	46
Discussion.....	46
Acknowledgements.....	50

Tables.....	51
Figures	53
Chapter 4: Physiological redundancy of H ⁺ excretion pathways in an estuarine teleost...	60
Authors	60
Abstract.....	60
Introduction.....	61
Results.....	63
Survival in response to exposure to elevated <i>p</i> CO ₂	63
Development of acid-base regulatory pathways.....	63
Impacts of hypercapnia on acid-base regulatory machinery	64
Larval H ⁺ excretion.....	64
Discussion.....	65
Methods	70
Animal husbandry.....	70
CO ₂ acclimation and survival assays.....	71
Molecular methods	72
Whole animal H ⁺ excretion.....	73
Statistical analysis.....	75
Acknowledgements.....	75
Tables.....	76
Figures	77
Supplementary Information	81
Methods	81

Preparing samples for confocal microscopy:	81
SIET:	81
Supplementary Tables.....	82
Supplementary Figures	83
Chapter 5: Mechanisms of acid-base regulation following respiratory alkalosis in red drum (<i>Sciaenops ocellatus</i>).....	84
Authors	84
Abstract.....	84
Introduction.....	85
Methods	87
Animal handling	87
Experimental design	88
Whole animal acid flux measurements.....	89
Gene expression.....	90
Enzymatic activity	91
Immunohistochemistry	92
NHE3 antibody validation	93
Statistical analysis.....	94
Results.....	94
Whole animal flux	94
Phenotypic differences in control fish	94
mRNA Expression and Enzymatic Activity	95
Protein localization and translocation.....	96
Discussion.....	96

Acknowledgments	102
Tables.....	103
Figures	104
Chapter 6: Summary and Conclusions.....	109
Perspectives on Ocean Acidification	109
Perspectives on Acid- Base Regulation.....	111
Future Directions	113
Caveats and Limitations.....	115
Bibliography	118

List of Tables

Table 2.1: Mean (± 1 SEM) temperature, salinity, pH, total alkalinity, and $p\text{CO}_2$ in experiments with red drum (<i>Sciaenops ocellatus</i>) embryos and early life stages.....	29
Table 2.2: Highest one-week recorded $p\text{CO}_2$ for 18 representative estuaries from across the United States and Puerto Rico, as well as corresponding temperature, salinity and pH.	30
Table 3.1: Mean (± 1 SEM) temperature, salinity, pH, total alkalinity, and $p\text{CO}_2$ in experiments with orange spotted grouper (<i>Epinephelus coioides</i>) embryos and early life stages.	51
Table 3.2: List of primers used for real-time PCR. All sequences are 5' to 3' and reverse primers are reverse compliments of the genetic sequence.	52
Table 4.1: Water quality parameters for all early life stage CO_2 exposures. Data are mean ± 1 SEM.	76
Table 4.2: List of primers used for real-time PCR. All sequences are 5' to 3' and reverse primers are reverse compliments of the genetic sequence.	82
Table 5.1: List of primers used for real-time PCR. All sequences are 5' to 3' and reverse primers are reverse compliments of the genetic sequence.	103

List of Figures

- Figure 1.1: Diagram of a representative ionocyte on the gill epithelium of a marine teleost highlighting proposed and documents mechanisms of apical H^+ excretion and basolateral HCO_3^- uptake. Diagram from Esbaugh (2018). ...11
- Figure 2.1: The number of publication per year returned in response to a combined topical search for ocean acidification and fishes.31
- Figure 2.2: Representative estimated pCO_2 tracing from the Guana Tolomato Matanzas National Estuarine Research Reserve in Florida.32
- Figure 2.3: Survival of red drum in response to elevated pCO_2 , and the effect of multi-generational exposure on survival.....33
- Figure 2.4: Mean (\pm SEM) **(a)** heart rate, and **(b)** standard length of red drum (*Sciaenops ocellatus*) after 48 h exposure to control, 1300 μ atm, and 3000 μ atm pCO_234
- Figure 2.5: Natural log of the mean yolk size (\pm 1 SEM) after 24 h, 48 h, and 72 h exposure to control, 1300 μ atm, and 3000 μ atm pCO_2 in red drum (*Sciaenops ocellatus*).35
- Figure 2.6: Light/dark preference for red drum (*Sciaenops ocellatus*) following acute and acclimated exposure to 1000 μ atm pCO_236
- Figure 3.1: Inverted microscope image of 60 hpf orange spotted grouper (*Epinephelus coioides*).53
- Figure 3.2: Confocal microscopy image of ionocyte density using 1 antibody for Na^+/K^+ ATPase (NKA) in 60 hpf orange spotted grouper (*Epinephelus coioides*).54
- Figure 3.3: Mean (\pm SEM) survival of orange spotted grouper (*Epinephelus coioides*) after 48 h exposure to control, 1500 μ atm, and 3100 μ atm pCO_255

Figure 3.4: Mean (\pm SEM) (a) heart rate, (b) standard length, and (c) yolk area of red drum orange spotted grouper (<i>Epinephelus coioides</i>) after 48 h exposure to control, 1500 μ atm, and 3100 μ atm $p\text{CO}_2$.	56
Figure 3.5: Whole animal gene expression of H^+ excretion pathways: (a) <i>nbc</i> (b) <i>nhe3</i> (c) <i>vha</i> , during development in orange spotted grouper (<i>Epinephelus coioides</i>).	57
Figure 3.6: Whole animal gene expression of H^+ excretion pathways: (a) <i>nbc</i> (b) <i>nhe3</i> (c) <i>vha</i> , during 24 and 48 h exposure to control, 1500 μ atm, and 3100 μ atm in orange spotted grouper (<i>Epinephelus coioides</i>).	58
Figure 3.7: Natural log of the mean ionocyte density per .0625 mm^2 area (± 1 SEM) after 48 h exposure to control, 1500 μ atm, and 3100 μ atm $p\text{CO}_2$ in orange spotted grouper (<i>Epinephelus coioides</i>).	59
Figure 4.1: Mean (\pm SEM) survival of red drum (<i>Sciaenops ocellatus</i>) after 72 h exposure to control, 1400, 3100, 5500, 12000 μ atm CO_2 . Sample size of each exposure group is annotated within the bar.	77
Figure 4.2: Development of acid-base regulatory pathways across early life stages of red drum (<i>Sciaenops ocellatus</i>).	78
Figure 4.3: Mean (\pm SEM) relative gene expression of <i>vha</i> (A) , <i>nhe2</i> (B) , and <i>nhe3</i> (C) in red drum (<i>Sciaenops ocellatus</i>) after exposure to elevated $p\text{CO}_2$ for 24 h and 72 h.	79
Figure 4.4: Mean (\pm SEM) $\Delta[\text{H}^+]$ (μM) of 72 hpf red drum (<i>Sciaenops ocellatus</i>) after exposure to both elevated $p\text{CO}_2$ and pharmacological inhibition.	80
Figure 4.5: Mean (\pm SEM) $\Delta[\text{H}^+]$ (μM) of 72 hpf red drum (<i>Sciaenops ocellatus</i>) across the various locations across the body.	83

Figure 5.1: A representative pH-HCO ₃ ⁻ - pCO ₂ diagram illustrating the experimental design using blood chemistry representative of red drum (<i>Sciaenops ocellatus</i>).....	104
Figure 5.2: Net H ⁺ excretion rates of red drum (<i>Sciaenops ocellatus</i>) following the onset of a respiratory alkalosis.....	105
Figure 5.3: Relative branchial gene expression of acid-base regulatory pathways following 16 h exposure to 15,000 μatm CO ₂ , or 2 h (series 1) or 24 h (series 2) to a respiratory alkalosis, as well as time matched control.	106
Figure 5.4: (A) NKA, (B) VHA, and (C) CA enzyme activity in the gills of red drum (<i>Sciaenops ocellatus</i>) following 16 h exposure to 15,000 μatm CO ₂ , or 2 h (series 1) or 24 h (series 2) to a respiratory alkalosis, as well as time matched control.....	107
Figure 5.5: Representative confocal microscope images of gill ionocytes under control conditions, after exposure to a respiratory acidosis, and after exposure to a respiratory alkalosis in red drum (<i>Sciaenops ocellatus</i>). Scale bar in all images is 20 microns.....	108

Chapter 1: General Introduction

OCEAN ACIDIFICATION

Anthropogenic carbon dioxide (CO₂) emissions are having measurable impacts on oceanic carbonate chemistry – a process known as ocean acidification (OA). Current models project that the oceans will reach approximately 1000 μatm partial pressure of CO₂ ($p\text{CO}_2$) by the end of this century, a 2.5x increase from the present oceanic $p\text{CO}_2$ level (Caldeira and Wickett, 2003; Doney et al., 2009; Solomon et al., 2007). Elevated $p\text{CO}_2$, at both end of the century OA levels and extreme levels, has been found to have numerous detrimental effects on marine life, including impairment of sensory systems and behavior (Dixson et al., 2010; Ferrari et al., 2015; Munday et al., 2009b; Nilsson et al., 2012), alterations in aerobic scope (Couturier et al., 2013; Munday et al., 2009a) and ionoregulatory physiology (Esbaugh et al., 2012; Heuer et al., 2012; Strobel et al., 2012), increased tissue damage (Chambers et al., 2014; Frommel et al., 2012; Frommel et al., 2014), and diminished growth and survival (Baumann et al., 2012; DePasquale et al., 2015; Miller et al., 2012). Early life stage fish are hypothesized to be especially susceptible to the impacts of elevated $p\text{CO}_2$, presumably because they are less capable of tolerating the associated acid-base disturbances (Esbaugh et al., 2016; Esbaugh et al., 2012; Green and Jutfelt, 2014; Strobel et al., 2012). It has been theorized that this susceptibility results from the lack of gill development, and the subsequently limited capacity for ion transport (Frommel et al., 2013; Tseng et al., 2013).

Notably, much of the current work has focused on species from marine or reef environments with less emphasis placed on estuarine-dependent species. Estuaries are able to have a variety of salinity regimes, with estuaries in Texas alone experience salinity values as low as 0 during heavy rain, and as high as 70 during major droughts (Armstrong,

1987). Estuaries are also important components of the marine ecosystem that commonly act as a nursery ground for early life stage fish and juveniles (Weinstein, 1979). Due to their near shore location and high productivity, estuaries are susceptible to a variety of environmental factors, including anthropogenic run-off, microbial processes, and upwelling (Cai et al., 2011; Feely et al., 2010). Furthermore, natural fluctuations of $p\text{CO}_2$ on a variety of time scales are prevalent in the estuarine environment (Feely et al., 2010), which has led many to conclude that the effects of OA may be exacerbated in these systems (Cai et al., 2011). For example, previous work has demonstrated $p\text{CO}_2$ in excess of 2000 μatm (Wallace et al., 2014) in estuaries in the northeast US, and 3000 μatm (Melzner et al., 2013) in an estuary in the Baltic region of Europe. These estuaries reach these peaks at different periods during seasonally, tides, and time of day (Wallace et al., 2014).

Studies on high $p\text{CO}_2$ have also defined the potential for tolerance and resilience in marine systems. This is especially important for fish as many species double as vital economic resources, and OA is predicted to have dramatic effects on global populations (See Reviews: Hofmann and Todgham, 2010; Kelly and Hofmann, 2013; Munday et al., 2010; Pfister et al., 2014). Tolerance to OA and climate change is thought to rely primarily on the presence of existing tolerant genotypes in a population, and the ability of individuals to alter their physiology to suit new environmental conditions; a process known as phenotypic plasticity (Bell, 2013; Gonzalez et al., 2013; Kelly et al., 2013; Pespeni et al., 2013). This is due to the relatively long-life spans of many marine organisms as compared to the rapidness of global climate change, which in many cases will negate traditional evolutionary processes. As such, species that inhabit pH variable environments are particularly interesting study organisms owing their potential for intrinsic resilience. Studies that have demonstrated plastic responses to high $p\text{CO}_2$ include previous work with red drum (*Sciaenops ocellatus*) (Allmon and Esbaugh, 2017; Esbaugh et al., 2016). To

date, the majority of work exploring intrinsically CO₂ tolerant organisms has focused on carbon vent habitats where genotypes that allow individual species, primarily invertebrates, to effectively cope with elevated *p*CO₂ levels have been described (Basso et al., 2015; Calosi et al., 2013). Interestingly, there has been relatively little effort to explore whether estuaries may act as a similar reservoir of tolerant species and genotypes, although this has been a growing topic of conversation (Baumann, 2019).

CURRENT PARADIGMS IN FISH ACID-BASE PHYSIOLOGY

Like many other physiological parameters, organisms strive to keep their acid-base balance within tightly controlled limits, which allow the organism to maintain key regulatory processes (Evans et al., 2005b). Acid-base balance is predicated on balancing of the bicarbonate system: $H^+ + HCO_3^- \rightarrow H_2O + CO_2$. There are four different ways that this acid-base balance can be altered, a respiratory acidosis, a respiratory alkalosis, a metabolic acidosis, and a metabolic alkalosis. A respiratory acidosis results from an increase in the *p*CO₂ in the blood plasma that subsequently reduces pH, while a respiratory alkalosis results from a decrease in *p*CO₂ in the blood plasma that raises pH. In contrast, a metabolic acidosis represents a decreased plasma pH that coincides with decreased plasma [HCO₃⁻], while a metabolic alkalosis results from a net increase in plasma [HCO₃⁻], which is due a decrease in [H⁺], that raises plasma pH. These acid-base disturbances can be compensated for via metabolic and/or respiratory processes.

Respiratory compensation involves the manipulation of ventilation so as to retain CO₂ or remove CO₂, which subsequently corrects plasma pH. This method is prominent in tetrapods when responding to a metabolic acid-base disturbances, but is predicated on the relatively high arterial *p*CO₂ (~40 mmHg) and CO₂ based ventilatory drive (Heisler, 1986; Swenson, 2000). In contrast, fishes live in oxygen poor environments and thus have an

oxygen based ventilatory drive combined with a gill morphology that maximizes gas diffusion. This results in a low arterial $p\text{CO}_2$ (~1 mmHg in normocapnic water) that limits the scope for respiratory compensation to correct acid-base disturbances (Gilmour, 2001; Gilmour and Perry, 2007; Perry and Abdallah, 2012). Furthermore, hyperventilation comes at the expense of potential physiological trade-offs, as outlined by the osmorepiratory compromise (Evans et al., 2005b; Perry et al., 2003b). This compromise simply refers to conflicting nature of osmotic water movement and diffusive gas transport across the gills. While hyperventilation can improve gas transport, it is hypothesized to result in greater energetic expenditures for osmoregulation. Even with these known limitations, hypercapnia induced hyperventilation has been shown to occur in many fish species (Ern and Esbaugh, 2016; Gilmour, 2001; Perry and Abdallah, 2012). This is hypothesized to have evolved in fish as a way to maintain O_2 uptake at the gills, because hypoxia and hypercapnia usually occur simultaneously in natural waters (Gilmour, 2001; Perry and Gilmour, 2002); however, it has also been shown to reduce the magnitude of subsequent metabolic compensation to low level hypercapnia (Ern and Esbaugh 2016).

Instead the primary route of acid-base regulation in most fish is the direct transfer of acid-base equivalents between the plasma and the external environment (Claiborne et al., 2002; Evans et al., 2005b; Perry and Gilmour, 2006). Fish gills have an epithelium that is in direct contact with seawater, which are capable of acting as an infinite source and sink of solutes, and thus acts as the predominate site of metabolic compensation (Claiborne et al., 2002; Evans et al., 2005b; Goss et al., 1992; Perry et al., 2003b). During periods of acidosis, net acid efflux across the gill is increased (equivalent to reduced base efflux) whereas during an alkalosis, the net efflux of acid across the gill is decreased (equivalent to increased base efflux).

The impressive metabolic compensatory capacity of teleosts is credited to the multiplicity of transport pathways for both H^+ and HCO_3^- across the basolateral and apical membranes (Figure 1.1). The salt secretory pathway of the marine teleost gill consists of basolateral entry of Na^+ , K^+ and Cl^- via the $Na^+-K^+-Cl^-$ cotransporter (NKCC), which is driven by electrochemical gradients established by Na^+/K^+ ATPase (NKA). Secretion of Cl^- across the apical membrane occurs through the cystic fibrosis transmembrane conductance regulator (CFTR) channel, while Na^+ exits via a paracellular pathway down its electrochemical gradient (Evans et al., 2005b). Hydration of CO_2 , facilitated by carbonic anhydrase (CAc), generates H^+ and HCO_3^- for exchange and co-transport across the apical and basolateral membranes (Esbaugh et al., 2005; Georgalis et al., 2006; Gilmour and Perry, 2009). Na^+/H^+ exchangers (NHEs) are expressed in the gill epithelium and are involved in dynamic adjustments of acid-base balance during an acidosis. Base efflux across the basolateral membrane complements acid secretion at the apical membrane, with the Na^+/HCO_3^- co-transporter (NBC) thought to be the primary facilitator of HCO_3^- transport into the plasma (Hirata et al., 2003; Perry et al., 2003a). Furthermore, a number of anion exchangers in the SLC26 and SLC4 families have been implicated in Cl^-/HCO_3^- exchange on the apical membrane in response to a metabolic alkalosis (Alper, 2009; Mount and Romero, 2004; Romero et al., 2013). In freshwater fish VHA is also known to contribute to branchial acid excretion; however, such a role in marine fish has been hypothesized.

Na^+/H^+ exchanger (NHEs)

NHEs have been proposed as the route of acid excretion from fishes in seawater, where the high Na^+ concentration favors Na^+ entry across the apical membrane in exchange for H^+ (Claiborne et al., 2002). To date, nine members of the mammalian NHE family have

been reported (NHE1-9). NHE1-5 are localized to the plasma membrane, NHE6, 7, and 9 are all localized intracellularly, and NHE8 is found both on the apical membrane and intracellularly, with each of the NHEs having specialized functions and membrane specificity (Donowitz et al., 2013; Noel and Pouyssegur, 1995; Ritter et al., 2001). Members of the NHE family play an important role in transepithelial ion movements, intracellular pH (pH_i) homeostasis, and cell volume regulation (Paillard, 1997). NHEs have also been shown to be expressed in the gills of many fishes, and recent studies have reported large increases in NHE3 mRNA expression following an acidosis. NHE1, a basolateral localized isoform, has been hypothesized to play a role in acid-base regulation in response to both a metabolic acidosis and hypercapnia-induced respiratory acidosis (Claiborne et al., 1999; Deigweiher et al., 2008; Edwards et al., 2005; Rimoldi et al., 2009). A common result of all these experiments is a down-regulation of NHE1 mRNA expression, which is consistent with reduced H^+ transport across the basolateral membrane into the blood plasma. The available evidence suggests that both NHE2 and NHE3 are localized to the apical membrane in marine fish gill ionocytes. NHE3 has generally been shown to be more dynamically regulated than NHE2 following an acidosis. For example, NHE3 showed elevated protein abundance and mRNA expression in response to both respiratory and metabolic acidosis, which is consistent with the increased need for acid excretion (Edwards et al., 2005; Laghmani et al., 1997; Tseng et al., 2013). Although, it is important to note that there are differences in acid-base regulatory responses to elevated pCO_2 in different species. At present there is little to no information about whether NHE2 plays any role in the compensatory response to an acidosis. It is also important to note that the functional evidence that points to a role for NHE2/3 in acid-base balance is largely restricted to freshwater fishes (Hwang, 2009; Yan et al., 2007) or freshwater species with seawater tolerance (Liu et al., 2016; Liu et al., 2013; Tseng et al., 2013). Work on truly

marine species is limited to localization and net H⁺ excretion experiments (Catches et al., 2006; Edwards et al., 2005), likely owing to the challenges of using pharmacological agents in seawater and the lack of marine models amenable to gene knockdown techniques.

V-type H⁺ ATPase (VHA)

In freshwater teleosts, VHA has also been shown to participate in apical acid excretion. Furthermore, VHA in freshwater fishes has been observed to increase in activity and mRNA expression in response to an acidosis, which indicates that VHA is dynamically regulated to enhance acid excretion during periods of stress (Lin and Randall, 1993; Perry et al., 2000; Perry et al., 2003b; Sullivan et al., 1995; Sullivan et al., 1996). In marine elasmobranchs, VHA has instead been established to play a role in net HCO₃⁻ excretion during an alkalosis by transporting H⁺ across the basolateral membrane into the blood plasma (Roa et al., 2014; Tresguerres et al., 2005; Tresguerres et al., 2007b). This is largely supported by a series of studies that demonstrated translocation of the VHA (B subunit) to the basolateral membrane in hagfish and elasmobranch species (Roa et al., 2014; Tresguerres et al., 2005; Tresguerres et al., 2007b). However, this translocation has not been demonstrated in a marine teleost. Furthermore, recent work has shown that marine teleost species upregulate the *vha* (B subunit) mRNA expression in response to hypercapnia (Allmon and Esbaugh, 2017; Michael et al., 2016). Similar evidence supporting the role of VHA in H⁺ excretion is available from hypersalinity transfer studies across a variety of species where increased activity and gene expression were observed (Guffey et al., 2011; Martin et al., In Review). As such, the role of branchial VHA in mediating acid-base disturbances in marine teleosts remains uncertain.

KEY POINTS ON OSMOREGULATORY PHYSIOLOGY

Previously we defined the key role of the gills and certain protein transporters in acid-base regulation, but the gills are also a critical site of osmosis and ionic diffusion. Freshwater fish live in a hypoosmotic environment and must balance the osmotic uptake of water by having high urine rates and minimizing renal salt loss. Furthermore, ion loss is balanced by active ion uptake mechanisms in the gills. The general mechanisms of ion uptake involves Na^+ and Cl^- being taken up from freshwater in exchange for intracellular ions such as NH_4^+ , H^+ , and HCO_3^- , which effectively function as counter ions to maintain electroneutrality across the epithelium (Evans et al., 2005b). Work has long suggested that the uptake of Na^+ by the fish gill epithelium may be electrically coupled to proton efflux, rather than directly coupled by a single exchanger (NHE) (Lin and Randall, 1995; Marshall, 2002). The V- H^+ -ATPase (VHA) specific inhibitor bafilomycin (1-10 μM in the freshwater medium) inhibited 60-90% of Na^+ uptake in tilapia, carp, and zebrafish (Boisen et al., 2003; Fenwick et al., 1999). This has been further corroborated by localized expression of VHA in the branchial epithelium of teleosts (Lin et al., 1994; Sullivan et al., 1995; Wilson et al., 2000). A major drawback of this model has long been the inability to identify the channel responsible for Na^+ uptake, since no ENaC, an epithelial Na^+ channel, have been identified in teleost fish genomes. Recently, work has investigated acid-sensing ion channels (ASICs), which share ~25% identity with ENaC (Kellenberger and Schild, 2002), and found that ASICs localize to NKA rich cells and found that pharmacological inhibition of ASICs reduced uptake of Na^+ (Dymowska et al., 2015; Dymowska et al., 2014).

Saltwater fish live in a hyperosmotic environment and must balance the osmotic loss of water and gain of NaCl with high ingestions rates of seawater, which subsequently induces intestinal uptake of water and NaCl extrusion by the gills. The mechanisms of NaCl excretion by the teleost gill epithelium is clear. Na^+ - K^+ -ATPase (NKA), localized to

the basolateral membrane, is critical for Na^+ and Cl^- extrusion because of its ability to maintain the necessary electrochemical gradients. This has been demonstrated by studies that have injected ouabain, a known inhibitor of NKA, causing the inhibition of the efflux of both ions (Silva et al., 1977). Furthermore, work has shown that NKA is localized to the basolateral aspect of the mitochondrial rich cells (MRCs) (Cutler et al., 2000; Lee et al., 1998). Furthermore, the expression and activity of gill NKA in teleosts is correlated with salinity (Hawkings et al., 2004; Hwang et al., 1989; Li et al., 2014; Lin et al., 2004; Seidelin et al., 2000; Tipsmark et al., 2004; Wilson et al., 2002). Although, work on some euryhaline species exhibit decreases in NKA activity and expression after acclimation to seawater (Lin et al., 2003; Marshall and Bryson, 1998; Piermarini and Evans, 2000), although the reason why has not been elucidated. $\text{Na}^+ - \text{K}^+ - 2\text{Cl}^-$ (NKCC) has been localized to the basolateral membrane (McCormick et al., 2003; Wilson et al., 2000), with expression being regulated by salinity (Hiroi and McCormick, 2007; Li et al., 2014).

The vast majority of fishes can only tolerate slight deviations in salinities, but a large sub-set of species are able to tolerate a much broader range of salinities (Evans et al., 2005b). Estuarine teleost species, like the red drum, are likely to be exposed to both freshwater and saltwater environments, requiring the ability to osmoregulate under a variety of conditions. One might assume that species that inhabit stable salinity environments lack the required mechanisms to accomplish the branchial salt transport. However, recent work has shown that branchial salt absorption mechanisms, such as VHA and ASICs (acid-sensing ion channels), are present in marine species, presumably for acid-base regulation. The importance of euryhalinity is in the context of discerning the role of VHA. The available data as described above indicates that VHA is basolateral in seawater and apical in freshwater, which leads us to hypothesize the role of VHA in euryhaline fishes.

OVERALL GOALS

On this background, my thesis will be divided into four major chapters with the goal of: 1) understanding the sensitivity of estuarine species to acid-base disturbances, 2) elucidating the mechanisms in epithelial tissues that offset these disturbances, and 3) exploring the capacity for acid-base plasticity in response to environmental disturbances. Chapters 2 and 3 of my thesis will explore the lethal and sub-lethal CO₂ sensitivity of early life stage estuarine fish species (red drum, *Sciaenops ocellatus*, and orange spotted grouper, *Epinephelus coioides*) in the context of ocean acidification. Chapter 4 will build on these results by exploring the role that the development of acid-base homeostatic pathways in early life stages using the red drum as a marine model species. The final chapter of my thesis will extend this work to sub-adult life stages and will explore the mechanisms by which estuarine fish compensate for respiratory alkalosis when high $p\text{CO}_2$ levels invariably return to control conditions.

FIGURES

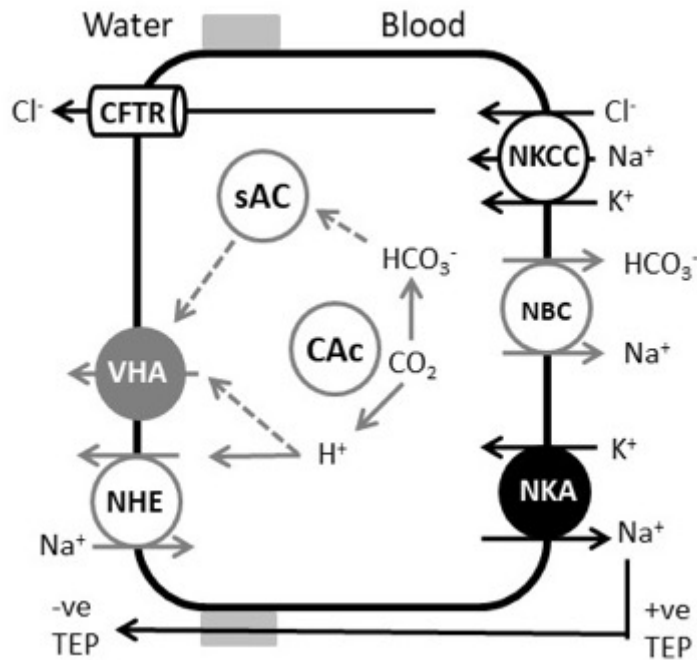


Figure 1.1: Diagram of a representative ionocyte on the gill epithelium of a marine teleost highlighting proposed and documents mechanisms of apical H^+ excretion and basolateral HCO_3^- uptake. Here we present all the transporters in a single ionocyte, but recent work has described multiple ionocytes. Metabolic CO_2 is hydrated by cytosolic carbonic anhydrase (CAc), which results in a H^+ and HCO_3^- ion. The H^+ ion is excreted across the apical membrane via either the Na^+/H^+ Exchanger (NHE) or the V-type H^+ ATPase (VHA). The HCO_3^- ion may interact with the soluble adenylyl cyclase (sAC), although sAC has yet to be shown in marine teleosts, to activate VHA and is also moved across the basolateral membrane by the Na^+/HCO_3^- Cotransporter (NBC). Here we have denoted accepted pathways by *solid lines* and suggested pathways by *dashed lines*. Furthermore acid-base pathways are denoted in gray, while osmoregulatory pathways are denoted in *black*. Diagram from Esbaugh (2018).

Chapter 2: The early life stages of an estuarine fish, the red drum (*Sciaenops ocellatus*), are tolerant to high $p\text{CO}_2$

AUTHORS

Joshua Lonthair*, Rasmus Ern, Andrew Esbaugh

Marine Science Institute, University of Texas at Austin, Port Aransas, TX, 78373,
USA

*Corresponding author: tel: +1 361 749 6827; fax +1 361 749 6749; e-mail:
jlonthair@utexas.edu¹

ABSTRACT

Ocean acidification (OA) and other climate change induced environmental alterations are resulting in unprecedented rates of environmental deterioration. This environmental change is generally thought to be too fast for adaptation using typical evolutionary processes, and thus sensitivity may be dependent on the presence of existing tolerant genotypes and species. Estuaries undergo natural $p\text{CO}_2$ fluctuations over a variety of time scales, and levels regularly exceed the predicted end of the century values. Interestingly, estuarine fish species have been overlooked in reference to the impacts of OA. Here we use the estuarine red drum (*Sciaenops ocellatus*) as a model to explore the hypothesis that early life stages of estuarine species have intrinsic tolerance to elevated $p\text{CO}_2$. Our sensitivity endpoints included: survival, growth, yolk consumption, heart rate, and scototaxis. Survival was significantly decreased when exposed to 1300 μatm and 3000 μatm and coincided with a significant increase in heart rate at the 3000 μatm exposure. However, these effects were less pronounced than the findings of previous studies on other

This work was published in ICES Journal of Marine Science (<https://doi.org/10.1093/icesjms/fsw225>)
J.L., R.E. and A.E. conceived the presented project. J.L. and R.E. carried out the experiments and data collection. J.L. and R.E. completed data analysis and interpretation. J.L. wrote the manuscript with editing and support from A.E. and R.E. A.E. provided support and supervision for the project.

marine fish species. Yolk depletion rate and standard length were not significantly affected by $p\text{CO}_2$. Scototaxis behavior was also not significantly affected by exposure to elevated levels of $p\text{CO}_2$ under both acute and acclimated exposure scenarios. Overall, these results support the hypothesis that estuarine life history and habitat usage may play a critical role in determining sensitivity of fish species to OA. Furthermore, estuarine species may provide present-day insight into the physiological and ecological foundation of OA tolerance.

Key Words red drum, development, larval, climate change, hypercapnia, estuary

INTRODUCTION

Anthropogenic carbon dioxide (CO_2) emissions are having measurable impacts on oceanic carbonate chemistry – a process known as ocean acidification (OA). Current models project that the oceans will reach approximately $1000 \mu\text{atm } p\text{CO}_2$ by the end of this century, a 250% increase from the present oceanic $p\text{CO}_2$ level (Caldeira and Wickett, 2003; Doney et al., 2009; Solomon et al., 2007). Estuaries are important components of the marine ecosystem that commonly act as a nursery ground for early life stage fish and juveniles. Estuaries are susceptible to a variety of environmental factors, including anthropogenic run-off, microbial processes, and upwelling (Cai et al., 2011; Feely et al., 2010). Furthermore, estuaries undergo natural fluctuations of $p\text{CO}_2$ on a variety of time scales (Feely et al., 2010), which has led many to conclude that the effects of OA may be exacerbated in these systems (Cai et al., 2011). For example, previous work has demonstrated $p\text{CO}_2$ in excess of $2000 \mu\text{atm}$ (Wallace et al., 2014) in estuaries in the northeast US, and $3000 \mu\text{atm}$ (Melzner et al., 2013) in an estuary in the Baltic region of Europe.

Previous studies have found negative responses to increased $p\text{CO}_2$ exposure on a variety of endpoints in early life stage marine teleosts, including: impaired sensory and behavior (Dixon et al., 2010; Ferrari et al., 2015; Munday et al., 2009b; Nilsson et al., 2012), alterations in aerobic scope (Couturier et al., 2013; Munday et al., 2009a) and ionoregulatory physiology (Esbaugh et al., 2012; Heuer et al., 2012; Strobel et al., 2012), increased tissue damage (Chambers et al., 2014; Frommel et al., 2012; Frommel et al., 2014), and diminished growth and survival (Baumann et al., 2012; DePasquale et al., 2015; Miller et al., 2012). Early life stage fish are especially susceptible to the impacts of elevated $p\text{CO}_2$, presumably because they are less capable of tolerating the associated acid-base disturbances (Esbaugh et al., 2016; Esbaugh et al., 2012; Green and Jutfelt, 2014; Strobel et al., 2012). Notably, much of the current work has focused on species from marine or reef environments with less emphasis placed on estuarine-dependent species.

Over the past few years, studies on high $p\text{CO}_2$ have gradually moved beyond defining the detrimental effects of elevated $p\text{CO}_2$ on marine life to exploring the potential for tolerance in marine systems. This is especially important for fish as many species double as vital economic resources, and OA is predicted to have dramatic effects on global populations (See Reviews: Hofmann and Todgham, 2010; Kelly and Hofmann, 2013; Munday et al., 2010; Pfister et al., 2014). Tolerance to OA and climate change is thought to rely primarily on the presence of existing tolerant genotypes in a population, and the ability of individuals to alter their physiology to suit new environmental conditions; a process known as phenotypic plasticity (Bell, 2013; Gonzalez et al., 2013; Kelly et al., 2013; Pespeni et al., 2013). Studies that have demonstrated plastic responses to high $p\text{CO}_2$ include previous work with red drum, which exhibited respiratory plasticity with only mild physiological trade-offs, as well as altered ventilatory parameters with little impact on the overall energy budget (Ern and Esbaugh, 2016; Esbaugh et al., 2016). To date, carbon vent

habitats have been of particular interest as a potential source of tolerant genotypes. These genotypes allow individual species, primarily invertebrates, to effectively cope with elevated $p\text{CO}_2$ levels and decreased pH (Basso et al., 2015; Calosi et al., 2013). Interestingly, there has been relatively little effort in exploring whether estuaries may act as a similar reservoir of tolerant species and genotypes.

On this background, the current study sought to examine the hypothesis that estuaries may act as a source of existing tolerant species and/or genotypes. We first explored the conceptual viability of the hypothesis that estuarine inhabitants may exhibit high $p\text{CO}_2$ tolerance by assessing carbonate chemistry in estuaries from across the United States through the National Estuarine Research Reserve network. We then explored the representation of estuarine fishes within the OA literature. Finally, we experimentally assessed the sensitivity of a fast-developing economically important estuarine species, the red drum (*Sciaenops ocellatus*). Parameters that were assessed for sensitivity to elevated $p\text{CO}_2$ include: survival, heart rate, yolk depletion rate, standard length, and scototaxis. Scototaxis has been verified to assess the anxiety-like behavior in fish (Maximino et al., 2010). Scototaxis or dark/light preference is based on the natural aversive quality of brightly lit environments. Using a standardized scototaxis test design that has been validated (Hamilton et al., 2014), we tested the influence of elevated $p\text{CO}_2$ on dark/light preference.

Red drum were selected as a representative due to their life history, as they broadcast spawn in the early fall in channels that interlink the open ocean and estuarine environment (Comyns et al., 1989; Holt et al., 1983). The embryos proceed into the estuarine environment where they hatch within 24 hours post fertilization (hpf) (Holt et al., 1983). Red drum are fast developing, with exogenous feeding occurring approximately 96 hpf. Comparatively, other teleosts species that have been studied have longer development

periods, including: Atlantic herring (Franke and Clemmesen, 2011), Atlantic cod (Frommel et al., 2013), *Menidia beryllina* (Baumann et al., 2012) We hypothesized that red drum, owing to their estuarine-dependent life history and fast development, will be tolerant to the impacts of elevated $p\text{CO}_2$ across a range of physiological, behavioral, and survival endpoints.

METHODS

Estuarine $p\text{CO}_2$ monitoring

Water chemistry data was obtained from the Central Data Management Office of the NOAA National Estuarine Research Reserve System, a network of 28 coastal sites designed to study and protect estuarine systems. Data included temperature, salinity, and pH, which was used to estimate $p\text{CO}_2$ levels using the CO2SYS software package (Lewis and Wallace, 1998; NOAA). Calculation preferences that were used in the software package include: CO_2 Constant – K1, K2 from Mehrbach et al., 1973 refit by Dickson and Millero, 1987; KHSO_4 – Dickson, 1990; pH Scale – NBS scale (mol/kg- H_2O); Total Boron – Uppstrom, 1974; and Air-Sea Flux – Wanninkhof, 2014. Two time points were analyzed each day, 12 am and 12 pm, for a yearlong period from September 2014 to August 2015. Because total alkalinity was not available through NERR resources, we estimated this parameter using a simple seawater dilution method. To estimate total alkalinity the measured salinity was divided by 32 ppt, typical ocean salinity, and multiplied by 2500 $\mu\text{mol kg}^{-1}$, an approximate total alkalinity for an alkaline rich estuary. A 7-day running average was used to smooth the data set. Data sets that had large gaps of missing information and those from estuaries with no direct interaction with the ocean were considered unrepresentative and not included in our analysis.

Rearing system

All embryos were produced by captive red drum broodstocks at both the University of Texas Marine Science Institute (UTMSI) Fisheries and Mariculture Laboratory (FAML) in Port Aransas, Texas and the Texas Parks and Wildlife – CCA Marine Development Center in Corpus Christi, Texas. Broodstock were collected as adults from the coastal waters off Corpus Christi, Texas. Broodstocks were exposed to seasonally varying temperature and photoperiod to mimic the natural environment and allowed to naturally spawn. At the time of embryo collection, water samples were obtained from the broodstock tank to determine $p\text{CO}_2$ levels at the time of spawning (Table 2.1). A single broodstock tank at FAML was retrofitted with a CO_2 scrubbing system to reduce $p\text{CO}_2$ levels, with the lowest obtainable level reaching approximately 1000 μatm . Note that a lower level could not be obtained without supplementing with flow through seawater; however, the required flow through would reduce temperature control and disrupt natural spawning behavior. The range in broodstock tank $p\text{CO}_2$ levels was used to assess the influence of parental exposure at the time of spawning on larval survival.

All larvae were reared on-site at FAML under control conditions in 150 L conical tanks with flow through seawater and constant aeration. Temperature ($25.6\pm 0.7^\circ\text{C}$), salinity (36.9 ± 0.4 ppt), and pH (8.08 ± 0.02) measurements were collected daily, and total alkalinity measurements were collected every 2-3 days (2317.7 ± 22.3 $\mu\text{mol kg}^{-1}$). Temperature and salinity were measured using a WTW Cond 3310 meter with a WTW Tetracon 325 probe. pH was measured with a combination pH electrode, calibrated immediately before use, attached to an Orion Star A121 pH meter (Thermo Scientific). Total alkalinity was measured with an automated open cell Gran titration system (ASALK2; Apollo SciTech). $p\text{CO}_2$ (526.3 ± 33.1 μatm) was then calculated using the CO2SYS package (Lewis and Wallace, 1998). At 18 days post fertilization (dpf) the fish

were divided into control, acclimated elevated $p\text{CO}_2$, and acute elevated $p\text{CO}_2$ treatments. Acute exposure fish were held at control conditions until 1 hour before testing, when they were exposed to elevated $p\text{CO}_2$ levels that mirror the acclimated $p\text{CO}_2$ treatment levels. Bubbling a mixture of CO_2 gas and air generated the water $p\text{CO}_2$ level in the elevated $p\text{CO}_2$ exposure tank. The CO_2 gas flow was controlled by a C100L gas mass flow controller (Sierra Instruments), and the nominal $p\text{CO}_2$ exposures verified by measuring pH and total alkalinity, as outlined for best practices in (Riebesell et al., 2010) (Table 2.1).

Embryonic incubation experiments

Embryos and larvae were reared at controlled temperature and salinity conditions in a VWR Low temperature diurnal illumination incubator that was programmed to have a 14 h light and 10 h dark cycle at 25°C . Tests were initiated at 12 hpf, with hatching occurring within 24 hpf. Seawater was autoclave sterilized and salinity corrected with deionized water to eliminate potential bacterial growth during testing. The process of sterilizing the water via the autoclave resulted in $p\text{CO}_2$ levels marginally lower than natural $p\text{CO}_2$ levels found in the environment. $p\text{CO}_2$ levels were achieved via methods outlined in Riebesell et al. (2010). Water quality analysis (temperature, salinity, pH, and TA) was completed on the sterilized seawater to determine the necessary volume of hydrochloric acid and sodium bicarbonate needed to reach the desired $p\text{CO}_2$ level. The three $p\text{CO}_2$ exposures included a control treatment, an OA relevant $p\text{CO}_2$ level, and a high $p\text{CO}_2$ level. These exposures were chosen due to their ecological relevance, with 3000 μatm representing the peak for the majority of estuaries (Wallace et al., 2014). A final water sample was collected and analyzed at the conclusion of the test to calculate the $p\text{CO}_2$ using the CO2SYS software package developed by Lewis and Wallace (1998) (Table 2.1).

Per spawn four replicates of 20 embryos at each of the three $p\text{CO}_2$ treatments were incubated in a 1L vacuum-sealed container in a VWR Low temperature diurnal illumination incubator. Survival was assessed at 72 hpf. Note that transition from endogenous to exogenous feeding occurs between 72 and 96 hpf, which is associated with a drop-in survival. Control survival exceeded 75% across all replicates, suggesting that tests were performed on high quality spawns. At the end of 72 h of exposure, unhatched and dead larval fish were removed and surviving larvae were anesthetized using a buffered MS-222 solution (250mg l^{-1}) and counted.

A second series of morphometric analyses were performed to assess standard length, yolk consumption, and heart rate. The experimental set-up was described as above, with exception that heart rate and standard length were assessed at 48 hpf, while yolk sac area was assessed at 24, 48 and 72 hpf. Each treatment consisted of 4 experimental replicates and 10 larvae were sampled per replicate. Heart rate was analyzed as described by Incardona et al. (2014). Videos and images were collected using a Nikon SMZ800N stereomicroscope and associated NIS Elements-D version 4.30 software (Nikon Instruments INC). Videos and images were randomly numbered to remove any potential bias during analysis. Heart rate was manually determined from video while images were analyzed for standard length and relative yolk sac area using the ImageJ free software program.

Behavior experiments

Scototaxic (light/dark preference) testing was performed as previously described in Holcombe et al. (2013). Testing took place between 8:00 and 21:00. The light/dark arena was 10cm wide by 38cm long and 10cm deep and had a white plastic floor and white walls; water level was 5cm. The walls of the dark zone were lined with black non-reflective

waterproof paper affixed to the sides with Velcro. The water in the arena was taken from the control and elevated $p\text{CO}_2$ treatment tanks, respectively. Food was withheld for 24 h prior to testing. In both groups the arena was rotated 180° after the first 5 trials. The fish was released into the arena along the border between the two zones to prevent biasing to the light or dark zone. Trials began 5 seconds after fish were released into the arena and lasted 15 minutes, consistent with other light/dark testing in fish (Hamilton et al., 2014; Holcombe et al., 2013; Maximino et al., 2010; Maximino et al., 2007). Fish movement was recorded using IDS 1.3 Megapixel camera and uEye software (IDS Imaging Development Systems, Obersulm, Germany). Time spent in the light and dark zones was quantified using EthoVision XT 10 (Noldus, Wageningen, Netherlands).

Statistical analysis

Statistical analyses were conducted using SigmaPlot version 12.5 (Systat Software, Inc., Chicago, IL, USA). All data passed normality and variance homogeneity tests unless otherwise indicated. Significant differences for survival were analyzed via a one-way analysis of variance (ANOVA) with the Holm-Sidak multiple comparisons test. The effect of broodstock $p\text{CO}_2$ level on larval survival was tested using linear regression. Heart rate was analyzed using a Kruskal-Wallis ANOVA on ranks with Dunnett's multiple comparisons test. Significant differences for standard length were analyzed via ANOVA. Yolk depletion rate was analyzed via one-way ANOVA following natural log transformation. Light/dark preference as a consequence of treatment and duration was analyzed via a two-way ANOVA with the Holm-Sidak pairwise multiple comparisons test following a square root data transformation.

RESULTS

Literature synthesis

We first performed a literature search to explore the breadth of OA research in fish that utilize different habitat types, methods for which can be found in supplementary materials. This review identified 129 peer-reviewed articles that focus on elevated $p\text{CO}_2$ effects on teleosts since 2001 (Figure 2.1). Studies on coral reef-associated fish comprised the largest portion of studies with 54 published articles, while studies on marine fish comprised 48 of the published articles. Estuarine fish comprised the smallest portion of published articles with 20. The relative proportion of work on estuarine fish has been increasing since 2012; however, it is important to note that the plurality (45%) of this work comes from only the three-spined stickleback (*Gasterosteus aculeatus*) and *Menidia spp.*

Estuarine $p\text{CO}_2$ monitoring

One year (September 2014 to August 2015) of publicly available monitoring data for 18 estuaries throughout the United States and Puerto Rico was analyzed, with 17 out of the 18 estuaries reaching $p\text{CO}_2$ levels that were in excess of end of century predictions (1000 μatm) (Table 2.2). Figure 2.2 depicts the variability in $p\text{CO}_2$ that can be found in a representative estuary, the Guana Tolomato Matanzas National Estuarine Research Reserve in Florida. In this estuary the $p\text{CO}_2$ reached a one-week maximum of 3024 μatm . Furthermore, this estuary exhibited $p\text{CO}_2$ levels that were well in excess of climate change relevant $p\text{CO}_2$ scenarios for approximately 6 months of the year.

Sensitivity experiments

Survival, heart rate, standard length, and yolk depletion rate

Water quality parameters were monitored for all embryonic incubation experiments throughout the exposure (Table 2.1). Increased $p\text{CO}_2$ caused a significant decrease in survival after a 72 h exposure at 1300 μatm and 3000 μatm ($P \leq 0.05$; ANOVA) (Figure 2.3a). Control survival was $77.6 \pm 1.2\%$, 1300 μatm survival was $66.6 \pm 2.5\%$, while 3000 μatm exposure survival was $61.7 \pm 2.8\%$, a decrease in survival of 11.0% and 15.9% respectively. There was also no apparent influence of broodstock $p\text{CO}_2$ on subsequent larval survival to either 1300 μatm or 3000 μatm exposures (Figure 2.3b). Heart rate was significantly increased after a 48 h exposure at 3000 μatm ($P \leq 0.05$; Kruskal-Wallis ANOVA on Ranks) (Figure 2.4a). Control heart rate was 132.2 ± 1.5 beats per minute while 3000 μatm exposure heart rate was 136.1 ± 1.7 beats per minute, an increase of 5.9 beats per minute. There was no significant difference in standard length after a 48 h exposure to increased $p\text{CO}_2$ (Figure 2.4b), and yolk depletion rate was not significantly different between exposure groups (Figure 2.5).

Behavior

Acute elevated $p\text{CO}_2$ exposure had no effect on light/dark preference with individuals from both treatments spending approximately 40% of their time in the dark section of the arena. Acclimated CO_2 exposure showed a similar lack of treatment effect; however, the acclimation experiment did show a group wide difference in light/dark preference as compared to the acute experiment (Figure 2.6) ($P \leq 0.05$; Two-way ANOVA).

DISCUSSION

The study of species tolerance is a crucial aspect of understanding the impacts that OA and other climate change induced environmental alterations will have on future marine ecosystems. An important facet of understanding tolerance is the identification of current species and habitats with traits that can defend against the physiological stresses of environmental deterioration. To this end, recent studies have begun examining the tolerance of species that survive in the proximity of CO₂ vents (Basso et al., 2015; Calosi et al., 2013), which often exhibit *p*CO₂ levels in excess of climate change scenarios. These studies have provided valuable insight into the natural tolerance of existing species and ecosystems. Here we suggest that estuaries are an underutilized resource for studying the tolerance of species to OA, owing to their natural elevations in ambient *p*CO₂. Furthermore, we demonstrate that a fast growing and economically important estuarine dependent species, the red drum, exhibits tolerance to high *p*CO₂ on a number of levels, ranging from survival to behavior.

It is well established that estuaries exhibit seasonally high *p*CO₂ levels owing to a number of factors, including proximity to upwelling zones and their naturally high productivity (Cai et al., 2011; Melzner et al., 2013). Our survey of estuarine *p*CO₂ levels from a variety of locations across the United States supports this viewpoint. It should be noted that we lack the ability to show that carbonate chemistry fluctuate over a 24 hour cycle in an estuary, because our data is based on a 10-day running average of *p*CO₂ levels. This fluctuation over 24 hours may allow a respite to high *p*CO₂ levels to its inhabitants. Nonetheless, the available data indicates that many of these systems exhibit persistently high *p*CO₂, which can extend up to 6 months in some cases. However, it is important to acknowledge that the data presented here are, at best, an estimate of environmental *p*CO₂ in these environments. This is simply because required water chemistry parameters such

as total alkalinity or dissolved inorganic carbon are not conducive to high throughput environmental monitoring programs. We therefore utilized a simple dilution method to estimate total alkalinity, which is based on the assumption that estuarine total alkalinity will be proportionally diluted with salinity. Importantly, this method is more likely to underestimate alkalinity by ignoring the geological contribution of riverine input. This would subsequently lead to an underestimation of $p\text{CO}_2$, and therefore we view our data as a conservative estimate.

Much of the discussion involving the effects of OA on estuarine environments has centered around the premise that OA will exacerbate the already high $p\text{CO}_2$ levels and thereby result in even greater costs than those found in more stable oceanic habitats (Cai et al., 2011). The current data supports this view while also demonstrating the difficulty in defining biologically relevant OA challenges in these systems. For example, a $p\text{CO}_2$ of 5000 μatm would typically be considered beyond the scope of OA relevant stress; however, this $p\text{CO}_2$ is far more relevant for estuarine species. Previous studies on estuarine systems have failed to acknowledge that the species inhabiting these zones may have an inherent tolerance to elevated $p\text{CO}_2$ stress. While this has been suggested as an explanation for tolerance in isolated cases (Franke and Clemmesen, 2011; Frommel et al., 2013), this is not being explored at an ecosystem wide level.

Despite the potential of estuaries to act as reservoirs of $p\text{CO}_2$ tolerant traits, there has been relatively less research concerning estuarine fish. The literature synthesis presented here attests to the fact that the majority of the previous work on the impacts of elevated $p\text{CO}_2$ on marine teleosts has focused on coral reef species and open ocean species. Note that we defined species as estuarine if these habitats are obligate during any portion of their life history. Furthermore, most of the work on estuarine fish has been limited to a select number of species, the primary species being the three-spined stickleback

(*Gasterosteus aculeatus*) and silversides (*Menidia spp.*), which accounted for 45% of the estuarine studies since 2012.

Early life survival is a particularly relevant endpoint when assessing the impacts of high $p\text{CO}_2$, as it is generally true that early life organisms are the most sensitive to environmental stress. To date, two species of teleost have been shown to exhibit decreased survival as a consequence of elevated $p\text{CO}_2$ exposure: the inland silverside (Baumann et al., 2012) and cinnamon anemonefish (*Amphiprion melanopus*) (Miller et al., 2012). Red drum exposed to both 1300 μatm and 3000 μatm $p\text{CO}_2$ exposure exhibited a significant decrease in survival (11.0% and 15.9% respectively); however, the magnitude of the response is relatively small in comparison to other studies. For example, the cinnamon anemonefish showed a 25% drop in survival during a 31-day 1000 μatm rearing exposure (Miller et al., 2012), while *Menidia beryllina* exhibited a 50% reduction during a 10-day 780 μatm exposure (Baumann et al., 2012). It should be noted that those impacts were the result of longer exposures to elevated $p\text{CO}_2$, which included portions of the lifecycle where larvae were exogenously feeding. Our study was limited to looking at the impacts of elevated $p\text{CO}_2$ over 72 h, owing to the steep drop in control survival associated with first feeding. It is possible that a greater effect of elevated $p\text{CO}_2$ would have been observed using longer exposures.

The 10% drop in survival as a consequence of $p\text{CO}_2$ exposure would suggest that the vast majority of early life stage red drum contain the physiological traits required for $p\text{CO}_2$ tolerance. This is in-line with work on Atlantic cod, which were exposed until hatch (12 dpf) to a maximum $p\text{CO}_2$ level of 4000 μatm (Frommel et al., 2013), and Atlantic herring, which were exposed until hatch (~8 dpf) at a maximum $p\text{CO}_2$ level of 4635 μatm (Franke and Clemmesen, 2011). Neither of these species showed significantly reduced survival. While these studies also had more prolonged exposure periods than the current

study, survival was assessed at a similar developmental stage. It is also important to note that our study had much larger sample sizes (N=19) than prior studies (N=4), which provides benefit when detecting small effect sizes. Interestingly, Atlantic cod and herring are known to inhabit and spawn in coastal upwelling zones (Franke and Clemmesen, 2011; Frommel et al., 2013), which can have significantly higher levels of $p\text{CO}_2$ than the open ocean (Melzner et al., 2013). It is also interesting to note that there is no apparent relationship between parental $p\text{CO}_2$ exposure and subsequent survival of offspring. Unfortunately, it was not possible to reduce broodstock exposures below 1000 μatm without jeopardizing spawning behavior, so we cannot say if the observed tolerance to 1000 μatm is the result of transgenerational plasticity. Such mechanisms have been demonstrated to confer tolerance in several fish species (Miller et al., 2012; Murray et al., 2014). Nonetheless, it is clear that further elevation of parental exposure did not provide offspring survival benefits at 3000 μatm .

Larval survival is an endpoint with clear population level outcomes; however, a number of studies have also explored sub-lethal effects of elevated $p\text{CO}_2$. Common endpoints include growth and aspects of energetics and metabolism (Baumann et al., 2012; Franke and Clemmesen, 2011; Frommel et al., 2013; Munday et al., 2016). Here we assessed larval growth, yolk size and heart rate in endogenous feeding larvae. Heart rate was significantly increased after exposure to 3000 μatm , which ostensibly could result in higher energetic costs. However, the very small increase in heart rate seems unlikely to have dramatic energetic implications. In adult red drum it was found that OA relevant $p\text{CO}_2$ exposures impacted ventilatory parameters, but there would be little impact on the overall energy budget (Ern and Esbaugh, 2016). This was based on the similarity in metabolic rate parameters in exposed and control fish. Standard length was not impacted by increased $p\text{CO}_2$ exposure, nor was yolk depletion rate. It seems likely that the increased heart rate is

simply a response to the developing sensory system related to cardiorespiratory control, which has been documented in zebrafish (Miller et al., 2014). Importantly, cardiorespiratory parameters do not drive oxygen uptake in larval fish, so this is unlikely to be related to increased oxygen requirements. Nonetheless, recent studies have theorized that exposure to elevated $p\text{CO}_2$ will result in greater energetic demands, and thus should result in a decrease in yolk size and standard length (Munday et al., 2016). Our results indicate that energy demands in red drum are not being altered by exposure to elevated $p\text{CO}_2$, which renders further support that these estuarine fish exhibit tolerance.

Fish behavior is one of the traits most consistently impacted by high $p\text{CO}_2$. Impacted behaviors include olfactory response (Cripps et al., 2011; Devine and Munday, 2013; Munday et al., 2009b), predation rate (Cripps et al., 2011; Ferrari et al., 2011; Ferrari et al., 2015), settlement rate (Devine and Munday, 2013), and learning (Chivers et al., 2014; Ferrari et al., 2012). Impacts on behavior are thought to be the result of CO_2 induced reversal of GABA-A receptor, the primary inhibitory neurotransmitter receptor in the vertebrate brain (Hamilton et al., 2014; Nilsson et al., 2012). Brain ion regulation is fine tuned to the ambient $p\text{CO}_2$ conditions, and alterations to these could lead to disruption (Nilsson et al., 2012). It is theorized that the elevated $p\text{CO}_2$ induced changes in blood CO_2 chemistry, including plasma $[\text{HCO}_3^-]$, (Esbaugh et al., 2012) alter the electrochemical driving forces governing chloride movement upon receptor activation (Heuer and Grosell, 2014). Thus, resulting in a misinterpretation of the sensory signal by the brain. Previous work has demonstrated that elevated $p\text{CO}_2$ results in a switch in light/dark preference, which can be reversed using an antagonist of GABA-A (Hamilton et al., 2014; Ou et al., 2015). Red drum were unaffected by elevated $p\text{CO}_2$ with control and exposed individuals showing no significant difference in light preference, regardless of the duration of $p\text{CO}_2$ exposure. Furthermore, recent work on other teleosts has found null-results of elevated

$p\text{CO}_2$ on behavior, lending further credence to our theory (Munday et al., 2016). It is noteworthy that a previous study on juvenile red drum demonstrated that these animals exhibit the typical elevated $p\text{CO}_2$ induced change in blood CO_2 chemistry (Esbaugh et al., 2016), which may suggest that these animals can more effectively control intracellular pH and thereby defend against GABA-A receptor reversal.

In conclusion, our study demonstrated that estuaries are dynamic environments whose natural fluctuations in $p\text{CO}_2$ can be representative of predicted climate change scenarios. As such, estuaries are excellent, yet underutilized, opportunities to explore current tolerance to elevated $p\text{CO}_2$ in biological systems. We have shown that the fast-growing estuarine-dependent red drum exhibit tolerance to elevated $p\text{CO}_2$ on a number of different levels. The only negative impact we observed to an increased $p\text{CO}_2$ level similar to end of century prediction was a marginal 10% decrease in survival.

ACKNOWLEDGEMENTS

This work was funded by a National Science Foundation grant (EF 1315290) to AJE. Additional support for JKL was provided by the Coastal Conservation Association (CCA) Texas and University of Texas at Austin: Summer Recruitment Fellowship. Red drum embryos were generously provided by Texas Parks and Wildlife – CCA Marine Development Center (Corpus Christi, Texas). Elizabeth Allmon assisted in imaging and sample collection with embryonic and early life stage work. The authors have no conflicts of interest with respect to this work.

TABLES

Table 2.1: Mean (± 1 SEM) temperature, salinity, pH, total alkalinity, and $p\text{CO}_2$ in experiments with red drum (*Sciaenops ocellatus*) embryos and early life stages.

Experiment	Treatment	Temp. ($^{\circ}\text{C}$)	Salinity	pH_{NBS}	A_{T} ($\mu\text{mol/kg}$)	$p\text{CO}_2$ (μatm)
<i>Broodstock</i>	Natural (n=6)	25.7 \pm 0.5	33 \pm 1	7.50 \pm 0.05	2592 \pm 445	2590 \pm 304
<i>Broodstock</i>	CO_2 Scrubber (n=2)	26.35 \pm 0.1	33.8 \pm 1	7.84 \pm 0.04	2610 \pm 337	1149 \pm 41
<i>Embryonic</i>	Control (n=24)	24.6 \pm 0.1	33 \pm 1	8.48 \pm 0.04	2234 \pm 15	193 \pm 30
	Medium $p\text{CO}_2$ (n=24)	24.7 \pm 0.1	33 \pm 1	7.73 \pm 0.02	2246 \pm 13	1326 \pm 54
	High $p\text{CO}_2$ (n=24)	24.6 \pm 0.1	33 \pm 1	7.43 \pm 0.03	2276 \pm 23	3021 \pm 172
<i>Behavioral</i>	Control (n=11)	22 \pm 0.1	35	8.21 \pm 0.01	2233 \pm 10	352 \pm 9
	Elevated $p\text{CO}_2$ (n=11)	22 \pm 0.1	35	7.73 \pm 0.03	2235 \pm 8	1258 \pm 87

Table 2.2: Highest one-week recorded $p\text{CO}_2$ for 18 representative estuaries from across the United States and Puerto Rico, as well as corresponding temperature, salinity and pH.

Name (State)	Temp. (°C)	Salinity	pH _{NBS}	A_T (μmol/kg)	$p\text{CO}_2$ (μatm)
Great Bay (NH)	16.3	21	7.4	1477	1600
Wells (ME)	17.8	31	7.6	2216	1175
Waquit Bay (MA)	26.8	27	6.9	1952	6943
Narragansett (RI)	22.9	30	7.5	2132	1520
Caribbean (PR)	30.8	37	7.4	2622	2772
Grand Bay (MS)	30.1	28	7.3	1997	2543
Rookery Bay (FL)	26.9	24	7.6	1704	1151
Delaware (DE)	25.7	14	6.8	996	5207
ACE Basin (SC)	29.4	17	6.8	1243	6171
GTM (FL)	30.4	25	7.2	1812	3024
North Inlet-Winyah (SC)	25.7	34	7.3	2399	2914
North Carolina (NC)	30	34	7.3	2419	2853
Elkhorn Slough (CA)	14.5	21	7.2	1481	2377
Kachemak Bay (AK)	3.4	31	7.9	2209	599
Padilla Bay (WA)	14	28	7.4	1964	1958
San Francisco (CA)	25.3	29	7.3	2032	2358
South Slough (OR)	18.5	30	7.4	2137	2205
Tijuana River (CA)	23	35	7	2497	5486

FIGURES

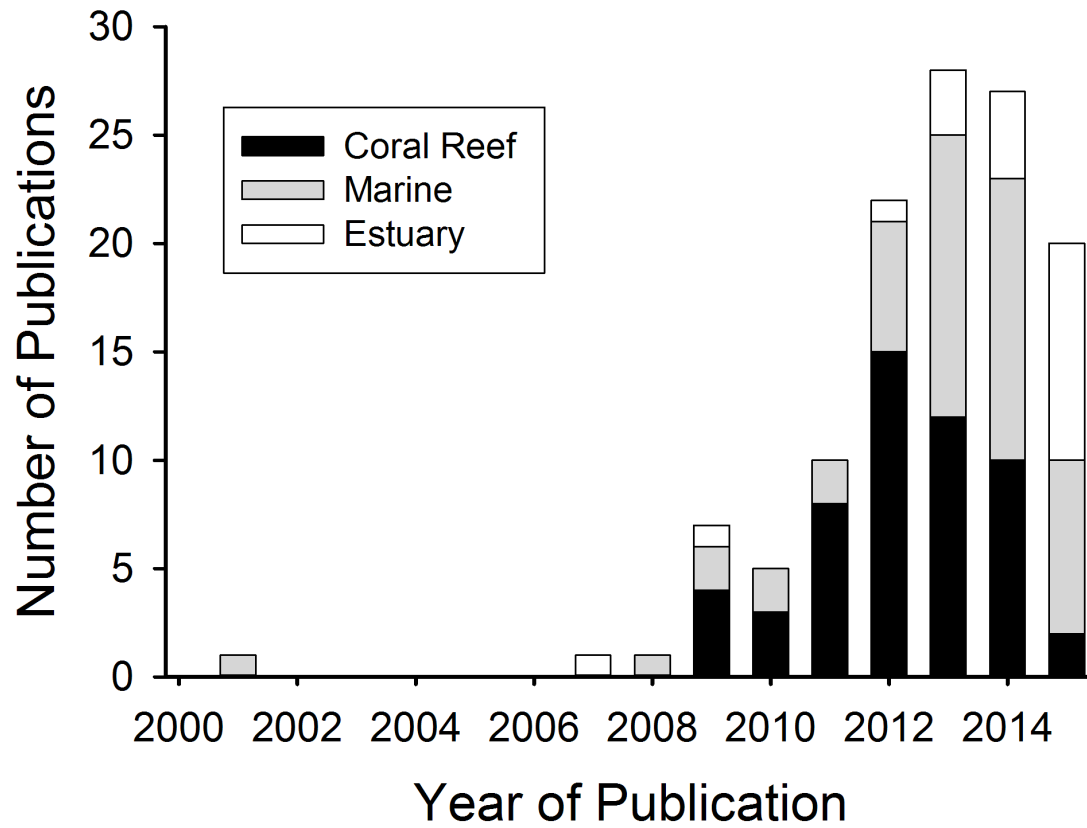


Figure 2.1: The number of publications per year returned in response to a combined topical search for ocean acidification and fishes. See Methods for a detailed description of the search parameters.

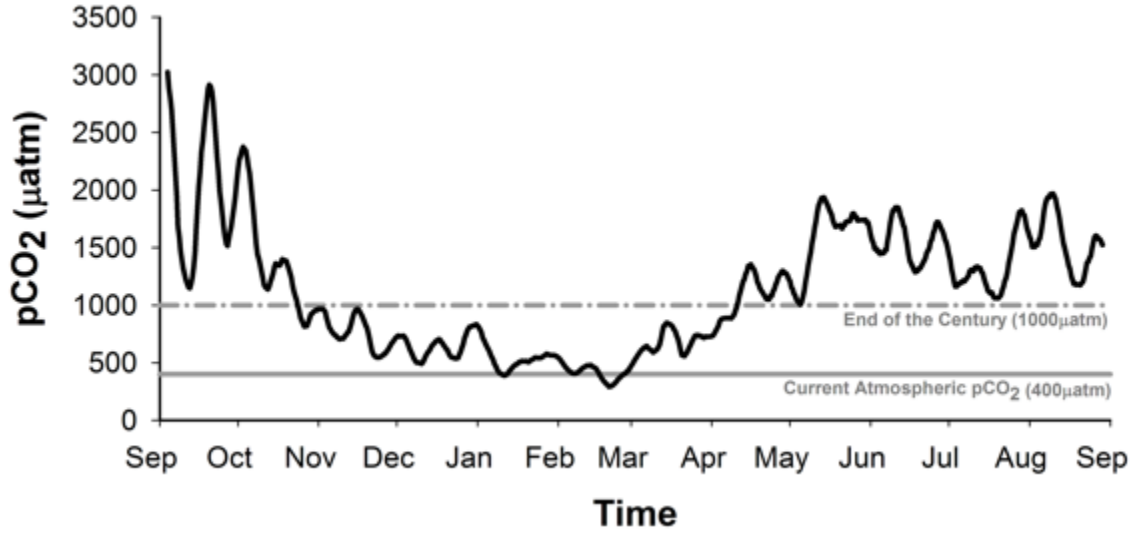


Figure 2.2: Representative estimated $p\text{CO}_2$ tracing from the Guana Tolomato Matanzas National Estuarine Research Reserve in Florida. Data is from September 2014 to August 2015. Data was smoothed using a 7-day running average.

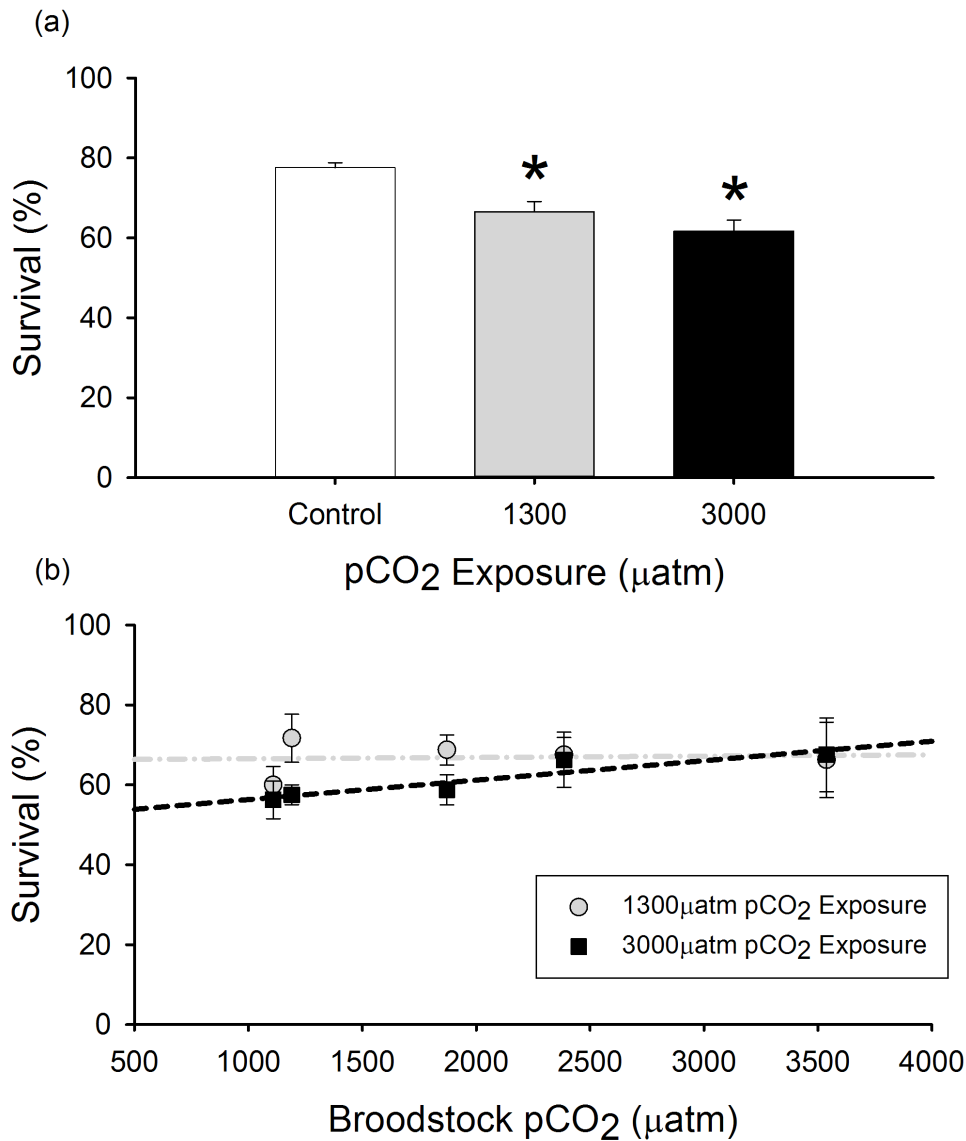


Figure 2.3: Survival of red drum in response to elevated $p\text{CO}_2$, and the effect of multi-generational exposure on survival. **(a)** Mean (\pm SEM) survival of red drum (*Sciaenops ocellatus*) after 72 h exposure to control, 1300 μatm , and 3000 μatm $p\text{CO}_2$. Asterisk indicated statistically significant difference from control ($P < 0.05$; $N = 19$). **(b)** Linear regression evaluating the mean (\pm SEM) survival of red drum (*Sciaenops ocellatus*) after 72 h exposure to 1300 μatm ($P = .835$; $R^2 = 0.003$) and 3000 μatm ($P = 0.125$; $R^2 = 0.09$) $p\text{CO}_2$ as a consequence of broodstock $p\text{CO}_2$ level. The broodstock $p\text{CO}_2$ varied owing to a combination of natural tank variability and selective installation of CO_2 scrubbers (≤ 1200 μatm $p\text{CO}_2$).

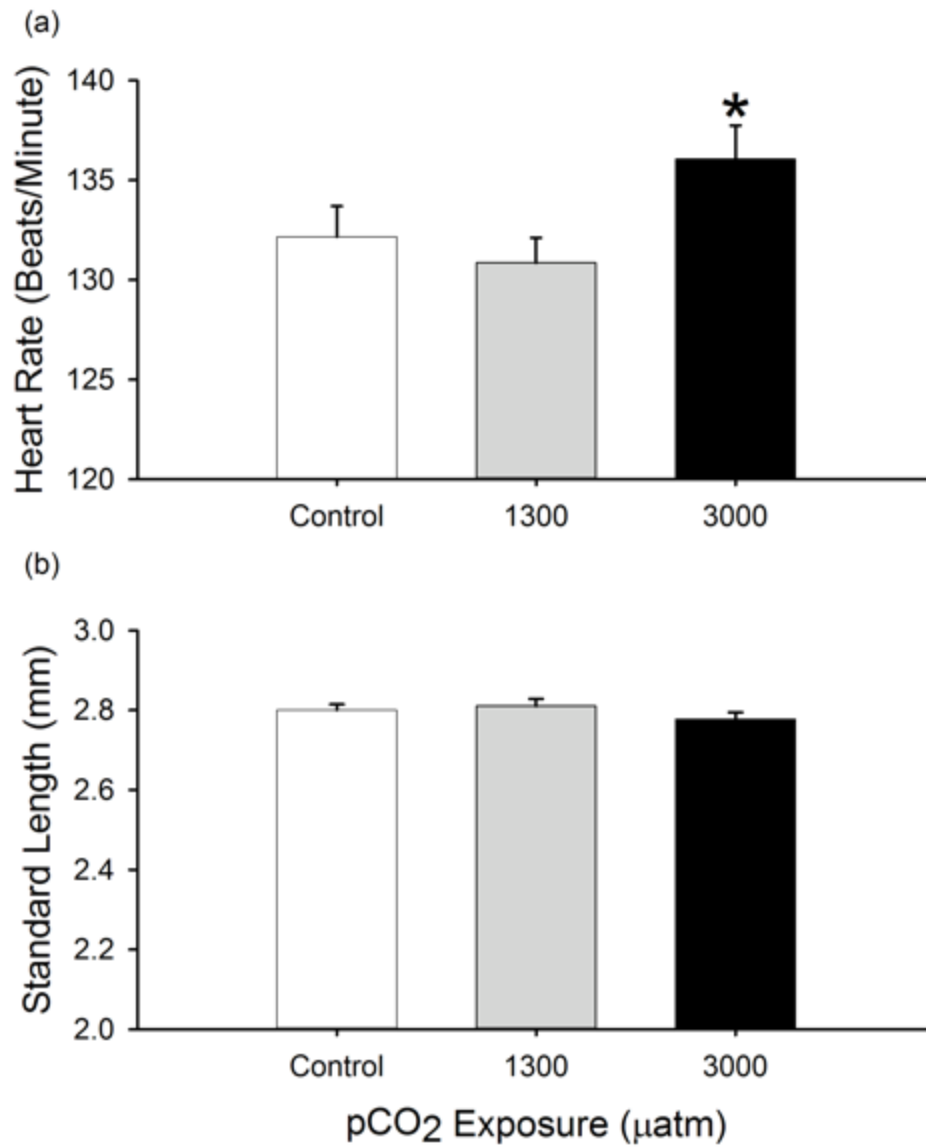


Figure 2.4: Mean (\pm SEM) (a) heart rate, and (b) standard length of red drum (*Sciaenops ocellatus*) after 48 h exposure to control, 1300 μatm , and 3000 μatm pCO₂. Asterisk indicated statistically significant difference from control (P < 0.05; N = 40 larvae per treatment).

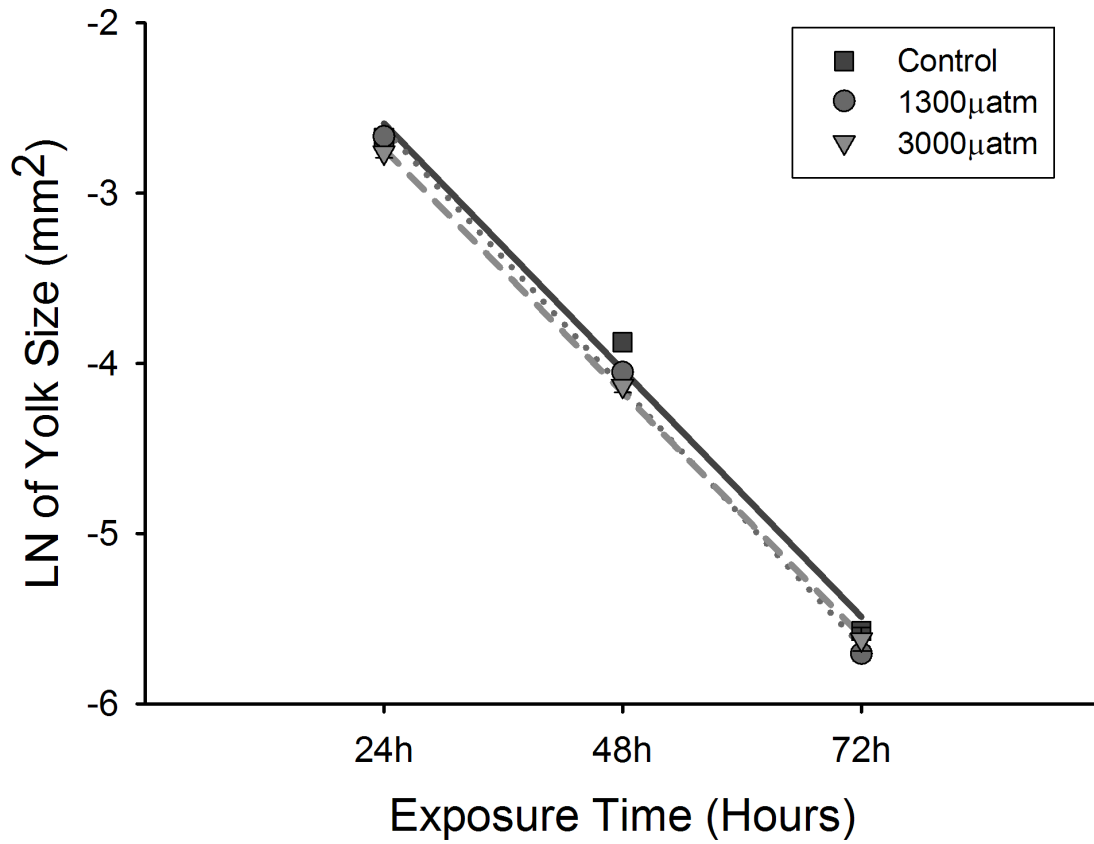


Figure 2.5: Natural log of the mean yolk size (± 1 SEM) after 24 h, 48 h, and 72 h exposure to control, 1300 μatm , and 3000 μatm $p\text{CO}_2$ in red drum (*Sciaenops ocellatus*). There were no significant differences between slopes, adjusted means, or intercepts (ANCOVA; N = 40 larvae per time point and treatment).

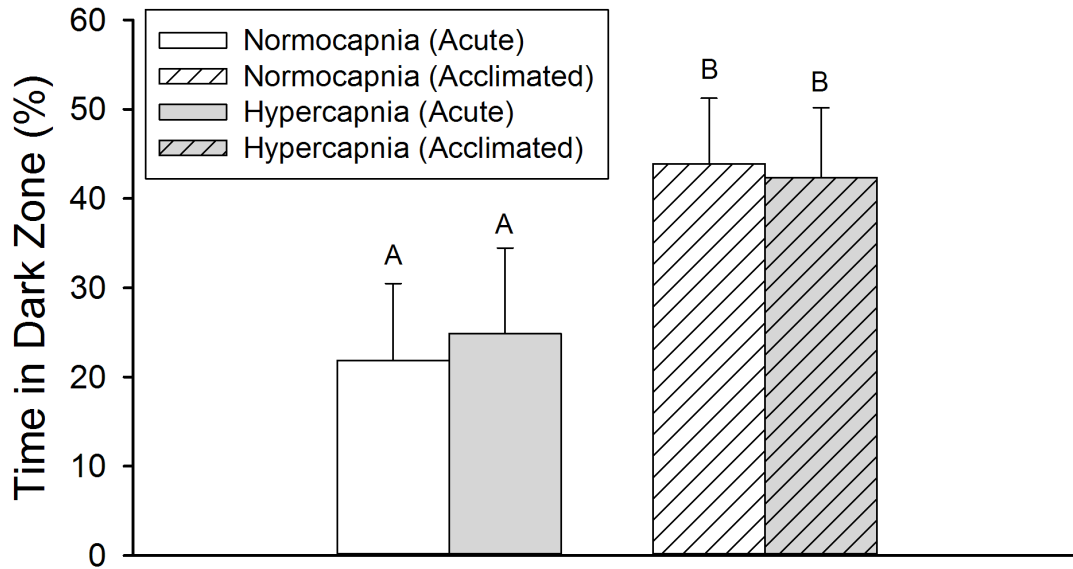


Figure 2.6: Light/dark preference for red drum (*Sciaenops ocellatus*) following acute and acclimated exposure to 1000 μatm $p\text{CO}_2$. There was no effect of $p\text{CO}_2$ treatment on light/dark preference and no significant interaction between treatment and group (2-way ANOVA; $N = 21$). Light/dark preference was significantly different between acute and acclimated tests.

Chapter 3: Impacts of hypercapnia on the early life stages of the orange spotted grouper, *Epinephelus coioides*

AUTHORS

Joshua Lonthair^{1*}, Pung-Pung Hwang², Andrew J. Esbaugh¹

¹Marine Science Institute, University of Texas at Austin, Port Aransas, TX, 78373, USA

²Institute of Cellular and Organismic Biology, Academia Sinica, Taipei 115, Taiwan

*Corresponding author: tel: +1 361 749 6827; fax +1 361 749 6749; e-mail: jlonthair@utexas.edu²

ABSTRACT

Ocean acidification (OA) and other climate change induced environmental alterations are resulting in environmental degradation. This environmental change is generally thought to be too fast for adaptation using typical evolutionary process, and thus resilience may depend on the presence of existing tolerant genotypes and species. Estuaries undergo natural $p\text{CO}_2$ fluctuations over a variety of time scales, with levels regularly exceeding predicted end of the century values. Here we use the estuarine orange-spotted grouper (*Epinephelus coioides*) to explore the intrinsic resilience to elevated $p\text{CO}_2$. Our sensitivity endpoints included: survival, heart rate, growth, and yolk consumption. Furthermore, we attempted to determine if their acid-base regulatory machinery was plastic in response to elevated $p\text{CO}_2$ by analyzing gene expression of key transporters and ionocyte density. Survival was not significantly altered by exposure to elevated $p\text{CO}_2$. Interestingly,

This work was conceived by J.L, P.P.H. and A.E. J.L. carried out the experiments and data collection. J.L. completed data analysis and interpretation. J.L. wrote the manuscript with editing and support from A.E. and P.P.H. P.P.H. provided technical support and resources. A.E. provided support and supervision for the project.

heart rate was significantly elevated at both 1500 μatm (30% increase) and 3100 μatm exposure (42% increase). However, other metrics of energetic consumption, like yolk consumption and growth, were not significantly altered. Furthermore, we observed significant upregulations of *vha* (4.1x increase) and *nbc* (4.9x increase) as the result of development, but we found no changes in gene expression in *vha*, *nhe3*, and *nbc*, as well as ionocyte density in response to elevated $p\text{CO}_2$. Overall, these results support the hypothesis that estuarine species exhibit resilience to early life exposure to OA but leads to questions about the long-term impacts of OA on teleost species.

INTRODUCTION

Since the beginning of the industrial revolution, anthropogenic carbon dioxide (CO_2) emissions have had measurable impacts on the oceanic carbonate chemistry – colloquially known as ocean acidification (OA). Models project that $p\text{CO}_2$ (partial pressure CO_2) could increase to 1000 μatm in open surface water by the end of the century, which would represent a 250% increase in $p\text{CO}_2$ from present oceanic levels (Caldeira and Wickett, 2003; Doney et al., 2009; McNeil and Sasse, 2016; Solomon et al., 2007). This increase in $p\text{CO}_2$ would result in a 0.3-0.4 units reduction in pH (Orr et al., 2005). Studies on the impacts of elevated $p\text{CO}_2$ exposure, at both extreme $p\text{CO}_2$ levels and end of the century OA levels, on marine teleosts have found a plethora of negative outcomes across a variety of endpoints (Esbaugh, 2018; Heuer and Grosell, 2014), including: impaired sensory and behavior (Ferrari et al., 2015; Munday et al., 2009b; Nilsson et al., 2012; Williams et al., 2019), alterations in aerobic scope (Couturier et al., 2013; Munday et al., 2009a), ionoregulatory physiology (Esbaugh et al., 2012; Heuer et al., 2012; Strobel et al., 2012), increased tissue damage (Chambers et al., 2014; Frommel et al., 2012; Frommel et al., 2014), and diminished growth and survival (Baumann et al., 2012).

The cumulative effects of OA are thought to largely stem from a compensated respiratory acidosis that results from the altered $p\text{CO}_2$ gradients between the water and blood. In fact, compensation to respiratory acidosis has been demonstrated in a number of marine fish species at OA relevant $p\text{CO}_2$ levels as evidenced by elevated plasma HCO_3^- and $p\text{CO}_2$ coincident with normal pH (Esbaugh et al., 2016; Esbaugh et al., 2012; Heuer et al., 2012; Strobel et al., 2012). The metabolic compensation pathways in teleosts generally involve apical excretion of H^+ into the water and basolateral absorption of HCO_3^- into the blood at the gills (Hwang et al., 2011). More specifically, the process occurs in a single branchial cell type called the ionocyte, whereby apical H^+ transport occurs through Na^+/H^+ exchangers (NHE2 and NHE3) and/or the V-type H^+ ATPase (VHA), although VHA acid excretion has only been verified in freshwater fish (Marshall and Grosell, 2006). The basolateral re-uptake of HCO_3^- is thought to occur mainly through the electrogenic $\text{Na}^+/\text{HCO}_3^-$ cotransporter (NBC), which is able to operate in the efflux direction owing to the favorable electrochemical gradients (Hirata et al., 2003). It is important to note that recent work has found that other transporters play a role in acid-secretion mechanisms in other saltwater-acclimated and estuarine species (Liu et al., 2016; Takei et al., 2014).

One major concern that has been hypothesized as the result of exposure to elevated $p\text{CO}_2$ is increased metabolic cost and potential metabolic reallocation that results from the increased transport of acid-base equivalents in larval teleosts. Previous work has used additional metabolic costs as an explanation for physiological responses to OA (Stumpp et al., 2012; Stumpp et al., 2011). Furthermore, recent work has shown that exposure to elevated $p\text{CO}_2$ in sea urchin larvae did not result in alterations in size, metabolic rate, biochemical content, and gene expression, but did result in a metabolic reallocation, specifically in protein synthesis and ion transport (Pan et al., 2015). Although there are limitations of comparing sea urchin and marine fish species due to basic physiological

differences, such as differences in acid-base mechanisms and calcification. Nevertheless, the alteration in energy allocation is critical for understanding the significance of sublethal stress, because individuals with maintenance costs less sensitive to environmental stressors are more likely to survive (Pan et al., 2015).

Recent studies on OA have moved beyond defining the detrimental effects of elevated $p\text{CO}_2$ on marine life to exploring the potential for resilience in marine systems. This is especially important for fish as most are vital economic resources, and OA is predicted to have dramatic effects on global populations (See Reviews: Hofmann and Todgham, 2010; Kelly and Hofmann, 2013; Munday et al., 2010; Pfister et al., 2014). The resilience of marine fish species to the long-term environmental degradation caused by OA is dependent on a number of factors. Evolutionary adaptation to ocean acidification may be a possible route for a few marine teleosts with short generation times, but typical evolutionary processes are too slow to provide a tangible route to resilience for long lived species. Thus, resilience to OA and climate change is thought to rely primarily on the presence of existing tolerant genotypes in a population, and the ability of individuals to alter their physiology to suit new environmental conditions; a process known as phenotypic plasticity (Bell, 2013; Gonzalez et al., 2013; Kelly et al., 2013; Pespeni et al., 2013). Previous studies have demonstrated resilient responses to OA amongst a variety of marine teleosts from across a variety of ecosystems, including species from: the Antarctic, estuaries, and coastal upwelling. These studies have found that various endpoints are not altered by elevated exposure to ocean acidification, including: survival, larval morphometrics, starvation rate, heart rate, enzymatic activity, and behavior (Allmon and Esbaugh, 2017; Baumann et al., 2018b; Davis et al., 2016; Lonthair et al., 2017; Munday et al., 2016).

On this background, the current study sought to examine whether a sub-tropical species with a delayed migration into an estuarine environment exhibits resilience. We first experimentally assessed the sensitivity of a fast-developing economically important teleost species, the orange-spotted grouper (*Epinephelus coioides*). We chose orange-spotted grouper, also known as estuary cod, because of their dependency of the tropical estuarine environment (Sheaves, 1993). We then tested whether this species exhibits plasticity of the acid-base regulatory machinery by measuring gene expression in key exchangers in the mechanism. We hypothesized that orange-spotted grouper, owing to their estuarine-dependent life history, will be tolerant to the impacts of elevated $p\text{CO}_2$ across a range of physiological, sub-lethal, and lethal endpoints.

METHODS

Lethal and sublethal impacts

All embryos were produced via common strip-spawning methods by captive orange spotted grouper broodstock at the Academia Sinica; Institute of Cellular and Organismic Biology (ICOB) Marine Research Station; Jiaoxi, Yilan 262, Taiwan. All larvae were reared on-site at Academia Sinica ICOB (Taipei City, Taiwan) at controlled temperature and salinity conditions (Table 1). Tests were initiated at 12 hpf, with hatching occurring within 24 hpf. Seawater was filter sterilized using a Millipore ExpressPlus 0.22 micron filter and salinity corrected with deionized water to eliminate potential bacterial growth during testing. $p\text{CO}_2$ levels were achieved via methods outlined in Riebesell et al. (2010).

Water quality analysis (temperature, salinity, pH, and TA) was completed on the sterilized seawater to determine the necessary volume of hydrochloric acid and sodium bicarbonate needed to reach the desired $p\text{CO}_2$ level. The three $p\text{CO}_2$ exposures included a control treatment, a medium predicted end-of-century $p\text{CO}_2$ level, and a predicted high

coastal-upwelling $p\text{CO}_2$ level. A final water sample was collected and analyzed at the conclusion of the test to calculate the $p\text{CO}_2$ using the CO2SYS software package developed by Lewis and Wallace (1998) (Table 3.1). Calculation preferences that were used in the software package include: CO_2 Constant – K1, K2 from Mehrbach et al., 1973 refit by Dickson and Millero, 1987; KHSO_4 – Dickson, 1990; pH Scale – NBS scale (mol/kg- H_2O); Total Boron – Uppstrom, 1974; and Air-Sea Flux – Wanninkhof, 2014. Temperature and salinity were measured using a standard thermometer and refractometer. pH was measured with a combination pH electrode, calibrated immediately before use (NBS scale), attached to an Orion Star A121 pH meter (Thermo Scientific). Titratable alkalinity was calculated via pH and total CO_2 , which was measured using a Corning 965 CO_2 analyzer.

Per spawn four replicates of 20 embryos at each $p\text{CO}_2$ treatment were incubated in a 1L vacuum-sealed container. Survival was assessed at 60 hpf. Note that transition from endogenous to exogenous feeding occurs at approximately 72 hpf, which is associated with a drop in survival. At the end of 48 h of exposure, unhatched and dead larval fish were removed, and surviving larvae were anesthetized using a buffered MS-222 solution (250mg l^{-1}) and counted.

A second series of morphometric analyses were performed to assess total length, yolk consumption, and heart rate. The experimental set-up was described as above, with heart rate, total length, and yolk area being assessed at 48 hpf. Each treatment consisted of 4 experimental replicates and 10 larvae were sampled per replicate. Heart rate was analyzed as described by Incardona et al. (2014). With only one beaker at a time being measured, so that all animals were anaesthetized for the same period of time. For all images, 2 to 3 larvae were mounted on top of 3% methylcellulose in sea water, which allowed for rapid processing of images and videos. Replicates were processed in random order, with controls being analyzed throughout the imaging process. After processing, videos and images were

randomly numbered to remove any potential bias during analysis. Heart rate was manually determined from video while images were analyzed for total length and relative yolk sac area using the ImageJ free software program. Figure 3.1 illustrates measurement methods of total length and yolk sac area.

Acid-base mRNA Expression

Real time PCR primers were developed for *efl α* , *nbc*, *vha* (B subunit), and *nhe3*. Full length sequences for both *efl α* , *nbc*, *vha*, and *nhe3* were identified from an in-house gill transcriptome. The identified sequences were then verified against the NCBI database using a standard Blast search. Primer pairs were identified using Primer3Plus software package. All primers and GenBank accession numbers for related sequences can be found in Table 3.2.

Whole larvae were collected at 12 hpf, 36 hpf, and 60 hpf under both control conditions and after exposure to elevated $p\text{CO}_2$ levels. Samples were flash frozen and stored in -80°C , until further processing was required. Total RNA isolation was performed using QIAzol (Qiagen) according to manufacturer protocols and quantified using an ND-1000 spectrophotometer (Thermo Scientific). Total RNA was treated for potential DNA contamination by incubating with DNase 1 (Roche), according to manufacturer protocols. cDNA synthesis was performed on 1 μg of total RNA using SuperScript IV reverse transcriptase (Invitrogen Life Technologies), according to manufacturer protocols. For all cDNA synthesis runs no reverse transcriptase controls were performed to test for genomic DNA contamination. Samples were diluted 10-fold using nuclease free water and stored at -20°C until qPCR analysis.

qPCR analysis was performed using the Maxima SYBR Green kit (Thermo Scientific). Reactions were prepared according to the manufacturer's protocols with the

exception that a 12.5 μ l total reaction volume was used. All reactions were processed using an MX3000P qPCR machine (Stratagene) with accompanying software. A serial dilution was used for standard curves to determine the reaction efficiency of each primer pair. PCR efficiencies ranged from 70 to 97.4% with an $R^2 \geq 0.97$. For all genes, negative and no reverse-transcriptase control reactions were performed. The CT values for each sample were used to assess relative abundance of each gene in relation to the control gene *efl α* using the delta-delta CT method.

Immunofluorescence methods

Prior to staining, larval samples were fixed overnight in Z-fix at 4°C. Samples were then washed 1 time with 100% methanol and then transferred to 100% methanol and stored at -20°C, this procedure constituted chill permeabilization of the sample. Samples were then washed with PBS 1% triton X (PBST) four times for 5 min followed by a 1 h in blocking buffer (PBST with 5% fetal calf serum) at room temperature. Blocking buffer was removed and samples were then incubated with primary antibodies for NKA (in 1:100 dilution in blocking buffer) at 4°C overnight on a rocker. The primary polyclonal rabbit antibody for NKA (sc-28800) was obtained from the Santa Cruz Biotechnology and its effectiveness was verified using a western blot (Allmon and Esbaugh, 2017). Following primary incubation, samples were washed in blocking buffer three times for 5 min then incubated with secondary antibodies – goat anti-rabbit Alexa Flour 488 [1:500] – in the dark for 6 h at 4°C on a rocker. Samples were then washed with blocking buffer four times for 5 min and mounted using Vectashield hard-mount with DAPI and stored in the dark at 4 °C until imaged. Imaging was completed using a Nikon C2+ confocal microscope system with a Nikon Eclipse Ti-E inverted microscope and utilizing NIS-Element imaging software for image acquisition, processing, and analysis. Images were randomly numbered

to remove any potential bias during analysis. Ionocyte density was determined by creating a 0.0625 mm² box over the yolk sac area and manually counting number of ionocytes using the ImageJ free software program. Figure 3.2 illustrates the immunofluorescence ionocyte density count methods.

Statistical methods

Survival and total length data across $p\text{CO}_2$ exposures was assessed using a one-way ANOVA. Heart rate across $p\text{CO}_2$ exposures was assessed via a Kruskal-Wallis One Way Analysis of Variance on Ranks due to failure of the Shapiro-Wilk normality test. Gene expression data across development was assessed using a one-way ANOVA and Holm-Sidak post-hoc test against control values. Gene expression data across $p\text{CO}_2$ exposures was assessed using a one-way ANOVA. Ionocyte density across $p\text{CO}_2$ exposures was natural log transformed and assessed using a one-way ANOVA.

RESULTS

Sensitivity experiments

Lethal and sub-lethal impacts

Water quality measures were monitored for all embryonic incubation experiments, and $p\text{CO}_2$ exposures were maintained throughout experiments (Table 3.1). Survival was not impacted by 48 h exposure to increased $p\text{CO}_2$ levels (Figure 3.3). Heart rate was significantly elevated by 48 h exposure to elevated $p\text{CO}_2$ levels at both the 1500 μatm and 3100 μatm ($P \leq 0.05$; Kruskal-Wallis ANOVA on Ranks) (Figure 3.4a). Control heart rate in mean \pm standard error of mean (SEM) was 134 ± 14 beats per minute (bpm) at 600 μatm , 1500 μatm heart rate was 174 ± 10 bpm with, while 3100 μatm heart rate was 190 ± 7 bpm, an increase of 40 bpm (30% increase) and 56 bpm (42% increase) respectively. No effects

were observed in response to 48 h exposure to elevated $p\text{CO}_2$ levels in both total length (Figure 3.4b), and yolk size (Figure 3.4c).

Acid-base regulatory pathway plasticity

Gene expression for *nbc* and *vha* exhibited significant up-regulation as a result of development at 60 hours post fertilization when compared to 12 hours post fertilization ($P \leq 0.05$; ANOVA) (Figure 3.5a and 3.5c). In contrast, *nhe3* exhibited no alterations in relative mRNA gene expression as development progressed (Figure 3.5b). Interestingly, at two time points, 24 h and 48 h, elevated $p\text{CO}_2$ exposure at both 1500 μatm and 3100 μatm had no effect on a variety of the transporters that we hypothesized to play a critical role in acid-base regulation in marine teleosts, including *nbc*, *nhe3*, and *vha* (Figure 3.6). Furthermore, NIKA-rich ionocyte density was not altered as a result of exposure to increased levels of $p\text{CO}_2$ (Figure 3.7).

DISCUSSION

Determining species resilience is a crucial aspect of understanding the impacts that OA and other climate change induced environmental changes will have on future marine ecosystems, specifically within the discussion of evolutionary rescue. Evolutionary rescue has been described as when genetic adaptation allows for a population to recover from deteriorating population effects, which were initiated by environmental change and would have otherwise caused a local extinction (Gonzalez et al., 2013). An important facet of evolutionary rescue is that a subset of individuals are resilient to the changing environment and have the appropriate phenotypic solutions. Thus, identifying species and ecosystems with tolerant traits that can defend against the physiological stresses of environmental degradation is critical. Here, we demonstrate that a fast growing and economically

important estuarine-dependent species, the orange-spotted grouper, exhibits no clear detrimental effects of OA when exposed during the most sensitive early life stages. These findings are consistent with the hypothesis that fish endemic to coastal and up-welling regions that commonly experience elevated CO₂ may have a level of intrinsic resilience.

Early work on the impacts of OA on early life stage fish has emphasized survival as a critical endpoint, because larval survival and recruitment represents a crucial population bottleneck. Baumann et al. (2012) is a foundational study in the field, which found a 73% reduction in survival of *Menidia beryllina* at elevated pCO₂. More recent studies have found that other species exhibit reduced survival but none with such extreme sensitivity as *M. beryllina*, which likely indicates that *M. beryllina* is an outlier (Chambers et al., 2014; DePasquale et al., 2015; Lonthair et al., 2017; Miller et al., 2012; Pimentel et al., 2014). Conversely, other studies have shown that a number of species exhibit resilience to high pCO₂. Furthermore, while a significant portion of the populations are unable to tolerate OA, there are tolerant individuals present in all species tested.

While larval survival is easy to interpret and has clear population level outcomes, it is also important to consider sub-lethal effects of OA that may indicate a poor prognosis for fish in later life. Following on our hypothesis that OA may place an additional energetic burden on endogenous feeding life stages, we sought to use two morphological traits that may indicate changing energy burdens: size at age and yolk sac area. Interestingly, there was no effect of elevated CO₂ on either endpoint, which argues against our hypothesis and supports the premise that this species may have a level of intrinsic resilience. Previous work has highlighted the impacts of OA on embryonic and larval growth can be variable depending on the model species. Some studies to OA relevant pCO₂ levels have found species exhibiting detrimental decreases in growth (Frommel et al., 2016; Miller et al., 2012), no effects on growth (Bignami et al., 2013; Frommel et al., 2013), and even

increases in growth and size at age (Bignami et al., 2014; Chambers et al., 2014). This indicates that energy utilization may vary considerably between species when exposed to elevated $p\text{CO}_2$, with some species allocating a larger portion of energy to maintaining growth.

Plasticity in the acid-base regulatory machinery is a critical metric to understand resilience of OA in a teleost species. Our study indicates that orange-spotted grouper maintains acid-base regulatory transporters do not require transcription changes in response to OA relevant $p\text{CO}_2$ levels. We saw no alterations in gene expression in any of the acid-base regulatory transporters that we measured, including: *nhe3*, *vha*, and *nbc*. Other studies on marine teleost species have observed a quick stabilization of net whole body titratable acid flux following $p\text{CO}_2$ exposure (Allmon and Esbaugh, 2017; Edwards et al., 2005) and the lack of alterations in acid-base transport gene expression, enzyme activity, and protein abundance (Allmon and Esbaugh, 2017; Esbaugh et al., 2012; Michael et al., 2016). Furthermore, when measuring ionocyte density as a result of exposure to elevated $p\text{CO}_2$, we found no significant change. This further supports the argument that the orange-spotted grouper maintains high enough levels of acid-base regulatory machinery at even the earliest life stages.

In contrast to the previously discussed data, the evidence provided from heart rate is consistent with the hypothesis that OA will result in elevated energetic costs of survival in orange spotted grouper. Our data demonstrate that the heart rate increases by almost 40% when exposed to elevated CO_2 . This trend is consistent with prior work (Lonthair et al. 2017); however, the magnitude of the response in grouper is much greater than previously described for other species. The significance of this finding is rooted in two physiological concepts. The first is that heart rate is an effective proxy for metabolic rate, whereby higher heart rates indicate greater energy utilization (Green, 2011). The second is

that larval fishes generally have limited metabolic scope (Killen et al., 2007), which is the difference between the baseline costs of living and the maximum capacity of the system. This would suggest that the energetic costs of increased heart rate will remove available energy from other functions, such as future growth or activity. Pan et al. (2015) showed that sea urchin larvae expend increased energy on protein synthesis and ion transport under OA conditions, despite no evidence of OA induced effects on size or gene expression. Our data may suggest that grouper are undergoing similar metabolic reallocations to maintain growth rate in the early life stage despite higher metabolic rates. While this would presumably aid the fish in reducing early life predation risk, the long-term cost of this putative metabolic reallocation is unknown.

It is also important to consider the physiological advantages of elevated heart rate to early life stage orange spotted grouper. Adult teleosts are known to control convective fluid movement across and through their respiratory epithelium in response to respiratory stress, such as reduced oxygen or elevated CO₂ (see review in Gilmour and Perry (2007)). In fact, OA relevant *p*CO₂ exposures resulted in significant elevation in ventilatory parameters that were found to significantly reduce the magnitude of the metabolic compensation response in juvenile life stages (Ern and Esbaugh, 2016). Yet as such a benefit would seem unlikely in the current study given that early life fishes use cutaneous gas exchange with little role for convective fluid movement (Fu et al., 2010; Rombough, 2002; Rombough, 2007; Wells and Pinder, 1996). It instead seems likely that the increased heart rate is a by-product of the developing sensory system related to cardiorespiratory control (Miller et al., 2014; Vulesevic and Perry, 2006).

In conclusion, our study has shown that the estuarine-dependent orange spotted grouper show no clear detrimental effects of OA exposure in the most sensitive life stage. This is consistent with the hypothesis that species that have evolved in habitats with natural

fluctuations in $p\text{CO}_2$ may have intrinsic resilience to the impact of OA. While these results are encouraging for the long-term prospects of orange spotted grouper, it is important to recognize that our conclusions are limited to the early life stages as we were unable to complete extended grow-out studies due to the severe drop in survival that occurs at first feeding. Furthermore, we cannot inform on the potential behavioral effects of OA that may occur in later life stages, nor the potential implication of elevated temperature and reduced oxygen as additive stressors, both of which can exacerbate concerns regarding the baseline energetic cost of living in the future oceans.

ACKNOWLEDGEMENTS

This work was funded by a National Science Foundation grants (EF 1315290) to AJE and (OISE 1614168) to JKL. Additional support for JKL was provided by the Coastal Conservation Association (CCA) Texas, University of Texas at Austin: Summer Recruitment Fellowship, and the University of Texas at Austin Marine Science Institute – Lund Endowment. Orange spotted grouper embryos were generously provided by Institute of Cellular and Organismic Biology (ICOB) Marine Research Station (Jiaoxi, Yilan 262, Taiwan). Elizabeth Allmon, Lee I-Chun, Kuan Bao-Long, and Amy Chow assisted in embryo collection, imaging, and sample collection with embryonic and early life stage work. The authors have no conflicts of interest with respect to this work.

TABLES

Table 3.1: Mean (± 1 SEM) temperature, salinity, pH, total alkalinity, and $p\text{CO}_2$ in experiments with orange spotted grouper (*Epinephelus coioides*) embryos and early life stages.

Treatment	Temp. (°C)	Salinity	pH_{NBS}	A_T (μmol/kg)	pCO₂ (μatm)
Control (n=14)	26.8±0.1	33.2±0.2	8.04±0.01	2498±16	656±18
Medium pCO ₂ (n=14)	27.0±0.1	33.5±0.3	7.72±0.02	2519±85	1545±84
High pCO ₂ (n=14)	27.0±0.1	33.2±0.3	7.43±0.01	2498±23	3143±101

Table 3.2: List of primers used for real-time PCR. All sequences are 5' to 3' and reverse primers are reverse compliments of the genetic sequence.

Gene	Accession #	Orientation	Sequence
<i>ef1-a</i>	#KU885470.1	L	CTTCAACATCAAGAACGTGTCC
		R	CATTAATCTGACCAGGGTGGTT
<i>nhe3</i>	#MN511303	L	TATCATGGTGTTTGGAGAGTCG
		R	ATTAATTTTGGGTCCTCCCAGT
<i>nbc</i>	#MN511305	L	TGAACGACATTTCTGACAAACC
		R	CCGAGCAAGATGAATAAAAACC
<i>vha</i>	#MN511304	L	CTAAGAAGACGGCCTGTGAGTT
		R	CTGGATCATCTCCTCTGGGTAG

FIGURES

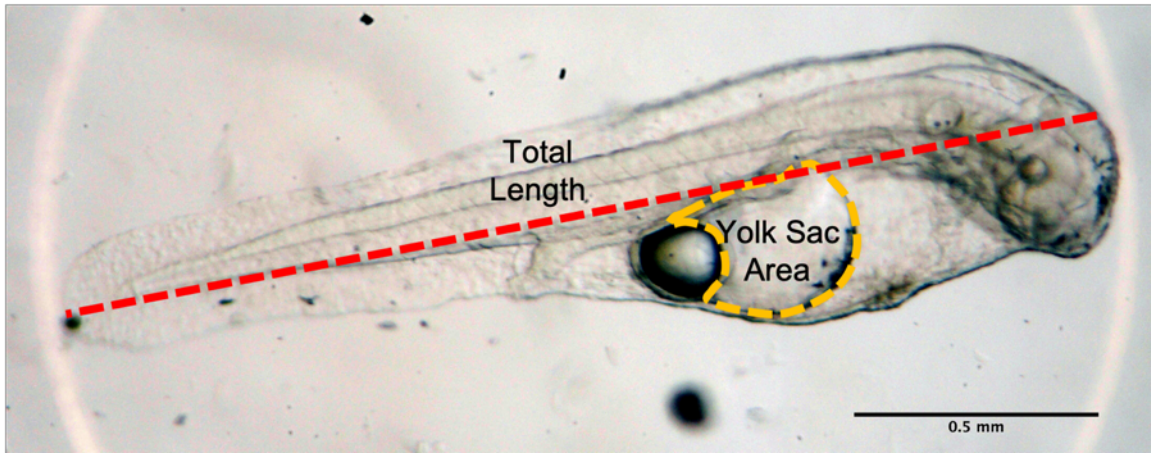


Figure 3.1: Inverted microscope image of 60 hpf orange spotted grouper (*Epinephelus coioides*). Overlaying illustration details methods used in ImageJ to determine total length (mm) and yolk sac area (mm^2) at varying $p\text{CO}_2$ conditions.

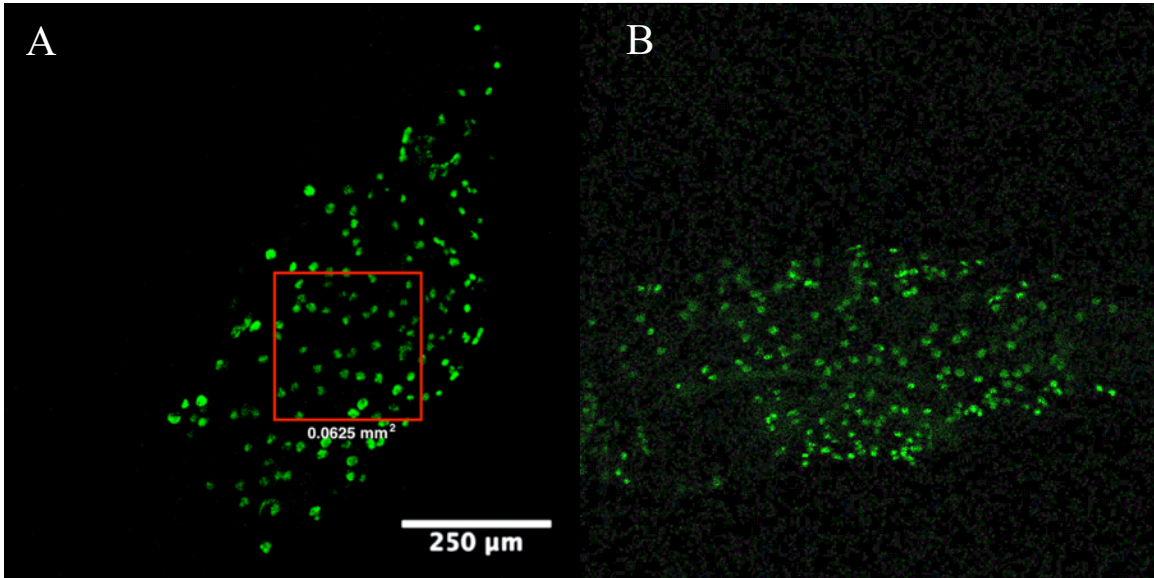


Figure 3.2: Confocal microscopy image of ionocyte density using 1 antibody for Na^+/K^+ ATPase (NKA) in 60 hpf orange spotted grouper (*Epinephelus coioides*). 0.0625 mm^2 illustrates methods used to complete counts of number of ionocytes at varying $p\text{CO}_2$ conditions. A) Ionocyte density after exposure to control conditions ($400 \mu\text{atm}$) B) Ionocyte density after exposure to $3000 \mu\text{atm}$

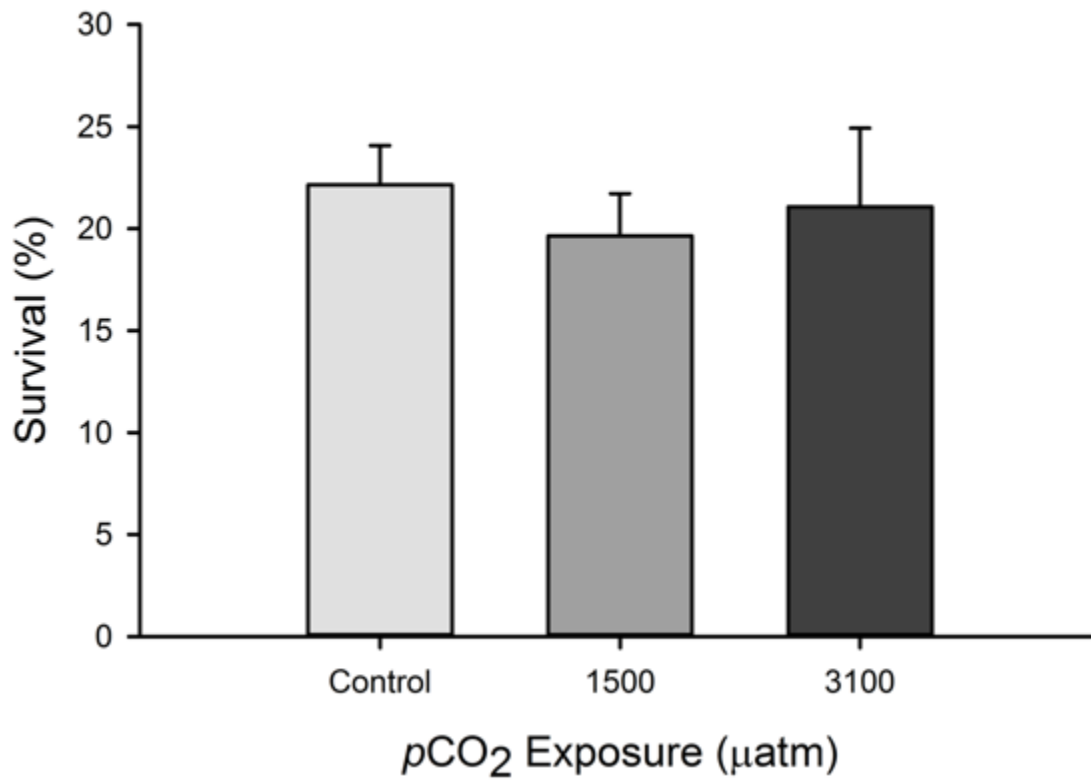


Figure 3.3: Mean (\pm SEM) survival of orange spotted grouper (*Epinephelus coioides*) after 48 h exposure to control, 1500 μatm , and 3100 μatm $p\text{CO}_2$. There were no significant differences between groups (ANOVA; $N = 7$ per treatment).

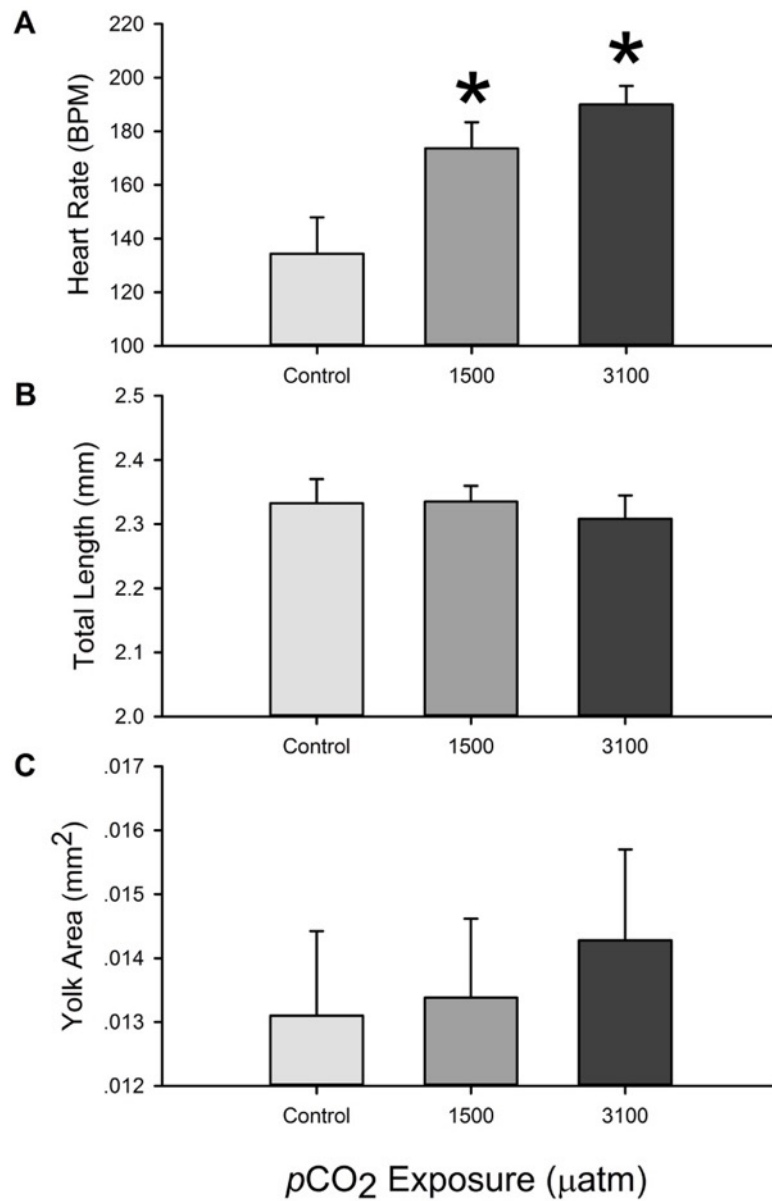


Figure 3.4: Mean (\pm SEM) **(a)** heart rate, **(b)** total length, and **(c)** yolk area of orange spotted grouper (*Epinephelus coioides*) after 48 h exposure to control, 1500 μatm , and 3100 μatm $p\text{CO}_2$. Asterisk indicated statistically significant difference from control ($P < 0.05$; $N = 19-21$ larvae per treatment).

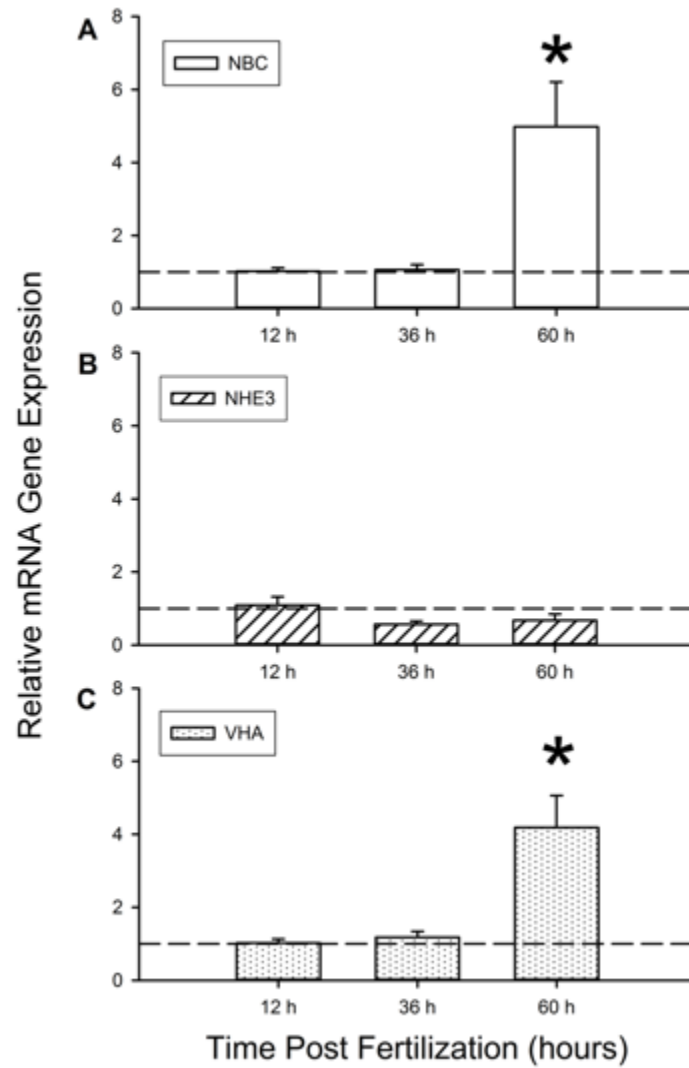


Figure 3.5: Whole animal gene expression of H⁺ excretion pathways: (a) *nbc* (b) *nhe3* (c) *vha*, during development under control conditions in orange spotted grouper (*Epinephelus coioides*). All values are relative to housekeeping gene *ef1a*. Values set relative to control values denoted by dashed lines at 1.0. Significant differences from initial time point (12 h) denoted by an asterisk (P<0.05; N = 8 per time point). All values are mean ± SEM.

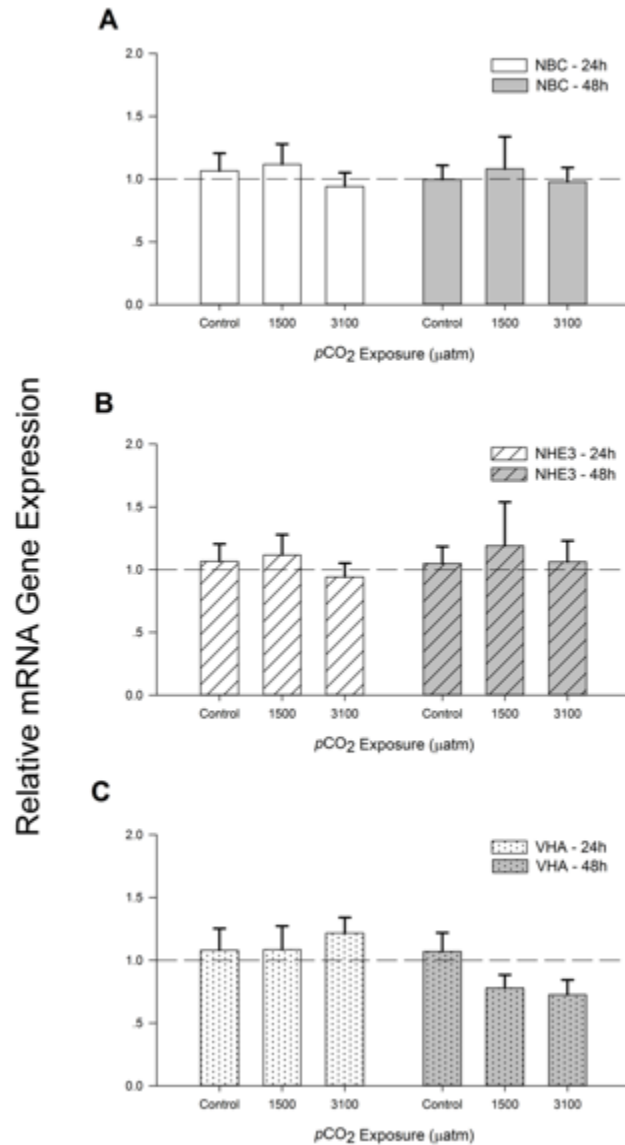


Figure 3.6: Whole animal gene expression of H⁺ excretion pathways: (a) *nbc* (b) *nhe3* (c) *vha*, during 24 and 48 h exposure to control, 1500 μatm, and 3100 μatm in orange spotted grouper (*Epinephelus coioides*). All values are relative to housekeeping gene *ef1a*. Values set relative to control values denoted by dashed lines at 1.0. There were no significant differences between groups (ANOVA; *N* = 8 per treatment). All values are mean ± SEM.

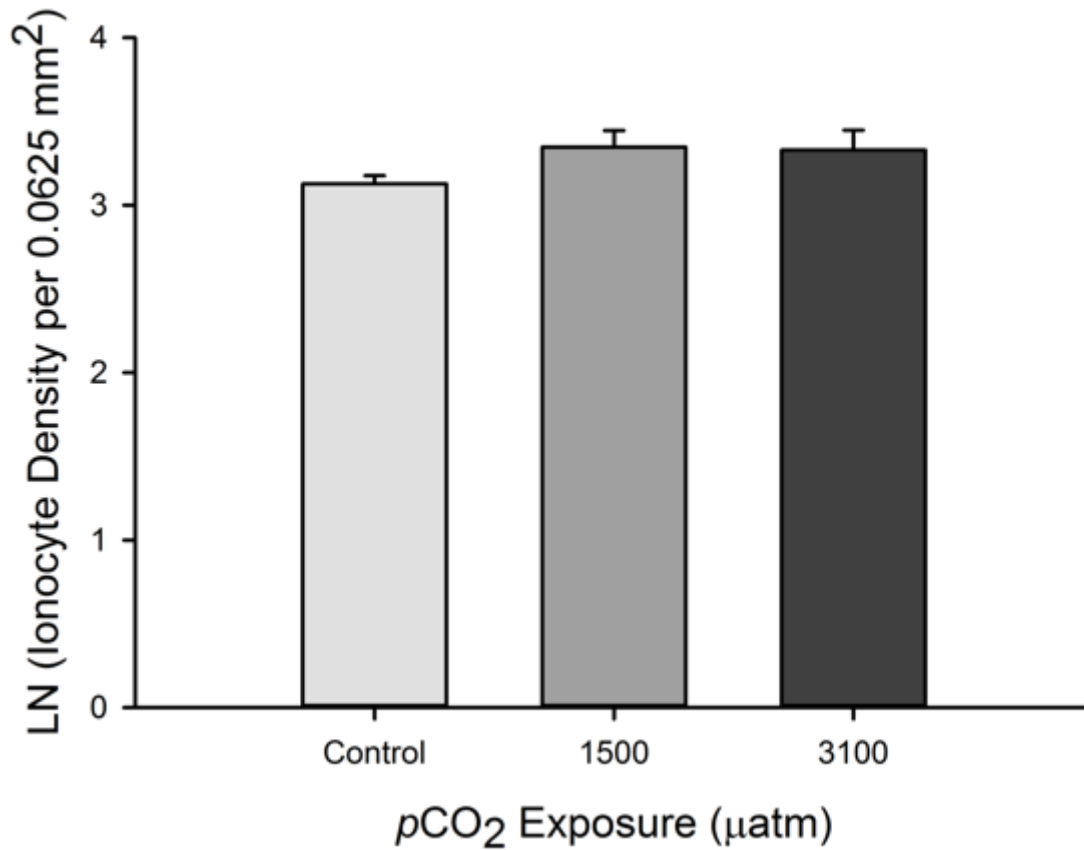


Figure 3.7: Natural log of the mean ionocyte density per .0625 mm² area (± 1 SEM) after 48 h exposure to control, 1500 μatm , and 3100 μatm $p\text{CO}_2$ in orange spotted grouper (*Epinephelus coioides*). There were no significant differences between $p\text{CO}_2$ exposure (ANOVA; $N = 8-12$ per treatment).

Chapter 4: Physiological redundancy of H⁺ excretion pathways in an estuarine teleost

AUTHORS

Joshua Lonthair* and Andrew J. Esbaugh

Marine Science Institute, University of Texas at Austin, Port Aransas, TX, 78373,
USA

*Corresponding author: tel: +1 361 749 6827; fax +1 361 749 6749; e-mail:
jlonthair@utexas.edu³

ABSTRACT

Ocean acidification (OA) has been shown to have severe impacts on early life stage (ELS) marine organisms. In fish, a variety of impacts have been documented, including reduced survival and growth, and increased tissue damage. Yet there is also substantial interspecies variability in the sensitivity of ELS fishes to OA, and it has been theorized that this may relate to the ontogeny of systemic acid-base regulatory pathways; an area that has been surprisingly understudied in obligate marine species. Here we use an integrative set of approaches to describe the role and plasticity of acid-base pathways in developing red drum, a marine fish native to the Gulf of Mexico. We demonstrate that red drum show significantly reduced survival in OA (1,000 $\mu\text{atm CO}_2$), yet over 50% of individuals were tolerant to 12,000 $\mu\text{atm CO}_2$. Consistent with the hypothesized role of acid-base pathways, we observed significant expression of relevant transporters and ionocytes ≤ 36 hours post fertilization (hpf), with only VHA exhibiting a significant upregulation at 84 hpf. Limited plasticity was observed in response to CO_2 exposure, with only Na^+/H^+ exchanger 2

This work was conceived by J.L and A.E. J.L. carried out the experiments and data collection. J.L. completed data analysis and interpretation. J.L. wrote the manuscript with editing and support from A.E. A.E. provided support and supervision for the project.

exhibiting a significant upregulation in gene expression in response to a 24 h exposure to 6000 and 12000 μatm ; however, ionocytes showed the capacity for dose-dependent acid excretion in response to elevated CO_2 , with significantly higher $\Delta[\text{H}^+]$ after exposure to 18000 and 28000 μatm . Furthermore, acid excretion was both EIPA and bafilomycin sensitive, which suggests that physiological redundancy may aid in resilience to acid-base stressors in early life.

INTRODUCTION

Anthropogenic release of carbon dioxide (CO_2) has caused measurable impacts on oceanic carbonate chemistry, also known as ocean acidification (OA) (Doney et al., 2009). Current models project that we could see a decline in pH of 0.4 units by 2100, with the highest changes occurring the arctic and nearshore environment (Ciais et al., 2013; Orr et al., 2005). Not, surprisingly these changes have caused a resurgence in the study of acid-base physiology in an effort to predict the outcomes of environmental change on organisms and ecosystems (Esbaugh, 2018; Heuer and Grosell, 2014; Lonthair et al., 2017). Much of the early work on the impacts of OA has focused on defining the detrimental impacts, and this still remains one of the most important focuses of climate change research. Specifically, reviews have synthesized various studies OA's impacts on behavior, development, and the acid-base regulatory machinery in several species of fish (Esbaugh, 2018; Heuer and Grosell, 2014), and it has become apparent that further work is needed to understand species resilience, adaptive capacity, and the physiological mechanisms defining the "winner's and loser's" of climate change (Kelly and Hofmann, 2013; Pfister et al., 2014). Teleost species that inhabit environments that exhibit natural fluctuations in CO_2 , likely act as a reservoir of resilient species, which would allow us to better investigate the above questions (Baumann et al., 2018b; Lonthair et al., 2017; Munday et al., 2016).

One of the most direct impacts of OA on teleosts is altered blood CO₂ chemistry (Esbaugh et al., 2012; Heuer et al., 2016b; Strobel et al., 2012). The subsequent metabolic compensation requires transporting H⁺ and HCO₃⁻ ions in and out of the body via acid-base regulatory pathways in the gill or skin (Evans et al., 2005b; Marshall and Grosell, 2006; Perry and Gilmour, 2006). The Na⁺/H⁺ exchangers (NHEs) have been proposed as the dominant route of acid excretion for marine fish, as the high Na⁺ concentration favors Na⁺ entry across the apical membrane (Claiborne et al., 2002; Evans et al., 2005b). Yet, our understanding of the role of NHEs in marine species is limited to localization and dynamic regulation experiments (Edwards et al., 2001; Edwards et al., 2005). More recent work, that has shown elevated levels of mRNA expression of VHA in response to elevated CO₂, has raised the possibility that VHA (V-type H⁺ ATPase) may also contribute to net acid excretion under elevated CO₂ conditions in marine teleosts (Allmon and Esbaugh, 2017; Michael et al., 2016). This would be similar to what occurs in freshwater fish (Perry et al., 2000; Perry et al., 2003b); however, this remains an open question. Furthermore, it should be noted that there is no evidence of translocation of VHA to apical membrane at any CO₂ level. Surprisingly, little is known about the development of these pathways in marine fish. The species with the most robust data sets (Mozambique tilapia and medaka) are best described as freshwater fish with seawater tolerance, as opposed to truly marine fishes (Ayson et al., 1994; Evans et al., 2005b; Hiroi et al., 1999; Hwang et al., 2011; Tseng et al., 2013), which limits the ability of researchers to extrapolate findings to the majority of marine fish.

On this background, this study sought to explore the development and plasticity of acid-base pathways in early life stages of a marine fish, and the implication of these pathways in species resilience to CO₂ stress. We used the economically important red drum (*Sciaenops ocellatus*) as a model for these studies, owing to the fact that they are spawned

offshore in full strength seawater yet regularly encounter high CO₂ during estuarine residence in the coastal estuaries of the Gulf of Mexico.

RESULTS

Survival in response to exposure to elevated pCO₂

Embryos exposed to elevated pCO₂ for 72 h exhibited significantly decreased survival at climate change relevant pCO₂ levels (One-way ANOVA; P<0.05; N = 8-26) (Figure 4.1). Surprisingly, no significant differences in survival were observed between exposure to 1400 µatm CO₂ and 12,000 µatm CO₂ exposure, with survival exceeding 50% even at the highest exposure.

Development of acid-base regulatory pathways

The relative gene expression of *nhe2* and *nhe3* plateaued at the earliest time point (12 hpf) and exhibited no changes across development. In contrast, *vha* (B subunit) showed consistent up-regulation until ~4 dpf (days post fertilization), after which the relative expression stabilized (One-way ANOVA; P<0.05; N = 6-8) (Figure 4.2a). Confocal microscopy found in excess of 640 ionocytes per mm² at the post-hatch time point (36 hpf), and density generally decreased throughout development. A significant decrease was observed by 10 dpf (N = 8) (Figure 4.2b), which coincides well with a qualitative assessment of gill development that began around 8 dpf. Note that the epithelial ionocytes co-localized for NKA and VHA (Figure 4.2c), as well as NKA and NHE3 (Figure 4.2d), which suggest that red drum have a single population of ionocytes, where VHA, NKA, and NHE3 are all colocalized together.

Impacts of hypercapnia on acid-base regulatory machinery

Acid-base plasticity was investigated in larval red drum after 24 h or 72 h of exposure to various $p\text{CO}_2$ levels. After 24 h of exposure only *nhe2* was significantly up-regulated, which occurred at 5,800 and 13,000 $\mu\text{atm CO}_2$ (One-way ANOVA; $P < 0.05$; $N = 8$) (Figure 4.3b), while we observed no alteration in *nhe3* (Figure 4.3c). Interestingly, *vha* was significantly down-regulated after exposure for 24 h to 13,000 $\mu\text{atm CO}_2$ (One-way ANOVA; $P < 0.05$; $N = 8$) (Figure 4.3a). We found no differences in gene expression after 72 h exposure (One-way ANOVA; $N = 8$) (Figure 4.3a-c). Similarly, ionocyte density was not altered in response to fish exposed for 72 h to any elevated $p\text{CO}_2$ level (One-way ANOVA; $N = 8$; data not shown).

Larval H^+ excretion

Note that very high acute $p\text{CO}_2$ exposures were used for these experiments to increase the resolution for detectable H^+ excretion. A first series of experiments measured $\Delta[\text{H}^+]$ at various locations along the body following acute exposure to a nominal 15,000 $\mu\text{atm CO}_2$. There was detectable net H^+ efflux at all areas tested; however, the yolk sac and pericardial area showed significantly higher excretion rates than other points (t-test; $P < 0.05$; $N = 8-9$) (Figure 4.5). As such, the yolk sac area was used for all subsequent experiments. The net H^+ efflux across the yolk sac area exhibited a dose-dependent relationship with $\mu\text{atm CO}_2$ (One-way ANOVA; $P < 0.05$; $N = 8-9$) (Figure 4.4b). When fish were exposed to high $p\text{CO}_2$ in the presence of EIPA, a known NHE inhibitor, they exhibited a significantly decreased $\Delta[\text{H}^+]$ as compared to vehicle-only controls (t-test; $P < 0.05$; $N = 6$) (Figure 4.4d). Similar results were found when exposed fish were treated with 10 μM bafilomycin, a known VHA inhibitor (t-test; $P < 0.05$; $N = 7$).

DISCUSSION

Larval fish exposed to elevated $p\text{CO}_2$ are solely dependent on metabolic acid-base compensation to maintain pH (Evans et al., 2005; Heuer and Grosell, 2014). As such, the early life sensitivity or resilience of fish to OA and other high CO_2 scenarios has been attributed to the relative capacity of acid-base pathways in early life (Esbaugh, 2018). Despite this assertion, there has been a paucity of studies specifically exploring the development and plasticity of these systems in marine fish – a fact made more relevant given the current concern relating to the detrimental effects of OA on marine life. The results of this study help to fill this crucial knowledge gap and support the hypothesis that animals native to habitats that regularly experience elevated CO_2 may have intrinsic physiological traits that confer resilience to OA and other high CO_2 scenarios. In this case, the estuarine-dependent red drum exhibits early onset of redundant acid-base homeostasis pathways that excrete H^+ in a dose-dependent fashion, with some indication of plasticity in the earliest time points.

As previously described, our survival data reinforce the idea that red drum demonstrate sensitivity to elevated $p\text{CO}_2$ at environmentally relevant partial pressures (Lonthair et al., 2017). Unexpectedly, a significant portion of the tested individuals were resilient to extremely high $p\text{CO}_2$, with approximately 50% of individuals surviving exposures of 12,000 $\mu\text{atm CO}_2$ (Figure 4.1). Early studies demonstrated severe survival consequences of OA, with a hallmark study on *Menidia beryllina* observing a 73% reduction in survival after exposure to 780 $\mu\text{atm CO}_2$ (Baumann et al., 2012). More recent work has supported that OA significantly decreases survival of ELS fish, but it is also clear that several species have a high degree of CO_2 tolerance (Esbaugh, 2018; Heuer and Grosell, 2014). Furthermore, many of the species that exhibit tolerance are native to estuarine and nearshore environments, which have high biological productivity, and thus

diel and seasonal fluctuations of 200-5000 $\mu\text{atm CO}_2$ are common (Caldeira and Wickett, 2003). A defined gradient also exists between these inshore highly productive areas and the stable $p\text{CO}_2$ conditions found in the open ocean (Duarte et al., 2013; Hofmann et al., 2011). Based on this natural gradient and recent research, Baumann (2019) has put forward the “Ocean Variability Hypothesis (OVH)”. The OVH states that marine organisms have adapted to the level of $p\text{CO}_2$ fluctuation present in their natural habitats, and if we assume that tolerance to elevated $p\text{CO}_2$ comes at a cost to the organism, species tolerance would decrease as you move from the nearshore environment to the open ocean environment. Exposure to elevated $p\text{CO}_2$ has been hypothesized to incite an elevated metabolic cost (Heuer and Grosell, 2016), but empirical evidence of this hypothesis is limited (Cattano et al., 2018; Esbaugh, 2018). It is possible that these costs are too small to be detectable in short-term exposures (Baumann et al., 2018b).

As hypothesized by the evolutionary rescue framework (Bell, 2013; Gonzalez et al., 2013), resilience to climate change related stressors will likely be predicated on existing traits or phenotypic plasticity. Here we suggest that the strong resilience to CO_2 in ELS red drum relates in part to both factors. As clearly shown, acid-base pathways are in place as early as 12 hpf, which is logical because metabolism is an acid-base stress, with a high density of epithelial ionocytes and stable expression of *nhe2* and *nhe3*. The *vha* (B subunit) exhibited a progressive up-regulation in gene expression until 84 hpf, which signifies that VHA-dependent pathways are in place early in development. It should be noted that both NHE2 and NHE3 are found in many cell types, and VHA is present throughout an organism. So, it is difficult to ascertain if the stable gene expression is the result of no changes in expression in gill epithelial ionocytes. The density of epithelial ionocytes decreased as development progressed, with a significant decrease occurring at the approximate onset of gill development, but confocal images did show that NKA, VHA,

and NHE3 are co-localized in the same cell type. Importantly, we were also able to validate ionocyte function following exposure to elevated CO₂ using a scanning ion electrode technique (SIET), which verified that H⁺ excretion did occur across the epithelium. As with work on other ELS fish, the highest rate of ion transport occurred at the yolk-sac (Lin et al., 2006; Liu et al., 2013). We observed Δ[H⁺] at yolk sac from .02 at control conditions to .072 after exposure to nominal 30,000 μatm. Similar excretion levels were observed in saltwater acclimated medaka exposed to a pH=8, although Δ[H⁺] ranged from .01 to .10 (Liu et al., 2013). More importantly, our data demonstrate that net H⁺ excretion responded to elevated CO₂ in a dose-dependent fashion. Overall, this collection of data indicate that red drum have a fully functional acid-base system that responds to CO₂ stress very early in their development.

Red drum reared under a series of elevated *p*CO₂ levels showed a dose-dependent increase in *nhe2* expression beginning at 5,800 μatm CO₂. Interestingly, this *p*CO₂ would represent the lowest test level beyond that typically found in the estuarine environment. These changes in gene expression were not coincident with significant alterations in ionocyte density (data not shown). Furthermore, the up-regulation in *nhe2* was only observed after 24 hpf, with red drum exposed for 72 h exhibiting no transcriptional changes. Also, of note is that neither *nhe3* nor *vha* exhibited up-regulation at either time point, and in fact, *vha* was significantly down-regulated following a 24 h exposure to the highest exposure level. The implications of this down-regulation is that extreme *p*CO₂ exposure could have a negative feedback on VHA. Unfortunately, red drum at 36 hpf are too small and delicate to subject to SIET, and thus we were unable to assess the effects of the observed plasticity on the rate of net H⁺ excretion. However, these data suggest red drum have a select window of sensitivity (≤ 36 hpf) that can be augmented through

phenotypic plasticity, and furthermore, that this plasticity manifest through only one of several possible routes of H⁺ excretion.

The data above clearly show that functional acid-base transporters and ionocytes are expressed in marine ELS fish, and that these fish show are capable of altering H⁺ excretion rates in respond to hypercapnia. We also we able to show that NHE2 gene expression is dynamically regulated by hypercapnia, but due to limitations on antibody availability we are unable to describe the location of this transporter in the ionocyte, although the literature hypothesizes that it is located on the apical membrane in NKA-rich ionocytes (Catches et al., 2006). Our final goal was to mechanistically link the expression of *nhe2*, *nhe3* and *vha* to the H⁺ excretion capacity of red drum using specific pharmacological blockers. Surprisingly, to our knowledge such validation is not available for fish with obligate marine life histories. In fact, the acceptance of *nhe2* and *nhe3* as the primary modes of acid excretion in adult marine fishes is based primarily on localization and the beneficial thermodynamic gradients (Catches et al., 2006; Edwards et al., 2005).

Here, we demonstrate that these pathways are functional in ELS red drum using the NHE specific inhibitor EIPA (200 μM) (Liu et al., 2013). As expected, EIPA resulted in an approximately 50% reduction in CO₂ induced acid excretion, as compared to the DMSO control. More surprising were the results obtained following bafilomycin A1 – a VHA specific inhibitor – exposure. While VHA is a well-known component of the H⁺ excretion pathways in freshwater fish, here we explore our hypothesis that VHA plays a role in H⁺ excretion in marine fish (Lin and Randall, 1993; Perry et al., 2000; Perry et al., 2003a). Here we demonstrate that exposure to 10 μM bafilomycin (10 min exposure) also reduced net H⁺ flux by 50%. It must be stated that the chosen concentration was on the significantly higher of those presented in the literature (Armstrong et al., 2018; Grosell and Wood, 2002) owing to solubility concerns in seawater. Yet 10 μM is also below the concentration where

bafilomycin would inhibit a significant portion of NKA (Bowman et al., 1998). In fact, 100 μM concentrations have been shown to be ineffective at inhibiting EIPA-sensitive H^+ excretion pathways (i.e. NHE and NKA dependent pathways) in freshwater medaka (Wu et al. 2010). Although, it must also be stated that VHA may be involved in other processes in eukaryotic cells, including: lysosomal macromolecule degradation, neurotransmission in synaptic vesicles, and vesicular trafficking (Beyenbach and Wieczorek, 2006). And while the standard caveats that accompany any study employing pharmacological agents as research tools must apply here (i.e. non-specific action), the available data supports a further investigation of the role of VHA in H^+ excretion, specifically with lower bafilomycin concentrations and another pharmacological inhibitor.

Assuming that the bafilomycin-sensitive H^+ excretion is due to VHA activity, the remaining question is why VHA would be required considering the beneficial thermodynamic conditions for NHE function? But it is important to remember that the relative alkaline seawater environment – as compared to the intracellular pH of an ionocyte – is also conducive to VHA function. In fact, previous work has shown that VHA is capable of transporting four H^+ per ATP at $\Delta\text{pH}=0$ (Kettner et al., 2003). The relative importance of VHA and NHE may reside in the cost of osmoregulation at the gills, which admittedly is difficult to address. Yet, a simple mass balance approach suggests that the NHE-mediated pathway may not yield the assumed energetic savings. A single NKA reaction cycle transports three Na^+ across the basolateral membrane, although alterations to this stoichiometry exist in some species (Esbaugh et al. 2019). Two of these Na^+ are excreted into the environment while one is transported back into the ionocyte via NKCC. The two Cl^- ions subsequently move through the apical membrane via CFTR. This mass balanced stoichiometry would suggest that a single ATP is capable of excreting two Na^+ and two Cl^- ions. While simplified, this analysis demonstrates that NHE function cannot be viewed

strictly on the premise that transport across the apical membrane does not require ATP. The incoming Na^+ adds to the osmoregulatory costs, which can be as high 0.5 ATP per Na^+/H^+ . Freshwater fish exhibit a wide range of functionally redundant acid-base pathways (Claiborne et al., 2002; Evans et al., 2005b; Hwang et al., 2011), so it seems reasonable that marine fish may also have evolved a number of distinct pathways capable to mitigating acid-base disturbances.

In conclusion, early life stage red drum have well-developed and plastic acid-base regulatory machinery, which likely contributes to their resilience to elevated $p\text{CO}_2$. To our knowledge, this is the first study to assess the ontogeny and hypercapnia response of acid-base pathways in a fish species with an obligate marine life history. The robust survival of red drum larvae to $p\text{CO}_2$ levels well in excess of OA combined with the evidence of plasticity and redundancy in acid-base homeostatic pathways provides support for the ocean variability hypothesis. While these data are encouraging with respect to the potential for estuaries and other “high CO_2 ” environments to act as a reservoir for tolerant species and genotypes in response to OA, caution should be used when extrapolating these findings to open ocean pelagic embryos. Furthermore, these data only relate to one of the many documented effects of OA. While it is tempting to suggest that tolerance in early life may correlate to a broader CO_2 tolerant phenotype, and in fact red drum have been shown to be behaviorally unaffected by CO_2 (Lonthair et al. 2017), more work is required before such conclusions can be made.

METHODS

Animal husbandry

All embryos were produced by captive red drum broodstock at the University of Texas Marine Science Institute (UTMSI) Fisheries and Mariculture Laboratory (FAML)

in Port Aransas, Texas and the Texas Parks and Wildlife – CCA Marine Development Center in Corpus Christi, Texas. Larvae were reared on-site at FAML under control conditions in 150 L conical tanks with flow through seawater and constant aeration. Temperature ($25.6\pm 0.7^{\circ}\text{C}$), salinity (36.9 ± 0.4 ppt), and pH (8.08 ± 0.02) measurements were collected daily, and total alkalinity measurements were collected every 2-3 days (2317.7 ± 22.3 $\mu\text{mol kg}^{-1}$). Temperature and salinity were measured using a WTW Cond 3310 meter with a WTW Tetracon 325 probe. pH was measured with a combination pH electrode, calibrated immediately before use, attached to an Orion Star A121 pH meter (Thermo Scientific). Total alkalinity (TA) was measured with an automated open cell Gran titration system (ASALK2; Apollo SciTech). $p\text{CO}_2$ (526.3 ± 33.1 $\mu\text{atm CO}_2$) was then calculated using the CO2SYS package (Lewis and Wallace, 1998).

CO₂ acclimation and survival assays

Embryos (12 hpf) were reared at controlled temperature and salinity in a low temperature diurnal illumination incubator (14:10 h light dark cycle; 25°C). Seawater was autoclaved and salinity corrected with either deionized water or instant ocean sea salt (Aquarium Systems Inc.). $p\text{CO}_2$ levels were achieved via established methods which uses the addition HCl and NaHCO_3 (Riebesell et al., 2010). Water samples were collected and analyzed (pH and TA) at the conclusion of all tests, and $p\text{CO}_2$ was calculated using CO2SYS (Table 4.1) (Lewis and Wallace, 1998). For survival assays per replicate at each of the five $p\text{CO}_2$ treatments 20 embryos were incubated in a 1L vacuum-sealed container. At the end of 72 h of exposure, unhatched and dead larval fish were removed, and surviving larvae were anesthetized using a buffered MS-222 solution (250mg l^{-1}) and counted.

Molecular methods

Embryos were exposed to elevated CO₂ using the methods described above, with the exception that tests were terminated at either 24 h or 72 h. All surviving larval fish per replicate were pooled and treated as n = 1. qPCR primers were previously developed for *eflα*, *nhe2*, *nhe3* and *vha* (B subunit) for red drum (Allmon and Esbaugh, 2017; Watson et al., 2014). All primers and GenBank accession numbers for related sequences can be found in Table 4.2. Total RNA isolation was performed using TriReagent according to manufacturer protocols and quantified using an ND-1000 spectrophotometer (Thermo Scientific). Total RNA was treated for potential DNA contamination by incubating with DNase 1 (Thermo Scientific), according to manufacturer protocols. cDNA synthesis was performed on 1 µg of total RNA using RevertAid M-Mulv reverse transcriptase (Thermo Scientific), according to manufacturer protocols. For all cDNA synthesis runs no reverse transcriptase controls were performed to test for genomic DNA contamination. Samples were diluted 10-fold using nuclease free water and stored at -20 °C until qPCR analysis.

qPCR analysis was performed using the Maxima SYBR Green kit (Thermo Scientific). Reactions were prepared according to the manufacturer's protocols with the exception that a 12.5 µl total reaction volume was used. All reactions were processed using an MX3000P qPCR machine (Stratagene) with accompanying software. A serial dilution was used for standard curves to determine the reaction efficiency of each primer pair. PCR efficiencies ranged from 85.3 to 101.1% with an $R^2 \geq 0.95$. For all genes, negative and no reverse-transcriptase control reactions were performed. The CT values for each sample were used to assess relative transcript abundance relative to the control gene *eflα* using the delta-delta CT method (Pfaffl, 2001). Note that *eflα* is a well-validated control gene for use in teleost fish that has been previously used in red drum (Allmon and Esbaugh, 2017; Esbaugh and Cutler, 2016; Esbaugh et al., 2016; Watson et al., 2014).

Samples collected for confocal microscopy were incubated with primary antibodies both for NKA α subunit (in 1:100 dilution in blocking buffer), and either VHA B subunit (in 1:200 dilution) or NHE3 (in 1:200 dilution). The primary polyclonal rabbit antibody for NKA (sc-28800) was obtained from the Santa Cruz Biotechnology and its effectiveness was verified (Allmon and Esbaugh, 2017). The primary monoclonal mouse antibody for VHA (sc-271832) was obtained from Santa Cruz Biotechnology and its effectiveness in red drum has been validated (Esbaugh and Cutler, 2016). The primary polyclonal rabbit antibody for NHE3 was custom made (GenScript) and its effectiveness in red drum was verified here based on the presence of a single 90 kDa band on gill protein Western blots (see Chapter 5). Following primary incubation, samples were washed and then incubated with secondary antibodies, goat anti-mouse Alexa Flour 488 [1:500] and goat anti-rabbit Alexa Flour 555 [1:500]. Samples were then washed and mounted using Vectashield hard-mount with DAPI and stored in the dark at 4 °C until imaged. Imaging was completed using established methods (Allmon and Esbaugh, 2017). Images were randomized to remove bias during analysis. Ionocyte density was determined by creating a 0.0625 mm² box over the yolk sac area and manually counting number of ionocytes using the ImageJ free software program.

Whole animal H⁺ excretion

The scanning ion-selective electrode technique (SIET) was used to measure H⁺ activity at the skin surface of larvae. Micropipettes were pulled, silanized, and filled using previous techniques (Lin et al., 2006; Liu et al., 2013). The ion-selective electrode was then connected to an operational amplifier (IA Amp ion polarographic amplifier; Applicable Electronics; East Falmouth, MA) via an Ag/AgCl wire electrode holder (World Precision Instruments). To calibrate the ion-selective probe, the Nernstian property of each

microelectrode were measured by placing the microelectrode in a series of standard solutions (pH 6, 7, and 10). By plotting the voltage output of the probe against the $\log[H^+]$ values, a linear regression yielded a Nernstian slope of 57.9 ± 0.23 (mean \pm SEM).

For all experiments, larvae were first exposed to elevated CO_2 for 2 h, in order to incite H^+ excretion. CO_2 exposures include 16883 ± 1167 and 26000 ± 935 $\mu\text{atm } CO_2$ (Table 4.1), with all pharmacological inhibition experiments occurring after exposure to 26000 ± 935 $\mu\text{atm } CO_2$. Larvae were anesthetized and positioned in the center of the chamber filled with recording medium at the same CO_2 / pH conditions. To measure the H^+ activity and pH at the surface of the larvae, the H^+ -selective probe was moved to the target position (~ 20 μm away from skin surface), voltages were recorded every 10 s over 3 min, and the median value was used to calculate the H^+ activity and pH. After recording at the skin surface, the probe was moved away from the skin (~ 1 cm), to record and calculate the background H^+ activity and pH. Before and after all measurements fish survival was confirmed via cardiac activity. In this study, $\Delta[H^+]$ was used to represent the H^+ gradient between the target position and background. The gradient reflects the integrated H^+ activity of skin cells near the target position (Liu et al., 2013).

The NHE inhibitor, EIPA (ethylisopropyl amiloride), was obtained from Fisher Scientific, and VHA inhibitor, Bafilomycin A1, was obtained from BioViotica. Stocks solutions were prepared by dissolving into DMSO (Fisher Scientific). The final concentration of DMSO in the working solutions (including the control group) was 0.1%. Larvae were incubated in 2 mL of exposure solution with either 10 μM bafilomycin A1 for 10 min or 200 μM EIPA for 1 h. Larvae were then transferred to recording medium that did not contain the inhibitor, which prevents the alteration of selectivity of the microelectrodes. Inhibitors were chosen based on previous work that details specificity

(Bowman et al., 1988; Masereel et al., 2003; Yoshimori et al., 1991) and concentration (Lin et al., 2006; Liu et al., 2013).

Statistical analysis

Data are reported as mean values \pm 1 standard error of the mean (SEM). All survival, gene expression, and ionocyte density data were evaluated using one-way ANOVA and Holm-Sidak post-hoc test. The statistical significance of effects of exposure to elevated $p\text{CO}_2$ on $\Delta[\text{H}^+]$ and the impacts of pharmacological inhibition on $\Delta[\text{H}^+]$ were evaluated using a one-tailed t-test. Where necessary, data transformation was completed to accommodate the assumption of normality and equal variance for parametric tests. If assumptions were not met, the equivalent non-parametric tests were employed. All statistical tests were carried out using SigmaPlot and a fiducial limit of significance of 0.05.

ACKNOWLEDGEMENTS

This work was funded by a National Science Foundation grant (EF 1315290) to AJE. Additional support for JKL was provided by the Coastal Conservation Association (CCA) Texas, University of Texas at Austin: Summer Recruitment Fellowship, and the University of Texas at Austin Marine Science Institute – Lund Endowment. Martin Tresguerres provided valuable insight and feedback during the development of this work. Red drum embryos were generously provided the Texas Parks and Wildlife CCA Marine Development Center in Corpus Christi, Texas. Elizabeth Allmon, Alexis Khursigara, Angelina Dichiera, Leighann Martin, Jeff Kaiser, and Cindy Faulk assisted in animal husbandry, larviculture, sample collection, and imaging. The authors have no conflicts of interest with respect to this work.

TABLES

Table 4.1: Water quality parameters for all early life stage CO₂ exposures. Data are mean \pm 1 SEM.

Experiment	Nominal pCO₂ (μatm)	N	Temp. (°C)	Salinity	pH_{NBS}	A_T (μmol/kg)	Calculated pCO₂ (μatm)
<i>Embryonic</i>	Control	25	24.6±0.1	34±1	8.31±0.04	2190±18	312±40
	1,000	22	24.8±0.1	34±1	7.69±0.01	2168±13	1380±38
	3,000	26	24.5±0.1	33±1	7.37±0.02	2220±26	3187±120
	6,000	8	24.7±0.2	30±1	7.16±0.06	2261±41	5518±532
	12,000	8	24.2±0.1	30±1	6.80±0.02	2253±35	12265±354
<i>SIET</i>	Control	17	26±0.2	34	8.47±0.04	2233±55	190±32
	15,000	15	27±0.1	34	6.68±0.04	2263±59	16883±1167
	30,000	18	25.3±0.2	33±0.06	6.44±0.02	2066±20	26000±935

FIGURES

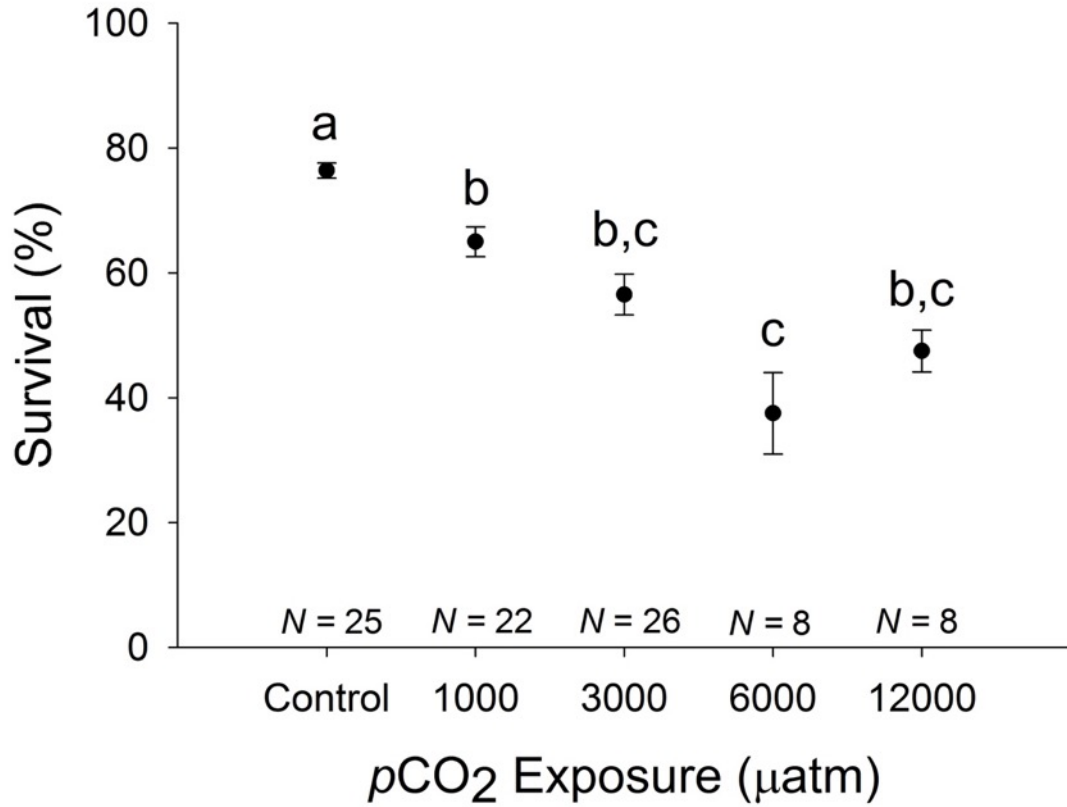


Figure 4.1: Mean (\pm SEM) survival of red drum (*Sciaenops ocellatus*) after 72 h exposure to nominal control, 1000, 3000, 6000, 12000 μatm CO₂. Sample size of each exposure group is annotated within the bar. A one-way ANOVA was used to analyze significant differences between treatment groups, with letters denoting significant differences ($P < 0.05$).

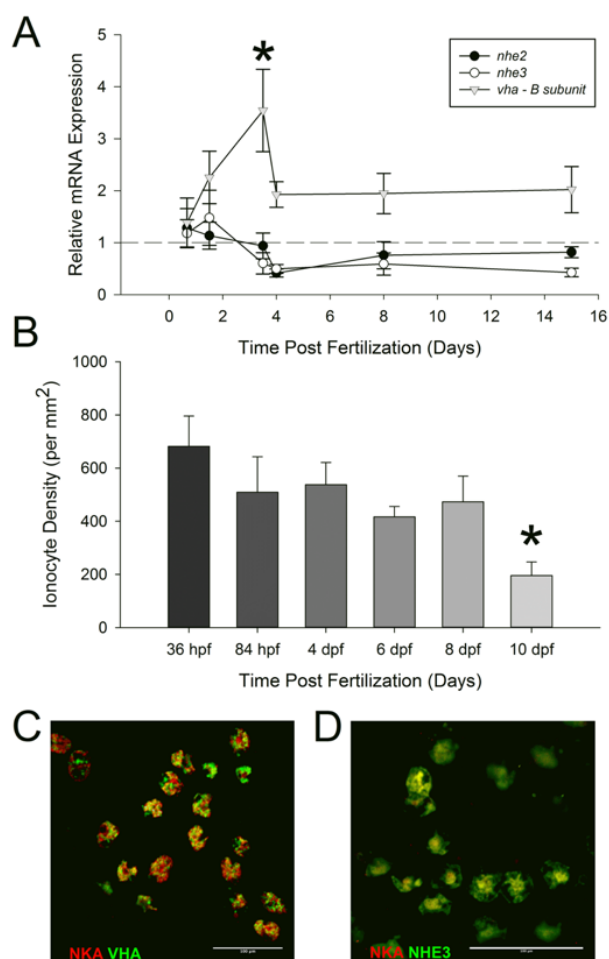


Figure 4.2: Development of acid-base regulatory pathways across early life stages of red drum (*Sciaenops ocellatus*). **(A)** Mean (\pm SEM) relative gene expression of acid-base regulatory pathways in red drum under control conditions at various time points across development. **(B)** Mean (\pm SEM) ionocyte density per mm² at various time points across development under control conditions in red drum (*Sciaenops ocellatus*). For both analyses, a one-way ANOVA was used to analyze differences from the initial time point (12 h), with significant differences denoted by an asterisk ($P < 0.05$; $N = 6-8$). Confocal microscopy images of red drum at 36 hpf. Larvae were stained with either NKA (red) and VHA (green) **(C)** or NKA (red) and NHE3 (green) **(D)**, with colocalization being perceived as yellow. A qualitative analysis of all photos taken found that colocalization of NKA with VHA and NHE3 is universal. A 100 μ m scale bar is included in each photo.

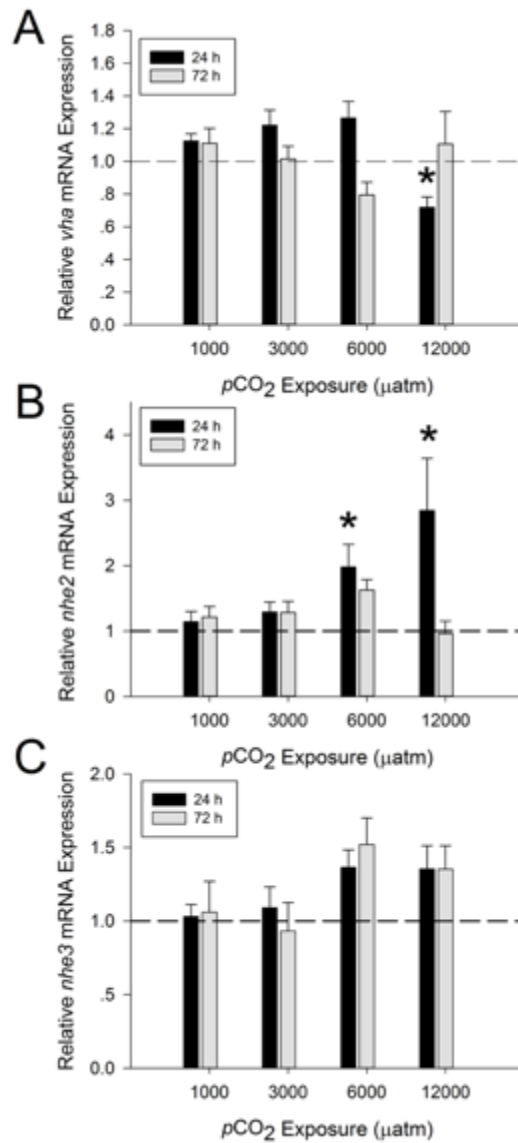


Figure 4.3: Mean (\pm SEM) relative gene expression of *vha* (A), *nhe2* (B), and *nhe3* (C) in red drum (*Sciaenops ocellatus*) after exposure to elevated $p\text{CO}_2$ for 24 h and 72 h. A one-way ANOVA was used to analyze differences from control $p\text{CO}_2$ exposure within an exposure time period, with significant differences denoted by an asterisk ($P < 0.05$; $N = 8$ per group).

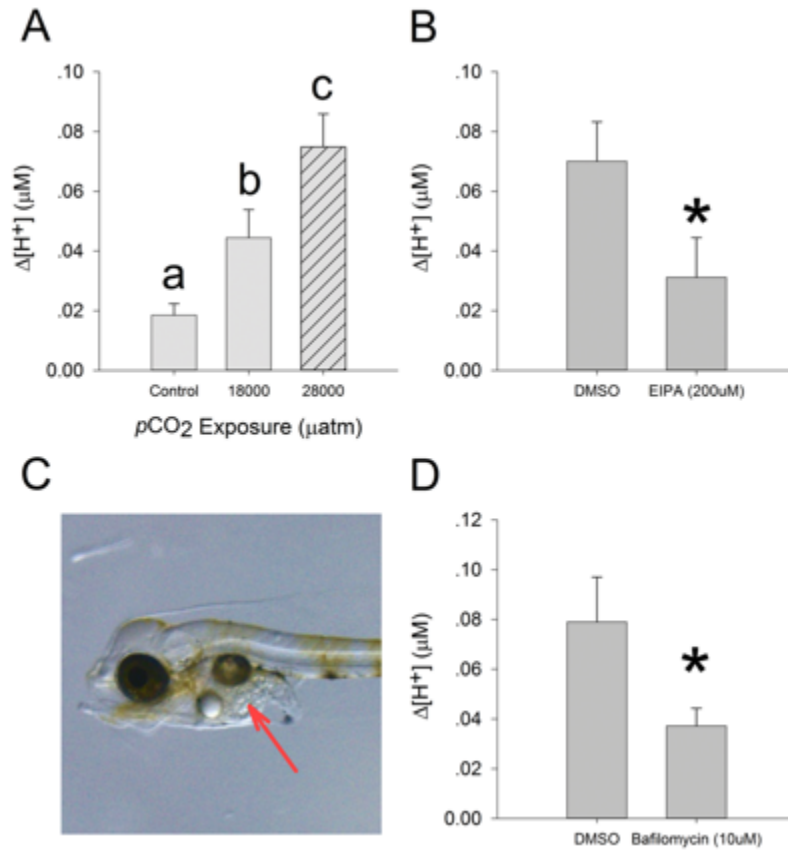


Figure 4.4: Mean (\pm SEM) $\Delta[H^+]$ (μM) of 72 hpf red drum (*Sciaenops ocellatus*) after exposure to both elevated pCO_2 and pharmacological inhibition. A one-way ANOVA was used to analyze the differences in $\Delta[H^+]$ (μM) after exposure to elevated pCO_2 , with a significant difference being denoted by an asterisk ($P < 0.05$; $N = 8-13$). Fish exposed to 28,000 μatm were also exposed to DMSO for 10 min to 1 h, following the acidosis exposure (A). A student t-test was used to analyze the differences in $\Delta[H^+]$ (μM) between 2 h hypercapnia exposed fish at 28,000 μatm , that have been either treated with 0.1% DMSO (Control) or 200 μM ethylisopropyl amiloride (EIPA) in 0.1% DMSO for 1 h (B) or 10 μM bafilomycin A1 in 0.1% DMSO for 10 min (D), with a significant difference being denoted by an asterisk ($P < 0.05$; $N = 6-7$). A microscope image of an 84 hpf red drum larvae, Red arrow indicates location of where $\Delta[H^+]$ were measured for all data shown in this study (C).

SUPPLEMENTARY INFORMATION

Methods

Preparing samples for confocal microscopy:

Prior to staining, larval samples were fixed overnight in Z-fix at 4°C. Samples were then washed 1 time with 100% methanol and then transferred to 100% methanol and stored at -20°C, this procedure constituted chill permeabilization of the sample.

SIET:

Pulling, silanizing, and filling microelectrodes

Borosilicate glass capillary tubes (B150-110-10; Sutter Instruments; San Rafael, CA) were pulled on a Sutter P-97 Flaming Brown pipette puller (Sutter Instruments; San Rafael, CA) into micropipettes with tip diameters of 3-4 μm . The micropipettes were then baked at 380°C overnight and then coated with Silanization Solution I (Sigma-Aldrich) for 10 min. The cover was then removed to allow fumes to dissipate, before being allowed to bake overnight again. The micropipettes were backfilled with a column of electrolytes, 100 mM NaCl, 10 mM NaOH, and 20 mM HEPES; pH 7.5, and frontloaded with a 20-30 μm column of liquid ionophore cocktail, hydrogen ionophore I cocktail (Sigma-Aldrich).

Preparing a recording medium:

The recording medium contained 350.9 mM NaCl, 45.7 mM $\text{MgCl}_2 \cdot 6\text{H}_2\text{O}$, 24.2 mM Na_2SO_4 , 8.9 mM $\text{CaCl}_2 \cdot 2\text{H}_2\text{O}$, 7.8 mM KCl, 2 mM NaHCO_3 , and 0.3 mg/L MS-222. pH values of the recording medium were altered using HCl and NaOH to mimic the exposure environment pH 8 for control $p\text{CO}_2$ exposure and pH 6.7 for high $p\text{CO}_2$ exposure.

Supplementary Tables

Table 4.2: List of primers used for real-time PCR. All sequences are 5' to 3' and reverse primers are reverse compliments of the genetic sequence.

Gene	Accession #	Reference	Orientation	Sequence
<i>ef1-a</i>	KJ958539	Watson et al., 2014	F	GTTGCTGGATGTCCTGCACG
			R	GTCCGTGACATGAGGCAGACTG
<i>vha</i>	KU899108	Allmon and Esbaugh, 2017	F	CCTACCATTGAGCGTATCATCA
			R	CGTAGGAGCTCATGTCAGTCAG
<i>nhe2</i>	KJ958540	Watson et al., 2014	F	CGGTTAAGCCTGATGGCCCTC
			R	TTGCAAACGAAGCCAGCAGC
<i>nhe3</i>	KJ958541	Watson et al., 2014	F	CAAGGTGCAGACCTTCACGCTG
			R	ACGAGGATGGCTCCCATGTT

Supplementary Figures

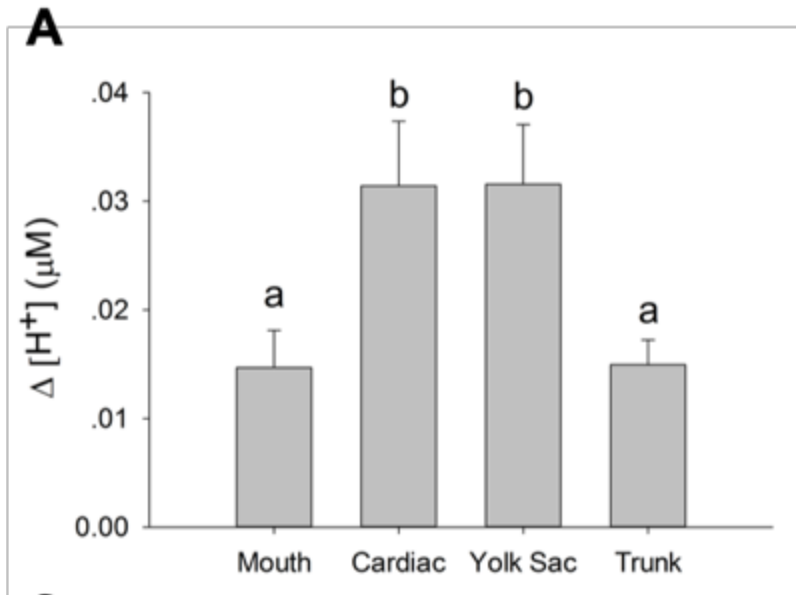


Figure 4.5: Mean (\pm SEM) $\Delta[H^+]$ (μM) of 72 hpf red drum (*Sciaenops ocellatus*) across the various locations across the body. A one-way ANOVA was used to analyze the difference in $\Delta[H^+]$ (μM) at different locations, with significant differences being denoted by lower case letter ($P < 0.05$; $N = 8-9$).

Chapter 5: Mechanisms of acid-base regulation following respiratory alkalosis in red drum (*Sciaenops ocellatus*)

AUTHORS

Joshua Lonthair*, Angelina M. Dichiera, Andrew J. Esbaugh

Marine Science Institute, University of Texas at Austin, Port Aransas, TX, 78373,
USA

*Corresponding author: tel: +1 361 749 6827; fax +1 361 749 6749; e-mail:
jlonthair@utexas.edu⁴

ABSTRACT

Respiratory acidosis and subsequent metabolic compensation are well-studied processes in fish exposed to elevated CO₂ (hypercapnia). Yet, such exposures in the marine environment are invariably accompanied by a return of environmental CO₂ to atmospheric baselines. This understudied phenomenon has the potential to cause a respiratory alkalosis that would necessitate base excretion. Here we sought to explore this question and the associated physiological mechanisms that may accompany base excretions using the red drum (*Sciaenops ocellatus*). As expected, when high *p*CO₂ (15,000 μatm CO₂) acclimated red drum were transferred to normal *p*CO₂ their net H⁺ excretion shifted from 0.157 ± 0.044 to -0.606 ± 0.116 μmol g⁻¹ h⁻¹ in the 2 h post-transfer period. Net H⁺ excretion returned to control rates during the 3 to 24 h flux period. Gene expression and enzyme activity assays demonstrated that while the acidosis resulted in significant changes in carbonic anhydrase enzymatic activity, Na⁺/K⁺ ATPase enzymatic activity, V-type H⁺ ATPase (VHA) gene expression, and Na⁺/H⁺ Exchanger 3 gene expression, no

This work was conceived by J.L, A.M.D. and A.E. Experiments and data collection were completed by J.L. and A.M.D. Specifically, A.M.D. provided expert support in the measurement of carbonic anhydrase. J.L. completed data analysis and interpretation. J.L. wrote the manuscript with editing and support from A.E. and A.M.D. A.E. provided support and supervision for the project.

significant changes accompanied the alkalosis exposure. Confocal microscopy was used to assess both acidosis and alkalosis-stimulated translocation of VHA to the basolateral membrane; however, no apparent translocation was observed. Overall, these data demonstrate that fluctuations in environmental CO₂ result in both acidic and alkalotic respiratory disturbances; however, red drum maintain sufficient regulatory capacity to accommodate base excretion. Furthermore, this work does not support a role for basolateral VHA translocation in metabolic compensation from a systemic alkalosis in teleosts.

INTRODUCTION

Acid-base balance is a fundamental homeostatic process that is required to maintain proper cellular function. The simplest description of this process is the ability of organisms to manipulate H⁺, HCO₃⁻ and CO₂ concentrations in the intracellular and extracellular compartments to defend metabolic or respiratory pH disturbances (Evans et al., 2005b; Marshall and Grosell, 2006; Perry and Gilmour, 2006). Metabolic disturbances refer to those that arise from the metabolic production of acid-base equivalents. The two most common examples are exercise and digestion, which produce metabolic acidosis and alkalosis, respectively. Respiratory disturbances occur when changes in the environment or ventilation rate result in an altered plasma partial pressure of CO₂ (*p*CO₂), which subsequently impacts pH (Evans et al., 2005a; Marshall and Grosell, 2006; Perry et al., 2009). Respiratory acidosis is particularly common in organisms inhabiting aquatic environments owing to the fact that many act as CO₂ sources or are impacted by up-welling (Cai et al., 2011; Caldeira and Wickett, 2003; Feely et al., 2010). In fish, this area of research has been buoyed in recent years owing to the interest in ocean acidification, which causes a mild respiratory acidosis and subsequent metabolic compensation (Esbaugh, 2018; Esbaugh et al., 2016; Esbaugh et al., 2012; Heuer and Grosell, 2016; Jutfelt and

Hedgarde, 2013; Strobel et al., 2012). Conversely, research into the organismal responses to a respiratory alkalosis is far less prominent. This form of acid-base disturbance is particularly relevant in coastal estuarine environments, sea grass habitats and coral reefs that experience daily fluctuations in ambient $p\text{CO}_2$. Put simply, a fish that metabolically compensates to a respiratory acidosis will experience a respiratory alkalosis when ambient $p\text{CO}_2$ falls to normal conditions.

In fish, most acid-base disturbances are compensated metabolically through the exchange of acid-base equivalents between the blood and environment via ionocytes found in the gills (Evans et al., 2005a; Marshall and Grosell, 2006; Perry et al., 2009). This organ accounts for at least 90% of acid-base transport (Claiborne et al., 2002). An acidosis is corrected by apical net acid (H^+) excretion, and parallel basolateral HCO_3^- uptake into the plasma. In seawater fish, the dominant apical transporters are thought to be Na^+/H^+ exchanger 2 and 3 (NHE2 and NHE3), which use the high Na^+ concentration in seawater to facilitate H^+ excretion (Allmon and Esbaugh, 2017; Claiborne et al., 1999; Claiborne et al., 2008; Edwards et al., 2001; Edwards et al., 2005). Cytosolic carbonic anhydrase (CAc) plays a critical role by catalyzing CO_2 hydration to produce HCO_3^- and H^+ , which provides the necessary acid-base equivalents for transport (Esbaugh et al., 2005; Georgalis et al., 2006; Gilmour et al., 2009). The $\text{Na}^+/\text{HCO}_3^-$ co-transporter (NBC) is localized on the basolateral membrane and is thought to be the primary mechanism for HCO_3^- uptake into the plasma (Perry et al., 2003a); however, other anion exchangers have also been implicated (Liu et al., 2016). The mechanisms by which marine teleosts excrete base are less well established; however, such information is available for sharks and hagfish. In these organisms metabolic alkalosis results in V-type H^+ ATPase (VHA) translocation to the basolateral membrane (Roa et al., 2014; Tresguerres et al., 2007b). VHA works in tandem with plasma accessible carbonic anhydrase IV (CA IV) to dehydrate plasma HCO_3^-

into CO₂ for excretion (Esbaugh et al., 2009; Gilmour et al., 2007a; Gilmour and Perry, 2004; Gilmour et al., 2001; McMillan et al., 2019), or recycling into the ionocytes where HCO₃⁻ is apically excreted via pendrin (Roa et al., 2014). To our knowledge, VHA translocation following an alkalosis has yet to be verified in teleost models, and in fact previous work in red drum has shown VHA mRNA up-regulation following exposure to elevated *p*CO₂, which is suggestive of a role in H⁺ excretion (Allmon and Esbaugh, 2017).

On this background, this study first sought to explore the whole animal acid-base flux responses to a respiratory alkalosis following exposure to, and compensation from, a respiratory acidosis. A second objective was to explore the branchial plasticity that may accompany respiratory alkalosis, as well as the preceding respiratory acidosis, using a combination of gene expression, enzyme activity assays and immunofluorescence microscopy. We hypothesized that red drum would quickly respond to a respiratory alkalosis via net base efflux across the gill. Furthermore, we hypothesized that exposure to a severe respiratory alkalosis would result in significant increases in the activity of relevant proteins including CA, VHA and Na⁺/K⁺ ATPase (NKA). Finally, we hypothesized that a respiratory alkalosis would stimulate basolateral translocation of VHA.

METHODS

Animal handling

Sub-adult red drum were collected from Ekstom Aquaculture, LLC in El Campo, Texas. Fish were housed in recirculating systems with UV treated natural seawater collected from the Port Aransas ship channel with intermittent partial renewal. All tanks were aerated, and ammonia was controlled by circulating water through a biofilter. Temperature was controlled using automated in-line heater/chiller units. *p*CO₂ was kept low through regular partial water replacement using ancillary flow-through lines. All fish

were held on a 14 h:10 h light dark cycle. Fish were fed daily with commercially available Aquamax pelleted dry food, and fish were acclimated to control conditions in the facility for a minimum of two weeks prior to experimentation. All experiments were conducted in accordance with protocols approved by the University of Texas at Austin Institutional Animal Care and Use Committee.

Experimental design

Figure 5.1 illustrates the methodology used in this study to incite a respiratory alkalosis. Fish were first exposed to elevated $p\text{CO}_2$ for 16 h, which is sufficient time for red drum to compensate for the initial respiratory acidosis by increasing plasma $[\text{HCO}_3^-]$ (Allmon and Esbaugh, 2017). Fish were then transferred to control seawater that would result in rapid off gassing of the elevated plasma $p\text{CO}_2$, which would raise plasma pH owing to the elevated plasma $[\text{HCO}_3^-]$. Control fish were put through the same tank transfer protocols; however, the $p\text{CO}_2$ of water was held constant at control conditions. Whole animal acid flux experiments were performed only during the final respiratory alkalosis phase of the experimental design. Tissue samples were collected from both control and treated fish following the 16 h acidosis phase, as well as 2 h (series 1) or 24 h (series 2) after the onset of the respiratory alkalosis phase. Mean fish mass across all groups was 18.0 ± 0.4 g ($n = 64$) with no significant differences between experimental groups. Prior to sampling, animals were euthanized using buffered MS-222 (250 mg L^{-1}) followed by spinal transection, after which the gills were perfused and dissected out of the animal. Samples for gene expression and enzyme analysis were stored at -80°C , while microscopy samples were immediately subjected to a fixing protocol (described below) and stored in 70% ethanol at room temperature.

Water quality was measured before and after all experimentation. Temperature and salinity were measured using a WTW 3310 conductivity meter with a WTW Tetracon 325 probe. pH was measured with a combination pH electrode, calibrated immediately before use, and attached to an Orion Star A121 pH meter (Thermo Scientific). Total alkalinity (TA) was measured with an automated open cell Gran titration system (ASALK2; Apollo SciTech). $p\text{CO}_2$ was then calculated using the CO2SYS package (Lewis and Wallace, 1998) using the CO_2 constants from Mehrbach et al., 1973 refit by Dickson and Millero, 1987, and the pHNBS scale. Ammonia concentrations were measured in each replicate using a colorimetric assay (Verdouw et al., 1978).

Whole animal acid flux measurements

Food was withheld from red drum for 24 h prior to and throughout the experiment to avoid digestive influences on acid-base regulation. In series 1, fish were placed into either a control (nominal 500 $\mu\text{atm } p\text{CO}_2$; $n = 8$) or hypercapnia (nominal 15,000 $\mu\text{atm } p\text{CO}_2$; $n = 8$) treatment for 16 h. After exposure, fish were transferred to individual static chambers (550 mL) with control seawater (salinity 34 ppt, temperature 23 °C, pH 8.06). In series 1, an initial water sample was taken 15 min after introduction to the chamber and a final sample was collected 2 h after introduction to the chamber. In series 2, fish were treated as above with the exception that water samples were collected at 15 min, 3 h, and 24 h after introduction to the flux chamber. All samples were measured for pH immediately after collection, as described above. A subset of each sample was frozen at -20°C until analysis as described above. Water samples subject to TA treatment were bubbled with N_2 for 15 min prior to analysis to remove the contributions of metabolically produced CO_2 . Net H^+ excretion rate was then calculated as previously described (Allmon and Esbaugh 2017).

Gene expression

Real time PCR primers were previously developed for *efl α* , *ca-c*, *nbc*, *nhe3*, and *vha* (B subunit) for red drum (Allmon and Esbaugh, 2017; Watson et al., 2014). All primers and GenBank accession numbers for related sequences can be found in Table 5.1. Total RNA isolation was performed using TriReagent according to manufacturer protocols and quantified using an ND-1000 spectrophotometer (Thermo Scientific). Total RNA was treated for potential DNA contamination by incubating with DNase 1 (Thermo Scientific), according to manufacturer protocols. cDNA synthesis was performed on 1 μ g of total RNA using RevertAid M-Mulv reverse transcriptase (Thermo Scientific), according to manufacturer protocols. No reverse transcriptase controls were performed to test for genomic DNA contamination for all cDNA synthesis batches. Samples were diluted 10-fold using nuclease free water and stored at -20°C until qPCR analysis.

qPCR analysis was performed using the Maxima SYBR Green kit (Thermo Scientific). Reactions were prepared according to the manufacturer's protocols with the exception that a 12.5 μ l total reaction volume was used. All reactions were processed using an MX3000P qPCR machine (Stratagene) with accompanying software. A serial dilution was used for standard curves to determine the reaction efficiency of each primer pair. PCR efficiencies ranged from 85.3 to 101.1% with an $R^2 \geq 0.95$. For all genes, negative and no reverse-transcriptase control reactions were performed. The CT values for each sample were used to assess relative abundance of each gene in relation to the control gene *efl α* using the delta-delta CT method (Pfaffl, 2001). Note that *efl α* is a well-validated control gene for use in teleost fish that has been previously used in red drum.

Enzymatic activity

Carbonic anhydrase activity was measured using the electrometric delta pH method (Henry, 1991; Henry et al., 1993). Gill filaments were cut from the arch and homogenized in buffer medium (225 mM D-mannitol, 13 mM Tris Base, 75 mM sucrose) at a 1:800 dilution. A 50 μ L aliquot of each sample was added to 5 mL of buffer medium (225 mM D-mannitol, 13 mM Tris Base, 75 mM sucrose) held at 4°C, and 200 μ L of CO₂ saturated deionized water was injected into the medium using a Hamilton syringe. The reaction velocity was measured over a 0.15 pH change, and each sample was measured in triplicate. The uncatalyzed reaction rate (the rate of pH change for CO₂ distilled water only) was subtracted from the observed rate to obtain the true catalyzed reaction rate. The buffer capacity of the medium was used to convert the rate from pH units min⁻¹ to mol H⁺ min⁻¹. CA activity was standardized by protein content (mol H⁺ min⁻¹ mg⁻¹ protein) measured via Coomassie Plus™ (Bradford) Assay Kit (Thermo Scientific).

Measurement of Gill Na⁺/K⁺ ATPase (NKA) activity and V-type H⁺ ATPase (VHA) activity was performed as previously described (Chowdhury et al., 2016; Gilmour et al., 2007b; McCormick, 1993). 5 mM sodium azide was used to inhibit background and mitochondrial ATPase activity, 500 μ M ouabain was used to target NKA, and 1 mM N-Ethylmaleimide (NEM) was used to target VHA. NKA activity was calculated as the difference between ouabain + sodium azide versus only sodium azide. VHA was calculated as the difference between ouabain + sodium azide versus the combination of all three inhibitors. The activity is expressed as mM of ADP mg protein⁻¹ h⁻¹ with protein concentration determined as described above.

Immunohistochemistry

After collection at both 2 h alkalosis and 24 h alkalosis gill samples were fixed by placing them into Z-fix solution overnight, and then transferred to 70% ethanol for long-term storage. Prior to staining, samples were dehydrated by 1) three washes with 95% ethanol for 60 min; 2) three washes with 100% ethanol for 45 min; 3) a 1 h butanol wash followed by an overnight soak in butanol. Samples were then washed twice for 90 min in Histochoice clearing agent. Two paraplast washes were then conducted at 58 °C for 1 h before samples were set in paraffin and allowed to harden at room temperature. Samples were then stored at 4 °C until sectioning. Samples were sectioned at 10 µm using a microtome and mounted onto Superfrost Plus slides where they were rehydrated, deparaffinized and soaked in DI water until ready to stain. Each slide contained two sections so that no-primary antibody controls could be run concurrently with each sample. Antigen recovery was performed by heating slides in boiling 10 mM citrate buffer solution three times for 5 min. Hydrophobic barriers were drawn around each sample and samples were washed in blocking buffer (PBST with 5% fetal calf serum) twice for 5 min. Samples were then incubated with either primary antibodies for NKA [1:1000] and VHA [1:200], or for NHE3 [1:200] and VHA [1:200] at 4 °C overnight. The primary polyclonal rabbit antibody for NKA (sc-28800) was obtained from Abcam Biotechnology and its effectiveness in red drum was previously validated (Allmon and Esbaugh, 2017). The primary monoclonal mouse antibody for VHA (sc-2713832) was obtained from Santa Cruz Biotechnology and its effectiveness in red drum had previously been validated (Esbaugh and Cutler, 2016). The primary polyclonal rabbit antibody for NHE3 was custom made (GenScript) and its effectiveness in red drum was verified here based on the presence of a single 90 kDa band on a gill protein western blot (see below). Following primary incubation, samples were washed in blocking buffer three times for 5 min, then incubated

with secondary antibodies – goat anti-rabbit Alexa Flour 555 [1:500] and goat anti-mouse Alexa Flour 488 [1:500] (Life Technologies) – in the dark for 1 h. Samples were washed with blocking buffer three times for 5 min, stained with Sudan Black for 20 min to eliminate autofluorescence, and washed in PBS for 10 min. Finally, samples were washed with blocking buffer three times for 5 min and mounted using Vectashield with DAPI and stored in the dark at 4 °C until imaged. Imaging was completed using a Nikon C2+ confocal microscope system with a Nikon Eclipse Ti-E inverted microscope at 600x magnification and utilizing NIS-Element imaging software for image acquisition, processing, and analysis. 8-10 images were taken from a minimum of three unique gills per treatment (acidosis, alkalosis, and control) to complete a qualitative analysis of VHA localization. Further analysis of apical membrane width and basolateral membrane width was completed using ImageJ. All images were also assessed for apical and basolateral membrane width, with measurements taken per image.

NHE3 antibody validation

The primary polyclonal antibody for NHE3 was custom made (GenScript) and thus its effectiveness and specificity in red drum was verified via a western blot (Figure 5.5). A western blot was completed using standard procedures as previously described for our lab (Esbaugh and Cutler, 2016). A primary antibody concentration of 1:400 in blocking reagent was tested against 5 and 10 µg of gill protein (multiple individuals). Protein was prepared from fresh gill using RIPA buffer and quantified using a bicinchoninic acid protein assay. A horse radish peroxidase (HRP) conjugated anti-rabbit secondary antibody (1:10,000 in blocking reagent) in combination with the Clarity HRP substrate kit (Bio-Rad) were used for protein detection. Briefly: 1) membranes were blocked with 5% skim milk powder in PBS for 2h at room temperature, 2) an overnight primary antibody incubation at 4°C, 3) 5

PBS washes, 4) 1 h secondary antibody incubation, and 5) 5 PBS washes, followed by detection.

Statistical analysis

Data are reported as mean \pm standard error of the mean (SEM). All data sets were evaluated for statistically significant differences using a two-way analysis of variance (ANOVA) with time and treatment as variables. In cases where an ANOVA indicated that significant difference existed, post hoc multiple comparison tests (Holm-Sidak method) were applied to identify the differences among individual means. All statistical tests were carried out using SigmaPlot and a fiducial limit of significance of 0.05.

RESULTS

Whole animal flux

Red drum exposed to hypercapnic conditions (15,000 μ atm) for 16 h and transferred to normocapnic waters (i.e. respiratory alkalosis) exhibited significantly different net H^+ excretion rates after 2 h and 3 h than fish that were maintained at normocapnic conditions (Figure 5.2). Negative H^+ excretion results indicate net base secretion (H^+ uptake or HCO_3^- excretion). In individuals exposed to a respiratory alkalosis, net H^+ uptake was significantly elevated at 0 - 2 h (series 1) and 0 - 3 h (series 2) post transfer, with the highest uptake rates observed for the 0 - 3 h flux period for series 2 fish. The final 3 - 24 h flux period showed that net H^+ excretion rates were comparable to those of control fish.

Phenotypic differences in control fish

Both gene expression and enzyme analysis demonstrated significant differences between fish batches used for series 1 and series 2 (Figure 5.3 and 5.4). The fish gills used

for series 2 experiments had significantly higher expression values for all measured genes, which included *nhe3*, *vha*, *ca-c* and *nbc*. The differences in expression ranged from approximately 3x for *ca-c* and *vha* to almost 20x for *nhe3*. Furthermore, CA activity in the gills of series 2 fish was almost double that of fish in series 1, while VHA and NKA activity was elevated by approximately 4x and 8x, respectively.

mRNA Expression and Enzymatic Activity

Given the observed differences in control fish from series 1 and series 2, the two experimental series were analyzed separately. The gene expression results for series 1 fish showed no effects at the 16 h post-acidosis time point or the 2 h post-alkalosis time point for *ca-c* (Figure 5.3a), *nhe3* (Figure 5.3b), and *nbc* (Figure 5.3c). Interestingly, a significant up-regulation of *vha* (B subunit) mRNA was observed at the 16 h post-acidosis time point; however, this mRNA returned to control condition by the 2 h post-alkalosis time point. These data are generally corroborated by the enzyme analysis with no effects of either treatment on NKA (Figure 5.4a) or VHA activity (Figure 5.4b). CA activity exhibited a significant elevation at the 16 h post-acidosis time point, and the activity did not return to control condition at the 2 h post-alkalosis time point.

The gene expression results for series 2 fish exhibited a greater variety of responses to exposure to an acidosis and an alkalosis. Expression of *ca-c* was unaffected at 16 h post-acidosis and 24 h post-alkalosis (Figure 5.3a). A significant down-regulation of *nhe3* mRNA was observed at the 16 h post-acidosis time point, and the mRNA did not return to control condition by the 24 h post-alkalosis time point (Figure 5.3b). A significant down-regulation of *nbc* mRNA was also observed at the 24 h post-alkalosis time point, but a significant down-regulation was also observed in the time matched control group (Figure 5.3c). A significant up-regulation of *vha* (B subunit) mRNA was observed at the 24 h post-

alkalosis time point, but again a significant up-regulation at the time matched control was also observed (Figure 5.3d). Enzymatic activity data followed a generally similar pattern. VHA activity exhibited no effect of either treatment (Figure 5.4b), while NKA and CA activity exhibited a significant decrease at the 16 h post-acidosis time point. The activity remained significantly decreased at the 24 h post-alkalosis time point.

Protein localization and translocation

Immunofluorescence analysis was used to determine if VHA translocated to the apical or basolateral membrane in response to an acidosis or alkalosis, respectively. NHE3 and NKA were used as indicators of apical and basolateral localization, respectively. Note that the NHE3 antibody was first validated by western blot (Figure 5.5), and also results in expected apical localization in gill ionocytes. These co-localization studies demonstrated that VHA, NKA and NHE3 show complete co-localization within a single ionocyte type. No occurrences of translocation in either direction (Figure 5.5) as a result of an acid-base disturbance was observed in either experimental series. The cellular localization of VHA was largely cytoplasmic as compared to NHE and NKA after a 16 h acidosis and a 2 h or 24 h alkalosis. A quantitative analysis of NHE3 signal width in response to an acidosis was performed as a proxy for apical microvilli depth. No significant differences in apical microvilli depth were observed between the three groups: control ($6.5 \pm 1 \mu\text{m}$; $n = 8$), acidosis ($5.4 \pm 0.2 \mu\text{m}$; $n = 8$), and alkalosis ($6.7 \pm 0.6 \mu\text{m}$; $n = 8$).

DISCUSSION

It is becoming increasingly recognized that many marine habitats, including sea grasses, estuaries and coral reefs, experience daily fluctuation in $p\text{CO}_2$ (Cai et al., 2011; Caldeira and Wickett, 2003; Feely et al., 2010). While this phenomenon has been getting

attention with respect to hypercapnia tolerance and ocean acidification (Baumann, 2019; Browman, 2017; Esbaugh, 2018; Heuer and Grosell, 2014), the full scope of acid-base consequences on fish endemic to these fluctuating CO₂ habitats has yet to be thoroughly addressed. Of particular importance is the counter-intuitive consequences of high CO₂ returning to normal conditions, which can result in a significant increase in plasma pH if animals have elevated plasma HCO₃⁻ to compensate for the high *p*CO₂ (Figure 5.1). The data presented here suggests that red drum, a species native to the coastal estuaries of the Gulf of Mexico, exhibit rapid and significant net base efflux in response to this respiratory alkalosis. Furthermore, the results presented here suggest that red drum are capable of quickly offsetting extreme fluctuations without changes to their baseline phenotype.

Previous work on red drum has suggested they are very effective acid-base regulators (Allmon and Esbaugh, 2017; Lonthair et al., 2017); however, such work has primarily focused on responses to an acidosis. Here we show that when fish are exposed to a respiratory alkalosis, they quickly respond by excreting base into the environment. More specifically, a respiratory alkalosis following a decrease in *p*CO₂ of approximately 15,000 μatm resulted in net HCO₃⁻ excretion of at least 0.61 μmol g⁻¹ h⁻¹ during the first 2 h post-transfer. Interestingly, the fish used for series 2 showed even greater excretion rates (1.16 μmol g⁻¹ h⁻¹) during the first 3 h post-transfer. While these rates are substantially higher than control fish, which showed approximately 0.1 μmol g⁻¹ h⁻¹ acid excretion, they are only 10 to 25% of those reported for an equivalent respiratory acidosis-type disturbance. For example, Allmon and Esbaugh (2017) observed mean net H⁺ excretion rates of 4 μmol g⁻¹ h⁻¹ in the first 2 h post-exposure to 15,000 μatm CO₂. Yet, our results are comparable to prior work investigating metabolic alkalosis via chronic or acute infusion of NaHCO₃, which have described net HCO₃⁻ excretion rates of ~0.3 μmol g⁻¹ h⁻¹ (Gilmour et al., 2007b; Goss and Perry, 1994).

One explanation for the discrepancy between acid and base excretion rates is that an alkalosis is not as physiologically severe as an acidosis, and thus fish have less cellular machinery dedicated to an alkalosis, although this is difficult to confirm with blood acid-base data. In this scenario base excretion would remain elevated for a longer duration than acid excretion when exposed to a respiratory stress of similar magnitude. Our data are equivocal on this point as the base excretion rates in the post 3 h interval of series 2 were similar to those observed in the opening 2 h of the series 1 exposures. However, the post 3 h interval was also not statistically different from the time matched control group, and this comparison seems most pertinent. This data would suggest that the alkalosis is largely compensated prior to 3 h, despite the much lower base excretion rates as compared to acid excretion rates. To reconcile these observations, we must consider the role of the intestine in acid-base regulation (Taylor et al., 2011). It seems probable that a respiratory alkalosis stimulates elevated intestinal transcellular HCO_3^- secretion (Heuer et al., 2012; Heuer et al., 2016a; Taylor et al., 2010); a phenomenon that has been observed following metabolic disturbances related to digestion in other species (Taylor et al., 2011; Taylor et al., 2007). While our whole animal acid-base flux measurements theoretically consider rectal base excretion, there remains the possibility of a significant lag time for the release of luminal fluid as well as the potential that much of the rectal base secretion may be in the unquantified precipitate fraction (Wilson et al., 2009). Future work on respiratory alkalosis should target the dynamic role of the intestine in a role akin to the freshwater fish kidney.

Series 1 experiments were intended to target the phenotypic plasticity that may occur in coordination with the highest rates of net base excretion. Interestingly, we observed few changes in transcriptional expression as a result of the 16 h exposure to hypercapnia (15,000 $\mu\text{atm CO}_2$) or the subsequent 2 h respiratory alkalosis. The lone significant up-regulation occurred for *vha* (B subunit) mRNA after 16 h exposure to

hypercapnia. This supports previous work in red drum that observed up-regulation of *vha* 24 h after exposure to 6,000 or 30,000 $\mu\text{atm CO}_2$ (Allmon and Esbaugh, 2017), and seems to suggest a role in acid excretion as opposed to net base excretion. Yet, this finding is tempered by the fact that VHA enzymatic activity, as well as NKA activity, was unaffected by either acid-base disturbance. Conversely, a significant increase in CA activity was observed after 16 h exposure to elevated $p\text{CO}_2$, with enzymatic activity levels remaining significantly elevated after 2 h of alkalosis. Overall these data suggest that dynamic regulation of acid-base transporters in the gill is more tightly linked to an acidosis with little to no effect of a respiratory alkalosis. On-going work in our lab is attempting to extend these results to the relevant *slc26* anion exchangers in the gills; the role of which remains poorly understood in marine fishes.

Series 2 experiments sought to target the phenotypic plasticity that may occur after the completion of compensation to an acid-base disturbance. This post-compensation plasticity has been observed before in red drum (Allmon and Esbaugh, 2017), and is largely attributed to the fish preparing for future acid-base disturbances. Surprisingly, the only observed treatment effects were down-regulation of *nhe3* expression, as well as reduced CA and NKA activity. All of these responses were again linked to the acidosis treatment. Note that observed down-regulations in *vha* and *nbc* were time point effects found in both treatment and control groups. It is curious as to why red drum would downregulate *nhe3* expression, as well as NKA and CA activity following exposure to elevated $p\text{CO}_2$. This is in opposition to the accepted models of acid-base regulation, which describe important roles for all three proteins in acid excretion (Perry and Gilmour, 2006). Yet similar findings have been previously demonstrated for NKA (Deigweiher et al., 2008; Esbaugh et al., 2012; Seidelin et al., 2001) and CA-c (Esbaugh et al., 2012). One explanation is that the signaling cascade governing the dynamic regulation of these transporters responds more

strongly to osmotic cues than acid-base cues. In these scenarios, the magnitude of the elevated influx of sodium through NHE3 may actually result in down-regulation of the NHE3 pathway, which also incorporates CA and NKA. It is important to state that this hypothesis is founded on our mRNA gene expression findings, which are known to not be directly correlated to protein abundance and activity (Maier et al., 2009), so further investigation is necessary.

An additional interesting observation from this work, which is important when considering the differential responses of series 1 and 2 fish to the 16 h hypercapnia exposure discussed above, is the dramatic difference in control phenotypes between experimental series. Both batches of fish were obtained from the same hatchery, but at different times, and were of the same size and acclimation temperature. Of particular significance is that series 2 two fish had substantially higher relative expression of acid-base transporters in their gills, as well as significantly higher enzyme activity across all proteins. As such, series 2 fish may be more effective at acid-base regulation. This is also consistent with the observed base excretion rates between the two batches, with the series 2 fish showing significantly higher rates in the 3 h post-exposure interval than observed in the 2 h post-exposure interval in series 1 fish. Note that the highest excretion rates would be expected at the earliest time points (e.g. Allmon and Esbaugh, 2017), so this is likely an underestimate of the difference in excretion rates between batches. The significance of individual variation in physiological traits is a growing area of interest in fish (Salin et al., 2019); however, such observations are not generally extended to acid-base physiology (Baumann, 2019). As the variation is more substantial between fish groups, as opposed to a high degree of variability within the groups, it seems likely that it may be the result of developmental plasticity that results in later life phenotypic effects. Such effects have been observed in the cardiac physiology of snapping turtles exposed to CO₂ in early

development (Filogonio and Crossley, 2019). It seems prudent for future work to assess whether fish exposed to acid-base stress in early life will have a more pronounced acid-base phenotype in later life.

The most surprising finding from the current study was the lack of VHA translocation following respiratory alkalosis for both series 1 (2 h alkalosis) and series 2 (24 h alkalosis). Based on previous work, we can estimate that plasma HCO_3^- reached in excess of 20 mM after compensation to 15,000 $\mu\text{atm CO}_2$ (Perry et al., 2010), and this is corroborated by unpublished work in our lab that revealed concentrations of 23 ± 1.3 mM ($n = 8$; mass = 103 ± 5 g) following metabolic compensation. Note that plasma HCO_3^- of only 6 to 7 mM was sufficient to drive translocation in dogfish sharks (Tresguerres et al., 2006), and a bolus injection that resulted in a peak of approximately 22 mM TCO_2 was sufficient to stimulate translocation in hagfish (Tresguerres et al., 2007a). We also did not observe translocation during the acidosis phase of the experiment, which supports previous work in red drum (Allmon and Esbaugh 2017). For all images, and under all acid-base conditions, the VHA signal was dominated by cytoplasmic signal. This is best represented by comparing the VHA signal to the basolateral NKA, and the apical NHE3. While this could suggest that VHA is not involved in systemic acid-base regulation in these animals, the mere presence of high levels of VHA in ionocytes would argue against such an interpretation. It is important to remember that VHA is a complex enzyme with two domains – a membrane associated V_0 domain and a peripherally associated V_1 domain. The B subunit is located in the latter, and cells can control VHA activity by the reversible assembly of the two domains (Oot et al., 2017). Unfortunately, antibodies targeting the V_0 domain are unavailable for fish species.

Our limited evidence for red drum suggests that VHA shows may play a role in acidosis, although a role for VHA in an alkalosis cannot be discounted. The gene

expression from series 1 – from fish with a lower overall abundance of gill ionoregulatory pathways – supported previous work that showed up-regulation of the B subunit gene expression with hypercapnia exposure (Allmon and Esbaugh 2017). Similar evidence of up-regulation in gene expression and activity was observed in Gulf toadfish following hypersalinity exposure, which the authors linked to the systemic metabolic acidosis that accompanies hypersalinity transition (Guffey et al., 2011). The role of VHA on the apical membrane has been clearly discussed in freshwater fish where it plays a role in ammonia excretion, ion regulation and systemic acidosis (Goss et al., 1998; Lin et al., 1994; Lin et al., 2006). Yet, the high sodium gradient in seawater has generally been used to suggest that NHE is the sole mechanism required for apical acid excretion in marine fishes. However, the same can be said for basolateral NHE1 and a systemic alkalosis owing to the co-localization of VHA and NKA in red drum gill ionocytes. This is not the case for the studied shark species, as the available evidence suggests that VHA is not located in NKA-rich ionocytes (Roa et al., 2014). Clearly future research is needed to fully elucidate the role of VHA with respect to acid-base and ion transport in the gills of marine fishes.

ACKNOWLEDGMENTS

This work was funded by a National Science Foundation grant (EF 1315290) to AJE. Additional support for JKL was provided by the Coastal Conservation Association (CCA) Texas, University of Texas at Austin: Summer Recruitment Fellowship, and the University of Texas at Austin Marine Science Institute – Lund Endowment. Alexis Khursigara, Benjamin Negrete, and Leighann Martin, assisted in animal collection, animal husbandry, and sample collection. The authors have no conflicts of interest with respect to this work.

TABLES

Table 5.1: List of primers used for real-time PCR. All sequences are 5' to 3' and reverse primers are reverse compliments of the genetic sequence.

Gene	Accession #	Reference	Orientation	Sequence
<i>ef1-a</i>	KJ958539	Watson et al., 2014	F	GTTGCTGGATGTCCTGCACG
			R	GTCCGTGACATGAGGCAGACTG
<i>ca-c</i>	KM387716.1	Watson et al., 2014	F	TGACATTCGCAGACGACTCCGA
			R	AGCAGGATACTTGGTCCCTCCA
<i>vha (B subunit)</i>	KU899108	Allmon and Esbaugh, 2017	F	CCTACCATTGAGCGTATCATCA
			R	CGTAGGAGCTCATGTGTCAGTCAG
<i>nbc1</i>	KM387714.1	Allmon and Esbaugh, 2017	F	TCTTCATCTACGACGCTTTCAA
			R	TCATATTGAGTGACGAGGTTGG
<i>nhe3</i>	KJ958541	Watson et al., 2014	F	CAAGGTGCAGACCTTCACGCTG
			R	ACGAGGATGGCTCCCATGTT

FIGURES

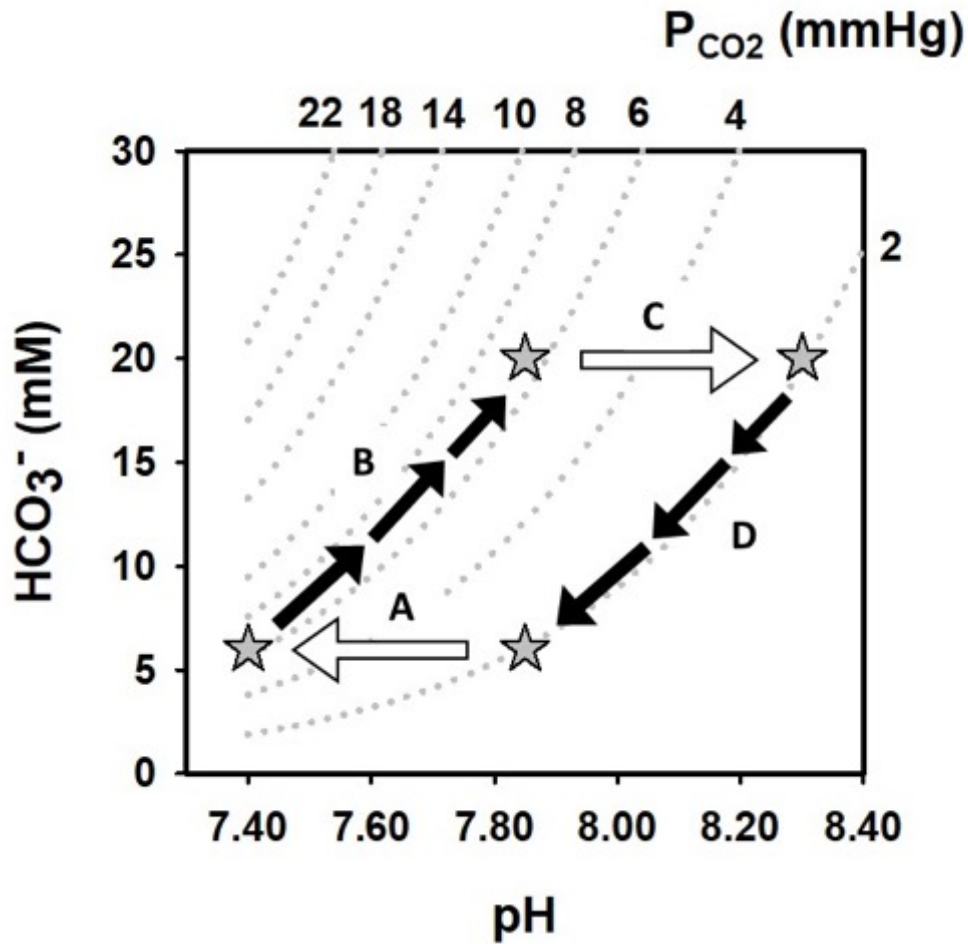


Figure 5.1: A representative pH- HCO_3^- - $p\text{CO}_2$ hypothetical diagram illustrating the experimental design using blood chemistry representative of red drum (*Sciaenops ocellatus*). White arrows depict respiratory acid-base disturbances, and black arrows depict metabolic compensation events. The experimental design will use hypercapnia to induce a respiratory acidosis (event A), which the fish will compensate for by elevating plasma HCO_3^- over the 16 h acclimation period (event B). The fish will then be returned to normocapnia resulting in a return of plasma $p\text{CO}_2$ to control levels resulting in elevated plasma pH (event C). Fish must correct this disturbance by lowering plasma HCO_3^- (event D). Treated fish will be sampled for tissue at following event B and at 2 h or 24 h after the onset of event D. Whole animal net acid-base excretion will be determined during event D.

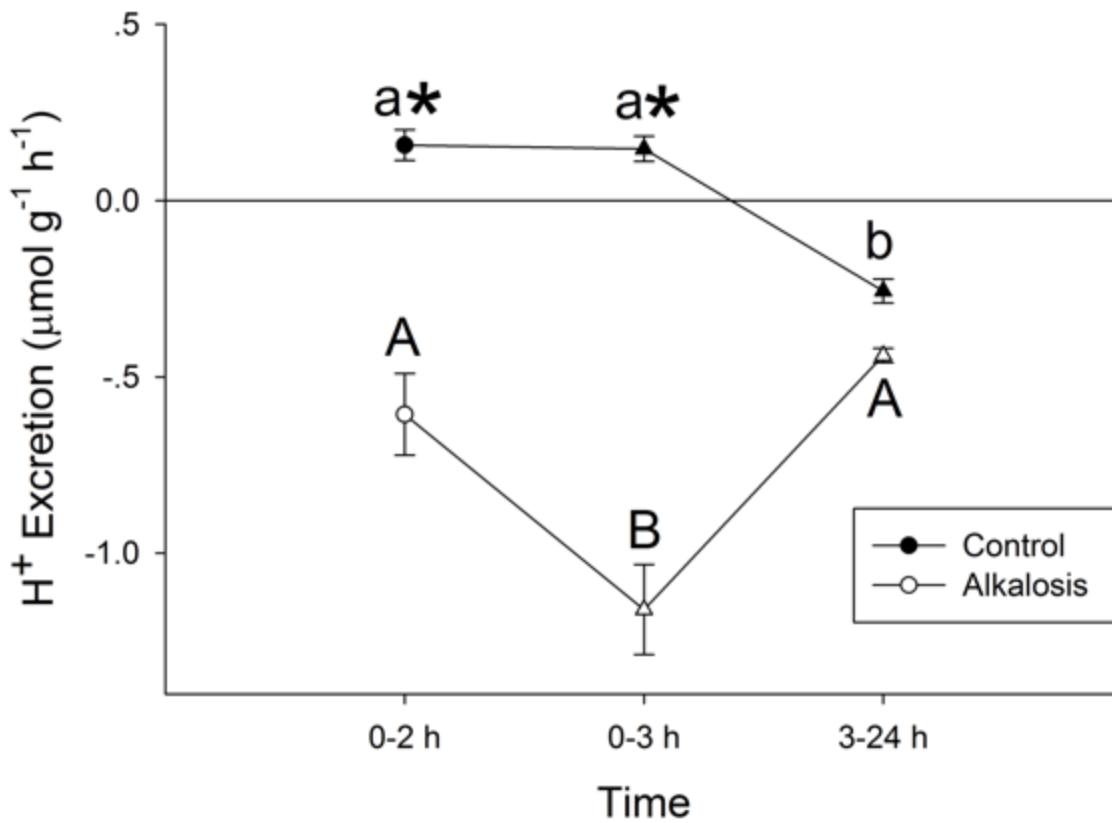


Figure 5.2: Net H⁺ excretion rates of red drum (*Sciaenops ocellatus*) following the onset of a respiratory alkalosis. Series 1 data is indicated by circles (○) and series 2 is indicated by triangles (△). Control fish net H⁺ excretion is denoted by filled shapes, and alkalosis fish are open shapes. Lower case letters denote significant differences across control treatment time points, and upper-case letters denote significant differences across alkalosis treatment. Asterisks indicate significant difference between treatments at a given time point. All values are mean ± S.E.M. (two-way ANOVA, P<0.05; Interaction P<0.001; n = 8 per group).

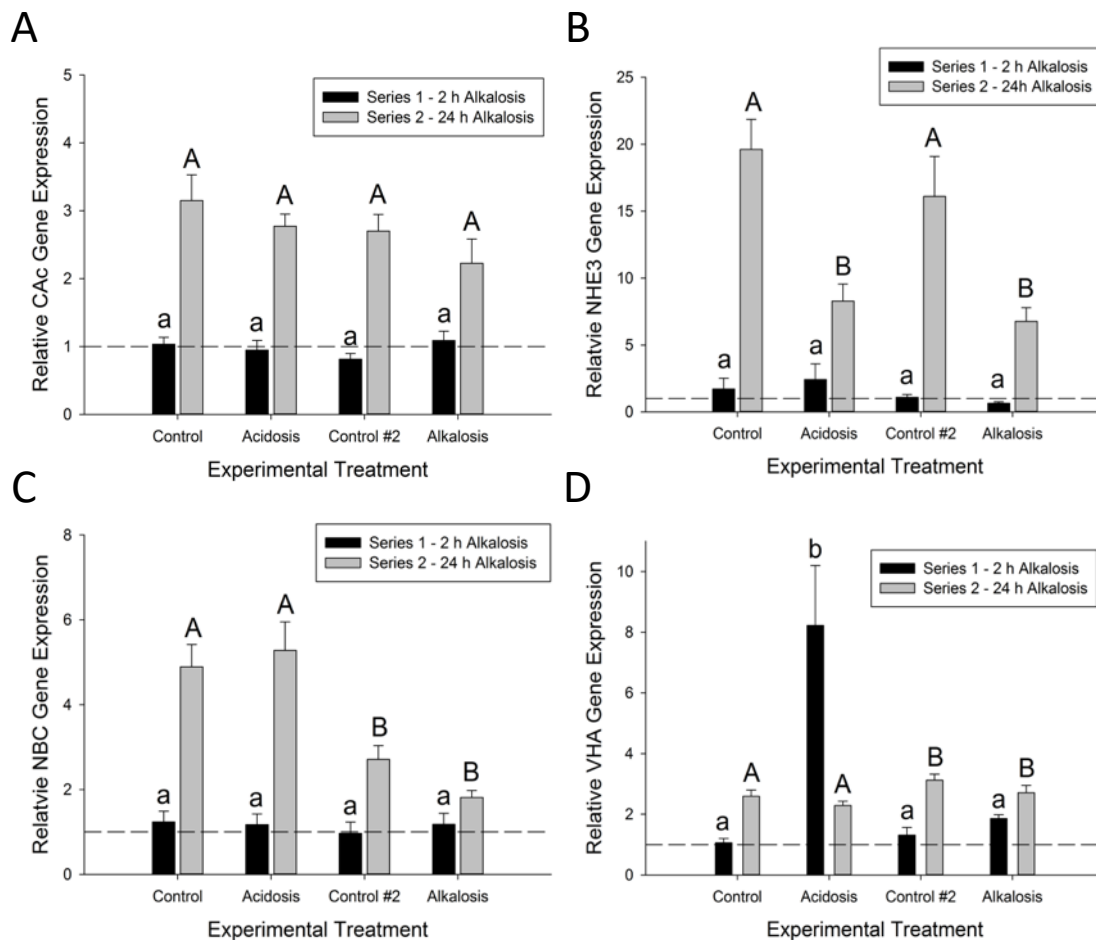


Figure 5.3: Relative branchial gene expression of acid-base regulatory pathways following 16 h exposure to 15,000 $\mu\text{atm CO}_2$, or 2 h (series 1) or 24 h (series 2) to a respiratory alkalosis, as well as time matched control. Control #2 were exposed to normocapnia and moved to normocapnia individual chambers, thus allowing for comparison to the alkalosis exposed fish. **(A)** CAC, **(B)** *nhe3*, **(C)** *nbc*, and **(D)** *vha*. Values set relative to housekeeping gene *ef1a*, which is denoted by the dash lines at 1.0. Lower case letters denote significant differences across series 1, and upper case letters denote significant differences across series 2 ($P < 0.05$). All values are mean \pm S.E.M. (two-way ANOVA, $P < 0.05$; $n = 8$ per group). Two-way ANOVA in *vha* series 1 was the only analysis that provided a significant interaction ($< .001$) between time and exposure, all other analyses found no significant interaction.

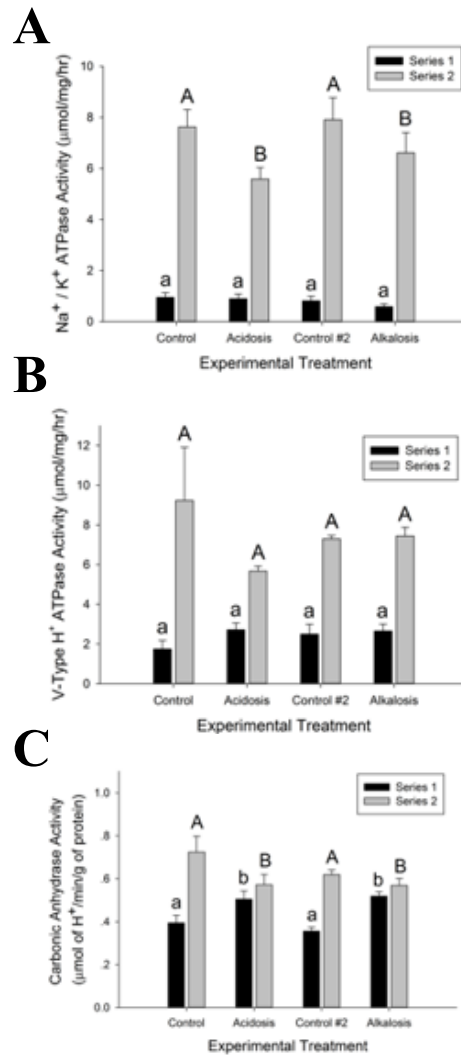


Figure 5.4: **(A)** NKA, **(B)** VHA, and **(C)** CA enzyme activity in the gills of red drum (*Sciaenops ocellatus*) following 16 h exposure to 15,000 μatm CO_2 , or 2 h (series 1) or 24 h (series 2) to a respiratory alkalosis, as well as time matched control. Control #2 were exposed to normocapnia and moved to normocapnia individual chambers, thus allowing for comparison to the alkalosis exposed fish. Lower case letters denote significant differences across series 1, and upper-case letters denote significant differences across series 2 ($P < 0.05$). All values are mean \pm S.E.M. (two-way ANOVA, $P < 0.05$; $n = 8$ per group). Two-way ANOVA analysis found no significant interaction between time and exposure across all groups.

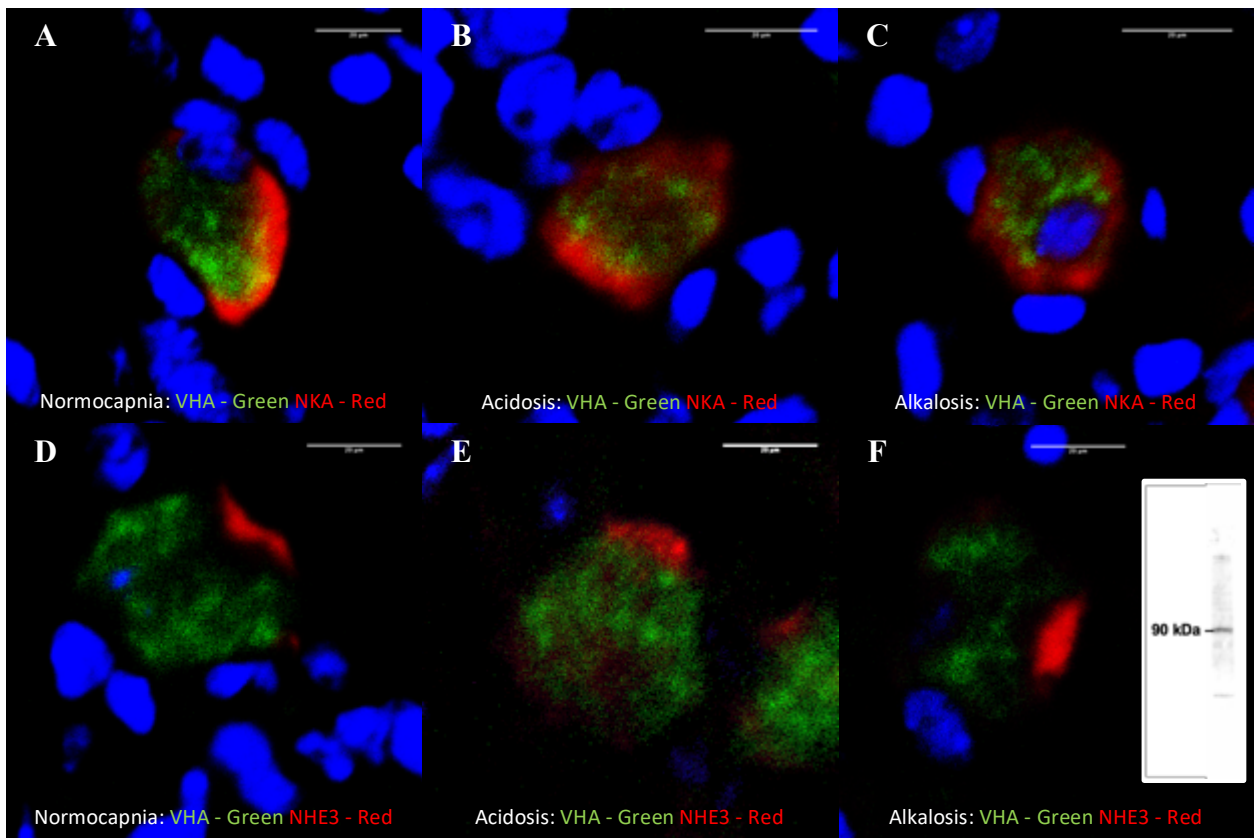


Figure 5.5: Representative confocal microscope images of gill ionocytes under control conditions, after exposure to a respiratory acidosis, and after exposure to a respiratory alkalosis (16 h exposure) in red drum (*Sciaenops ocellatus*). Scale bar in all images is 20 microns. VHA (green) was localized in the cytoplasm in the ionocyte, and no co-localization on the basolateral membrane with NKA (red) was evident under normocapnia conditions (A), after exposure to acidosis (B), and after 16 h exposure to alkalosis (C). VHA (green) was localized in the cytoplasm in the ionocyte, and no co-localization on the apical membrane with NHE3 (red) was evident under normocapnia conditions (D), after exposure to acidosis (E), and after 16 h exposure to alkalosis (F). Western blot verification showed a single NHE3 band at 90 kDa. Images were collected after 2 h alkalosis exposure (not shown), with no evidence of translocation.

Chapter 6: Summary and Conclusions

PERSPECTIVES ON OCEAN ACIDIFICATION

From 2001 to 2015 the number of publications exploring the impacts of elevated $p\text{CO}_2$ on marine teleosts exponentially increased, and among those publications a majority of the work had been completed on species native to open ocean or coral reef environments. A relatively small portion of published articles examined nearshore and estuarine species. Thus, my thesis investigated this important knowledge gap. The results of my work demonstrate that species native to the estuarine environment exhibit a great degree of resilience to the impacts of ocean acidification when compared to many of the species previously tested. I examined this tolerance through both lethal and sub-lethal metrics, including survival, growth, energetics, and behavior. The results from this dissertation further emphasize that species that inhabit naturally variable pH environments, like the near shore and estuaries, may be pre-adapted for resilience against ocean acidification – at least for the common endpoints tested here. These data generally agrees with recent work on the resilience of other estuarine species to acid-base disturbance (Baumann et al., 2018a; Murray and Baumann, 2018; Schade et al., 2014).

Estuarine and nearshore environments have high biological productivity, and therefore diel and seasonal $p\text{CO}_2$ fluctuations between 200-5000 μatm are common (Caldeira and Wickett, 2003; Lonthair et al., 2017). Furthermore, a defined gradient exists between these inshore productive areas and the stable $p\text{CO}_2$ conditions found in the open ocean (Duarte et al., 2013; Hofmann et al., 2011). Based on this natural gradient and recent evidence, Baumann (2019) has put forward the “Ocean Variability Hypothesis (OVH)”. The OVH states that marine organisms have adapted to the level of $p\text{CO}_2$ fluctuation present in their natural habitats, and because tolerance to elevated $p\text{CO}_2$ comes at a cost to

the organism, it can be assumed that species tolerance would decrease as you move from the nearshore environment to the open ocean. Our data on two different estuarine species further supports the argument that estuaries likely act as a genetic reservoir for CO₂ tolerance. This is important because tolerance to OA and climate change is thought to rely primarily on the presence of existing tolerant genotypes in a population, and the ability of individuals to alter their physiology to suit new environmental conditions; a process known as phenotypic plasticity (Bell, 2013; Gonzalez et al., 2013; Kelly et al., 2013; Pespeni et al., 2013). This is due to the relatively long-life spans of many marine organisms as compared to the rapidness of global climate change, which in many cases will negate traditional evolutionary processes.

There are a number of stressors that result from global climate change, with ocean warming, acidification, and oxygen decline comprising the main symptoms (Baumann, 2016; Portner, 2012). Furthermore, there is a plethora of evidence describing the concurrent rise of ocean temperature and CO₂ or the co-occurrence of high CO₂ and low oxygen (Baumann and Smith, 2018; Breitburg et al., 2015; Cai et al., 2011). This evidence has recently demanded an assessment of the sensitivity of organisms to multiple stressors, which may elicit different effects than each stressor alone (Breitburg et al., 2015). The study of the impacts of CO₂ and temperature on organisms has been the most extensive, with studies on the impacts of high CO₂ and low oxygen being rare (Baumann, 2019). What is evident is that the response to multi-stressors are variable, and that our predictive capacity of when these responses will occur is limited. Studies that have been completed on teleost species have found that exposing individuals to multiple stressors often incites either an additive or synergetic negative effect. For example, work on *Menidia menidia* found that exposure to low pH and low dissolved oxygen exhibited synergistic effects on survival, while work on *Menidia beryllina* found additive effects on survival (DePasquale

et al., 2015; Miller et al., 2016). These studies also found negative effects of multiple stressor exposures on growth, opercula ventilation rates, and aquatic surface respiration. Here, we have described the resilience of red drum to one stressor, but it would be interesting to examine if exposure to elevated $p\text{CO}_2$ in congruence with increased temperature or decreased oxygen causes a synergistic impact on survival in red drum exhibit.

PERSPECTIVES ON ACID- BASE REGULATION

This work also attempted to elucidate the mechanisms that allow for the increased tolerance to increased $p\text{CO}_2$ in an estuarine teleost. It is clear that marine fish larvae can excrete H^+ across the skin under control conditions, and this has been attributed to the NHE (Na^+/H^+ Exchanger) pathway (Liu et al., 2013). Additionally, we have hypothesized that VHA (V-type H^+ ATPase) may be playing a role in acid-excretion in marine teleosts (Allmon and Esbaugh, 2017; Michael et al., 2016). Nevertheless, prior to my thesis our understanding of the development and plasticity of acid excretion pathways under hypercapnia in estuarine species was limited, with the most robust data sets coming from species that would be best described as freshwater fish with seawater tolerance (Ayson et al., 1994; Evans et al., 2005b; Hiroi et al., 1999; Hwang et al., 2011; Tseng et al., 2013). Even more interestingly, alterations in development have not been described with respect to OA, with the only study observing a wide array of expression changes, including up-regulation of *nhe3* and *nbc* at various ontogenetic stages (Tseng et al., 2013). In Chapter 4, I described the developmental progression of hypothesized acid-excretion pathways in a true marine teleost. I observed that these fish had well developed acid-excretion systems even at the earliest time points, with the only increased expression across the early developmental window occurring at 84 hpf for *vha*. In Chapter 3 and 4, I describe the

alterations of hypothesized acid-excretion pathways in early life stages of a true marine teleost. The available evidence suggests that transcriptional alterations in response to hypercapnia is limited, with the only significant up-regulation occurring in *nhe2* after 24 h exposure to 5,500 and 12,000 μatm . I also provide the first evidence that estuarine teleosts may have multiple pathways for H^+ excretion, and specifically provide evidence to further hypothesize that VHA is used in apical H^+ excretion.

Investigations into the role of VHA in fish species have described a wide range of functions. In freshwater teleosts, the role of VHA in acid and ammonia excretion has been discussed in depth (Goss et al., 1998; Lin et al., 1994; Lin et al., 2006). Conversely, work on marine elasmobranch and hagfish has clearly shown that VHA plays a pivotal role in H^+ transport in the basolateral membrane in response to alkaline tide (Roa et al., 2014; Tresguerres et al., 2007a; Tresguerres et al., 2007b). The role of VHA in marine teleosts has been less described, but the current paradigm suggests that NHEs are the single pathway for acid-excretion in these animals. This idea is predicated on the premise that NHE is more energetically efficient due to the high Na^+ gradient (Claiborne et al., 1999; Claiborne et al., 2008; Edwards et al., 2001; Edwards et al., 2005; Guffey et al., 2015). I hypothesize that VHA can play a role in H^+ excretion in estuarine teleosts, if not all marine fish. This is because estuarine teleosts have the ability to inhabit both the marine and freshwater environments, which may necessitate the use of apical VHA in freshwater conditions for Na^+ uptake. Furthermore, these freshwater environments are inherently low in Na^+ , which would affect the function of the NHE acid excretion pathway. It seems reasonable to assume that if VHAs play a role in H^+ excretion in estuarine teleosts when inhabiting the freshwater environment, this may also extend to their residence in marine environments. This would have a secondary benefit of providing physiological redundancy in H^+ excretion pathways.

FUTURE DIRECTIONS

My dissertation's investigation of the tolerance estuarine species to ocean acidification and the development and plasticity of the acid-base regulatory machinery in red drum provides an opportunity to explore new and exciting questions that have evolved organically from said findings. First, we were unable to identify clear translocation of VHA in response to either an acidosis or alkalosis. A very unlikely conclusion from this data is that VHA is not involved in systemic acid-base balance at the gill, which would be in opposition to the data presented in Chapter 4 and Chapter 5. Furthermore, confocal microscopy has demonstrated that VHA is always co-localized with NKA. NKA is known to drive electrochemical ion gradients in the cell, which allows for ion and acid-base regulatory pathways to function (Evans et al., 2005b; Perry and Gilmour, 2006). Because of this, high NKA density in a cell has long been used as an identifier for an ionocyte using immunohistochemical techniques (Kwan et al., 2019; Varsamos et al., 2002). Thus, the colocalization of VHA and NKA would suggest a role in ion regulation of some kind. A more likely reason for the inability to observe translocation is due to the abundance in the cytoplasm, which limits our ability to observe VHA in other locations within the cell. As discussed in Chapter 4, our study of VHA cellular localization is likely constrained by the currently available tools for fish physiologist. Our antibody stained for the 'B subunit' of VHA, which is located in the V_1 complex in the cytoplasm, and in certain species it is not always attached to the V_0 complex of VHA (Beyenbach and Wieczorek, 2006). However, it is always attached when VHA is functional. Unfortunately, a commercial antibody is not available for the VHA 'a subunit', so a custom designed antibody is necessary. For future investigation it would be interesting if we could examine the VHA 'a subunit', the largest subunit in the V_0 complex, location in response to control, acidosis, and alkalosis conditions.

This study shows that there is wide variability in tolerance within a species, specifically with respect to survival metrics. I first observed that early life stages of red drum exhibited decreased survival in response to OA, but interestingly we also observed that there are individuals with tolerance to levels of $p\text{CO}_2$ in excess of 12,000 μatm . Intraspecies variation of physiological traits has been described since the mid-20th century (Roche et al., 2016), but a shift of focus to understanding the functional basis and eco-evolutionary implication of differences among individuals has incited a resurgence of interest in the field (Bolnick et al., 2003; Crawford and Oleksiak, 2007). In this study I investigated the underlying physiological traits that may promote this tolerance and have hypothesized that one mechanism is a redundancy of acid excretion pathways, which includes multiple NHEs and VHA. It should be noted that VHA data is limited to mRNA data, which has been inconsistent, and SIET data which has shown that VHA is only function at $p\text{CO}_2$ levels beyond 20,000 μatm . A future direction would be to measure gene expression of acid-base regulatory machinery in individuals in response to elevated $p\text{CO}_2$ and attempt to discern whether the variations in the development of the acid-base regulatory machinery result in differences in lethal and sub-lethal endpoints.

This study also lacked the ability to examine how widespread these physiological traits are among fish species. By investigating both tolerant and sensitive species we can increase our understanding of the physiological traits that confer tolerance (Esbaugh, 2018). We know that phenotypic diversity among individuals promotes the efficiency with which natural selection can generate an adaptive response across generations, and individual genotypes play a critical role in the robustness of a species to environmental stress (Gonzalez et al., 2013). A future direction would be replicating parts of this work in an offshore species that we would hypothesize is more sensitive to the impacts of ocean acidification. We would then be able to describe their physiological traits, which would

provide the opportunity to further describe differences and similarities between the resilient estuarine species and.

Finally, a majority of published experiments on the impacts of ocean acidification have focused on acute exposures to vulnerable early life stages. Interestingly, a recent study found that Atlantic silverside (*Menidia menidia*) exhibited decreased growth in response to elevated $p\text{CO}_2$, but this effect was only observable after raising individuals from fertilization to adult stages at high $p\text{CO}_2$ (Murray et al., 2017). This evidence supports the argument that future work should attempt to investigate the long-term ramifications of ocean acidification on survival, growth, and other sub-lethal endpoints. Recently, CO_2 rearing systems have been developed which allow for extended periods of CO_2 exposure at a decreased cost, making it possible to complete studies that can span multiple life stages, whole life cycles, or in some cases generations. Red drum mature at 2 to 3 years of age, which makes raising to full maturity likely unfeasible (Ross et al., 1995), although it would be interesting to see if these energetically costly metabolic compensatory pathways result in changes in growth, reproduction, and other morphometric metrics across different life stages at minimum.

CAVEATS AND LIMITATIONS

Even the most well planned and orchestrated research has caveats and limitations due to issues that are both in and out of the researcher's control, and this dissertation is no exception. The first limitation of this work is the inability to clearly define the long-term consequences of ocean acidification on exposed ELS fish. The importance of long-term impacts was highlighted above and has been discussed in recent work (Baumann, 2019). This is of specific importance in the context of the observed elevation in heart rate. In both species investigated, red drum (*Sciaenops ocellatus*) and orange spotted grouper

(*Epinephelus coioides*), I observed a significant increase in heart rate with increased exposure to CO₂, while being unable to discern significant impacts on energetic outcomes, yolk depletion rate and length. This could indicate that the observed increase has little impact on the whole animal energetics, but more likely this represents a key limitation in my conclusions. Thus, as previously stated the long-term impacts is an important avenue of future research.

Another limitation of our investigation is on defining the role of V-type H⁺ ATPase (VHA) in H⁺ excretion using the pharmacological inhibitor, bafilomycin A1. As previously stated, all forms of inhibition have caveats. Gene knock-down approaches, like morpholinos, have limitations that reduce the efficiency of the technique, including: non-specific effects and the necessity for injection before the first cell division, which is difficult for fast developing species like the red drum (Bedell et al., 2011; Zimmer et al., 2019). Knock-in approaches, like CRISPR, reduce the limitation of non-specific inhibition, but limitations do exist in the form of cost, time, and the difficulty of use of non-traditional model organisms (Auer and Del Bene, 2014; Simone et al., 2018; Zimmer et al., 2019). Furthermore, both approaches suffer from the possibility that knock-down individuals will augment their physiology to compensate for the knock-down, thus giving spurious results relative to the control animals. Pharmacological inhibitors are not limited as severely by time, cost, and development rate, but do have serious limitations in the form of non-specific inhibition and solubility in seawater (Xie et al., 1997). In our experiment design, pharmacological inhibition was chosen due to the limitations of the use of genetic tools on red drum were deemed to be too great. To overcome the solubility issues inherent in seawater a bafilomycin concentration of 10 μM was used, although this raises the risk of non-specific inhibition on other ATPases, including NKA, and could impair mitochondrial function (Bowman et al., 1988; Teplova et al., 2007). Future work could overcome these

concerns by completed additional experiments using an inhibitor dose response experiment and incorporating a second VHA specific inhibitor such as concanamycin A (Huss and Wieczorek, 2009).

The last limitation discussed here is that much of this work has used RT-qPCR to investigate the impacts of an acid-base disturbance on acid-base regulatory pathways. A key limitation of studying mRNA expression is that it may not be directly correlated to protein activity or even protein abundance (Maier et al., 2009; Vogel and Marcotte, 2012). What mRNA expression does provide is a snapshot of the pathway that is taking place in response to an environmental exposure, and this what we have used this technique for in this dissertation. Nevertheless, we should understand this limitation and think of mRNA expression as a box rather than an arrow, and that it contributes to a better understanding of mechanisms but cannot be solely relied upon to define physiological findings. While comparative physiologists are always limited by available tools (e.g. NHE2 antibody), future studies should attempt to use a greater array of endpoints in order to thoroughly describe the phenotypic plasticity of fishes in response to an environmental exposure.

Bibliography

- Allmon, E. B. and Esbaugh, A. J.** (2017). Carbon Dioxide Induced Plasticity of Branchial Acid-Base Pathways in an Estuarine Teleost. *Scientific Reports* **7**, 10.
- Alper, S. L.** (2009). Molecular Physiology and Genetics of Na⁺-Independent Slc4 Anion Exchangers. *Journal of Experimental Biology* **212**, 1672-1683.
- Armstrong, E. J., Roa, J. N., Stillman, J. H. and Tresguerres, M.** (2018). Symbiont Photosynthesis in Giant Clams Is Promoted by V-Type H⁺-Atpase from Host Cells. *Journal of Experimental Biology* **221**, 7.
- Armstrong, N. E.** (1987). The Ecology of Open-Bay Bottoms of Texas: A Community Profile, vol. 85 (ed. U. S. F. W. S. B. Rep.).
- Auer, T. O. and Del Bene, F.** (2014). Crispr/Cas9 and Talen-Mediated Knock-in Approaches in Zebrafish. *Methods* **69**, 142-150.
- Ayson, F. G., Kaneko, T., Hasegawa, S. and Hirano, T.** (1994). Development of Mitochondrion-Rich Cells in the Yolk-Sac Membrane of Embryos and Larvae of Tilapia, *Oreochromis-Mossambicus*, in Fresh-Water and Seawater. *Journal of Experimental Zoology* **270**, 129-135.
- Basso, L., Hendriks, I. E., Rodriguez-Navarro, A., Gambi, M. C. and Duarte, C. M.** (2015). Extreme Ph Conditions at a Natural Co₂ Vent System (Italy) Affect Growth, and Survival of Juvenile Pen Shells (*Pinna Nobilis*). *Estuaries and Coasts* **38**, 1986-1999.
- Baumann, H.** (2016). Combined Effects of Ocean Acidification, Warming, and Hypoxia on Marien Organisms. *Limnology and Oceanography e-Lectures* **6**.
- Baumann, H.** (2019). Experimental Assessments of Marine Species Sensitivities to Ocean Acidification and Co-Stressors: How Far Have We Come? *Canadian Journal of Zoology* **97**, 399-408.
- Baumann, H., Cross, E. L. and Murray, C. S.** (2018a). Robust Quantification of Fish Early Life Co₂ Sensitivities Via Serial Experimentation. *Biology Letters* **14**, 5.
- Baumann, H., Parks, E. M. and Murray, C. S.** (2018b). Starvation Rates in Larval and Juvenile Atlantic Silversides (*Menidia Menidia*) Are Unaffected by High Co₂ Conditions. *Marine Biology* **165**, 9.
- Baumann, H. and Smith, E. M.** (2018). Quantifying Metabolically Driven Ph and Oxygen Fluctuations in Us Nearshore Habitats at Diel to Interannual Time Scales. *Estuaries and Coasts* **41**, 1102-1117.
- Baumann, H., Talmage, S. C. and Gobler, C. J.** (2012). Reduced Early Life Growth and Survival in a Fish in Direct Response to Increased Carbon Dioxide. *Nature Climate Change* **2**, 38-41.
- Bedell, V. M., Westcot, S. E. and Ekker, S. C.** (2011). Lessons from Morpholino-Based Screening in Zebrafish. *Briefings in Functional Genomics* **10**, 181-188.
- Bell, G.** (2013). Evolutionary Rescue and the Limits of Adaptation. *Philosophical Transactions of the Royal Society B-Biological Sciences* **368**, 6.

- Beyenbach, K. W. and Wieczorek, H.** (2006). The V-Type H⁺ Atpase: Molecular Structure and Function, Physiological Roles and Regulation. *Journal of Experimental Biology* **209**, 577-589.
- Bignami, S., Sponaugle, S. and Cowen, R. K.** (2013). Response to Ocean Acidification in Larvae of a Large Tropical Marine Fish, *Rachycentron Canadum*. *Glob Chang Biol* **19**, 996-1006.
- Bignami, S., Sponaugle, S. and Cowen, R. K.** (2014). Effects of Ocean Acidification on the Larvae of a High-Value Pelagic Fisheries Species, Mahi-Mahi *Coryphaena Hippurus*. *Aquatic Biology* **21**, 249-260.
- Boisen, A. M. Z., Amstrup, J., Novak, I. and Grosell, M.** (2003). Sodium and Chloride Transport in Zebrafish Soft Water and Hard Water Acclimated (*Danio Rerio*). *Biochimica Et Biophysica Acta-Biomembranes* **1618**, 207-218.
- Bolnick, D. I., Svanback, R., Fordyce, J. A., Yang, L. H., Davis, J. M., Hulsey, C. D. and Forister, M. L.** (2003). The Ecology of Individuals: Incidence and Implications of Individual Specialization. *American Naturalist* **161**, 1-28.
- Bowman, E. J., Siebers, A. and Altendorf, K.** (1988). Bafilomycins - a Class of Inhibitors of Membrane Atpases from Microorganisms, Animal-Cells, and Plant-Cells. *Proceedings of the National Academy of Sciences of the United States of America* **85**, 7972-7976.
- Breitburg, D. L., Salisbury, J., Bernhard, J. M., Cai, W. J., Dupont, S., Doney, S. C., Kroeker, K. J., Levin, L. A., Long, W. C., Milke, L. M. et al.** (2015). And on Top of All That... Coping with Ocean Acidification in the Midst of Many Stressors. *Oceanography* **28**, 48-61.
- Browman, H. I.** (2017). Towards a Broader Perspective on Ocean Acidification Research Introduction. *Ices Journal of Marine Science* **74**, 889-894.
- Cai, W.-J., Hu, X., Huang, W.-J., Murrell, M. C., Lehrter, J. C., Lohrenz, S. E., Chou, W.-C., Zhai, W., Hollibaugh, J. T., Wang, Y. et al.** (2011). Acidification of Subsurface Coastal Waters Enhanced by Eutrophication. *Nature Geoscience* **4**, 766-770.
- Caldeira, K. and Wickett, M. E.** (2003). Anthropogenic Carbon and Ocean Ph. *Nature* **425**, 365-365.
- Calosi, P., Rastrick, S. P. S., Graziano, M., Thomas, S. C., Baggini, C., Carter, H. A., Hall-Spencer, J. M., Milazzo, M. and Spicer, J. I.** (2013). Distribution of Sea Urchins Living near Shallow Water Co₂ Vents Is Dependent Upon Species Acid-Base and Ion-Regulatory Abilities. *Marine Pollution Bulletin* **73**, 470-484.
- Catches, J. S., Burns, J. M., Edwards, S. L. and Claiborne, J. B.** (2006). Na⁺/H⁺ Antiporter, V-H⁺-Atpase and Na⁺/K⁺-Atpase Immunolocalization in a Marine Teleost (*Myoxocephalus Octodecemspinosus*). *Journal of Experimental Biology* **209**, 3440-3447.
- Cattano, C., Claudet, J., Domenici, P. and Milazzo, M.** (2018). Living in a High Co₂ World: A Global Meta-Analysis Shows Multiple Trait-Mediated Fish Responses to Ocean Acidification. *Ecological Monographs* **88**, 320-335.
- Chambers, R. C., Candelmo, A. C., Habeck, E. A., Poach, M. E., Wieczorek, D., Cooper, K. R., Greenfield, C. E. and Phelan, B. A.** (2014). Effects of Elevated Co₂

in the Early Life Stages of Summer Flounder, *Paralichthys Dentatus*, and Potential Consequences of Ocean Acidification. *Biogeosciences* **11**, 1613-1626.

Chivers, D. P., McCormick, M. I., Nilsson, G. E., Munday, P. L., Watson, S. A., Meekan, M. G., Mitchell, M. D., Corkill, K. C. and Ferrari, M. C. O. (2014). Impaired Learning of Predators and Lower Prey Survival under Elevated Co₂: A Consequence of Neurotransmitter Interference. *Global Change Biology* **20**, 515-522.

Chowdhury, M. J., Girgis, M. and Wood, C. M. (2016). Revisiting the Mechanisms of Copper Toxicity to Rainbow Trout: Time Course, Influence of Calcium, Unidirectional Na⁺ Fluxes, and Branchial Na⁺, K⁺ Atpase and V-Type H⁺ Atpase Activities. *Aquatic Toxicology* **177**, 51-62.

Ciais, P., Sabine, C., Bala, G., Bopp, L., Brovkin, V., Canadell, J., Chhabra, A., DeFries, R., Galloway, J., Heimann, M. et al. (2013). Carbon and Other Biogeochemical Cycles. In *Climate Change 2013: The Physical Science Basis. Contribution of Working Group I to the Fifth Assessment Report of the Intergovernmental Panel on Climate Change*, eds. T. F. Stocker D. Qin G.-K. Plattner M. Tignor S. K. Allen J. Boschung A. Nauels Y. Xia V. Bex and P. M. Midgley), pp. 465–570. Cambridge, United Kingdom and New York, NY, USA: Cambridge University Press.

Claiborne, J. B., Blackston, C. R., Choe, K. P., Dawson, D. C., Harris, S. P., Mackenzie, L. A. and Morrison-Shetlar, A. I. (1999). A Mechanisms for Branchial Acid Excretions in Marine Fish: Identification of Multiple Na⁺/H⁺ Antiporter (Nhe) Isoforms in Gills of Two Seawater Teleosts. *Journal of Experimental Biology* **202**, 315-324.

Claiborne, J. B., Choe, K. P., Morrison-Shetlar, A. I., Weakley, J. C., Havird, J., Freiji, A., Evans, D. H. and Edwards, S. L. (2008). Molecular Detection and Immunological Localization of Gill Na⁺/H⁺ Exchanger in the Dogfish (*Squalus Acanthias*). *American Journal of Physiology-Regulatory Integrative and Comparative Physiology* **294**, R1092-R1102.

Claiborne, J. B., Edwards, S. L. and Morrison-Shetlar, A. I. (2002). Acid-Base Regulation in Fishes: Cellular and Molecular Mechanisms. *Journal of Experimental Zoology* **293**, 302-319.

Comyns, B. H., Lyczkowskishultz, J., Rakocinski, C. F. and Steen, J. P. (1989). Age and Growth of Red Drum Larvae in the North-Central Gulf of Mexico. *Transactions of the American Fisheries Society* **118**, 159-167.

Couturier, C. S., Stecyk, J. A. W., Rummer, J. L., Munday, P. L. and Nilsson, G. E. (2013). Species-Specific Effects of near-Future Co₂ on the Respiratory Performance of Two Tropical Prey Fish and Their Predator. *Comparative Biochemistry and Physiology a-Molecular & Integrative Physiology* **166**, 482-489.

Crawford, D. L. and Oleksiak, M. F. (2007). The Biological Importance of Measuring Individual Variation. *Journal of Experimental Biology* **210**, 1613-1621.

Cripps, I. L., Munday, P. L. and McCormick, M. I. (2011). Ocean Acidification Affects Prey Detection by a Predatory Reef Fish. *Plos One* **6**, 7.

Cutler, C. P., Brezillon, S., Bekir, S., Sanders, I. L., Hazon, N. and Cramb, G. (2000). Expression of a Duplicate Na,K-Atpase Beta(1)-Isoform in the European Eel

(*Anguilla Anguilla*). *American Journal of Physiology-Regulatory Integrative and Comparative Physiology* **279**, R222-R229.

Davis, B. E., Miller, N. A., Flynn, E. E. and Todgham, A. E. (2016). Juvenile Antarctic Rockcod (*Trematomus Bernacchii*) Are Physiologically Robust to Co₂-Acidified Seawater. *J Exp Biol* **219**, 1203-13.

Deigweiher, K., Koschnick, N., Portner, H. O. and Lucassen, M. (2008). Acclimation of Ion Regulatory Capacities in Gills of Marine Fish under Environmental Hypercapnia. *American Journal of Physiology-Regulatory Integrative and Comparative Physiology* **295**, R1660-R1670.

DePasquale, E., Baumann, H. and Gobler, C. J. (2015). Vulnerability of Early Life Stage Northwest Atlantic Forage Fish to Ocean Acidification and Low Oxygen. *Marine Ecology Progress Series* **523**, 145-156.

Devine, B. M. and Munday, P. L. (2013). Habitat Preferences of Coral-Associated Fishes Are Altered by Short-Term Exposure to Elevated Co₂. *Marine Biology* **160**, 1955-1962.

Dixson, D. L., Munday, P. L. and Jones, G. P. (2010). Ocean Acidification Disrupts the Innate Ability of Fish to Detect Predator Olfactory Cues. *Ecology Letters* **13**, 68-75.

Doney, S. C., Fabry, V. J., Feely, R. A. and Kleypas, J. A. (2009). Ocean Acidification: The Other Co₂ Problem. *Ann Rev Mar Sci* **1**, 169-92.

Donowitz, M., Tse, C. M. and Fuster, D. (2013). Slc9/Nhe Gene Family, a Plasma Membrane and Organellar Family of Na⁺/H⁺ Exchangers. *Molecular Aspects of Medicine* **34**, 236-251.

Duarte, C. M., Hendriks, I. E., Moore, T. S., Olsen, Y. S., Steckbauer, A., Ramajo, L., Carstensen, J., Trotter, J. A. and McCulloch, M. (2013). Is Ocean Acidification an Open-Ocean Syndrome? Understanding Anthropogenic Impacts on Seawater Ph. *Estuaries and Coasts* **36**, 221-236.

Dymowska, A. K., Boyle, D., Schultz, A. G. and Goss, G. G. (2015). The Role of Acid-Sensing Ion Channels in Epithelial Na⁺ Uptake in Adult Zebrafish (*Danio Rerio*). *Journal of Experimental Biology* **218**, 1244-1251.

Dymowska, A. K., Schultz, A. G., Blair, S. D., Chamot, D. and Goss, G. G. (2014). Acid-Sensing Ion Channels Are Involved in Epithelial Na⁺ Uptake in the Rainbow Trout *Oncorhynchus Mykiss*. *American Journal of Physiology-Cell Physiology* **307**, C255-C265.

Edwards, S. L., Claiborne, J. B., Morrison-Shetlar, A. I. and Toop, T. (2001). Expression of Na⁺/H⁺ Exchanger Mrna in the Gills of the Atlantic Hagfish (*Myxine Glutinosus*) in Response to Metabolic Acidosis. *Comparative Biochemistry and Physiology a-Molecular and Integrative Physiology* **130**, 81-91.

Edwards, S. L., Wall, B. P., Morrison-Shetlar, A., Sligh, S., Weakley, J. C. and Claiborne, J. B. (2005). The Effect of Environmental Hypercapnia and Salinity on the Expression of Nhe-Like Isoforms in the Gills of a Euryhaline Fish (*Fundulus Heteroclitus*). *Journal of Experimental Zoology Part a-Ecological and Integrative Physiology* **303A**, 464-475.

- Ern, R. and Esbaugh, A. J.** (2016). Hyperventilation and Blood Acid-Base Balance in Hypercapnia Exposed Red Drum (*Sciaenops Ocellatus*). *Journal of comparative physiology. B, Biochemical, systemic, and environmental physiology* **186**, 447-60.
- Esbaugh, A. J.** (2018). Physiological Implications of Ocean Acidification for Marine Fish: Emerging Patterns and New Insights. *Journal of Comparative Physiology B-Biochemical Systems and Environmental Physiology* **188**, 1-13.
- Esbaugh, A. J. and Cutler, B.** (2016). Intestinal Na⁺, K⁺, 2Cl⁻ Cotransporter 2 Plays a Crucial Role in Hyperosmotic Transitions of a Euryhaline Teleost. *Physiological Reports* **4**, 12.
- Esbaugh, A. J., Ern, R., Nordi, W. M. and Johnson, A. S.** (2016). Respiratory Plasticity Is Insufficient to Alleviate Blood Acid-Base Disturbances after Acclimation to Ocean Acidification in the Estuarine Red Drum, *Sciaenops Ocellatus*. *Journal of Comparative Physiology B-Biochemical Systemic and Environmental Physiology* **186**, 97-109.
- Esbaugh, A. J., Gilmour, K. M. and Perry, S. F.** (2009). Membrane-Associated Carbonic Anhydrase in the Respiratory System of the Pacific Hagfish (*Eptatretus Stouti*). *Respiratory Physiology & Neurobiology* **166**, 107-116.
- Esbaugh, A. J., Heuer, R. and Grosell, M.** (2012). Impacts of Ocean Acidification on Respiratory Gas Exchange and Acid-Base Balance in a Marine Teleost, *Opsanus Beta*. *J Comp Physiol B* **182**, 921-34.
- Esbaugh, A. J., Perry, S. F., Bayaa, M., Georgalis, T., Nickerson, J., Tufts, B. L. and Gilmour, K. M.** (2005). Cytoplasmic Carbonic Anhydrase Isozymes in Rainbow Trout *Oncorhynchus Mykiss*: Comparative Physiology and Molecular Evolution. *Journal of Experimental Biology* **208**, 1951-1961.
- Evans, C. W., Cziko, P., Cheng, C. C. and Devries, A. L.** (2005a). Spawning Behaviour and Early Development in the Nakes Dragonfish *Gymnodraco Acuticeps*. *Antarctic Science* **17**, 319-327.
- Evans, D. H., Piermarini, P. M. and Choe, K. P.** (2005b). The Multifunctional Fish Gill: Dominant Site of Gas Exchange, Osmoregulation, Acid-Base Regulation, and Excretion of Nitrogenous Waste. *Physiol Rev* **85**, 97-177.
- Feely, R. A., Alin, S. R., Newton, J., Sabine, C. L., Warner, M., Devol, A., Krembs, C. and Maloy, C.** (2010). The Combined Effects of Ocean Acidification, Mixing, and Respiration on Ph and Carbonate Saturation in an Urbanized Estuary. *Estuarine, Coastal and Shelf Science* **88**, 442-449.
- Fenwick, J. C., Bonga, S. E. W. and Flik, G.** (1999). In Vivo Bafilomycin-Sensitive Na⁺ Uptake in Young Freshwater Fish. *Journal of Experimental Biology* **202**, 3659-3666.
- Ferrari, M. C. O., Dixon, D. L., Munday, P. L., McCormick, M. I., Meekan, M. G., Sih, A. and Chivers, D. P.** (2011). Intrageneric Variation in Antipredator Responses of Coral Reef Fishes Affected by Ocean Acidification: Implications for Climate Change Projections on Marine Communities. *Global Change Biology* **17**, 2980-2986.

Ferrari, M. C. O., Manassa, R. P., Dixon, D. L., Munday, P. L., McCormick, M. I., Meekan, M. G., Sih, A. and Chivers, D. P. (2012). Effects of Ocean Acidification on Learning in Coral Reef Fishes. *Plos One* **7**, 10.

Ferrari, M. C. O., Munday, P. L., Rummer, J. L., McCormick, M. I., Corkill, K., Watson, S. A., Allan, B. J. M., Meekan, M. G. and Chivers, D. P. (2015). Interactive Effects of Ocean Acidification and Rising Sea Temperatures Alter Predation Rate and Predator Selectivity in Reef Fish Communities. *Global Change Biology* **21**, 1848-1855.

Filogonio, R. and Crossley, D. A. (2019). Long Term Effects of Chronic Prenatal Exposure to Hypercarbia on Organ Growth and Cardiovascular Responses to Adrenaline and Hypoxia in Common Snapping Turtles. *Comparative Biochemistry and Physiology a-Molecular & Integrative Physiology* **234**, 10-17.

Franke, A. and Clemmesen, C. (2011). Effect of Ocean Acidification on Early Life Stages of Atlantic Herring (*Clupea harengus* L.). *Biogeosciences* **8**, 3697-3707.

Frommel, A. Y., Maneja, R., Lowe, D., Malzahn, A. M., Geffen, A. J., Folkvord, A., Piatkowski, U., Reusch, T. B. H. and Clemmesen, C. (2012). Severe Tissue Damage in Atlantic Cod Larvae under Increasing Ocean Acidification. *Nature Climate Change* **2**, 42-46.

Frommel, A. Y., Maneja, R., Lowe, D., Pascoe, C. K., Geffen, A. J., Folkvord, A., Piatkowski, U. and Clemmesen, C. (2014). Organ Damage in Atlantic Herring Larvae as a Result of Ocean Acidification. *Ecological Applications* **24**, 1131-1143.

Frommel, A. Y., Margulies, D., Wexler, J. B., Stein, M. S., Scholey, V. P., Williamson, J. E., Bromhead, D., Nicol, S. and Havenhand, J. (2016). Ocean Acidification Has Lethal and Sub-Lethal Effects on Larval Development of Yellowfin Tuna, *Thunnus albacares*. *Journal of Experimental Marine Biology and Ecology* **482**, 18-24.

Frommel, A. Y., Schubert, A., Piatkowski, U. and Clemmesen, C. (2013). Egg and Early Larval Stages of Baltic Cod, *Gadus morhua*, Are Robust to High Levels of Ocean Acidification. *Marine Biology* **160**, 1825-1834.

Fu, C., Wilson, J. M., Rombough, P. J. and Brauner, C. J. (2010). Ions First: Na⁺ Uptake Shifts from the Skin to the Gills before O₂ Uptake in Developing Rainbow Trout, *Oncorhynchus mykiss*. *Proceedings of the Royal Society B-Biological Sciences* **277**, 1553-1560.

Georgalis, T., Perry, S. F. and Gilmour, K. M. (2006). The Role of Branchial Carbonic Anhydrase in Acid-Base Regulation in Rainbow Trout (*Oncorhynchus mykiss*). *Journal of Experimental Biology* **209**, 518-530.

Gilmour, K. M. (2001). The CO₂/pH Ventilatory Drive in Fish. *Comparative Biochemistry and Physiology a-Molecular and Integrative Physiology* **130**, 219-240.

Gilmour, K. M., Bayaa, M., Kenney, L., McNeill, B. and Perry, S. F. (2007a). Type IV Carbonic Anhydrase Is Present in the Gills of Spiny Dogfish (*Squalus acanthias*). *American Journal of Physiology-Regulatory Integrative and Comparative Physiology* **292**, R556-R567.

Gilmour, K. M., Euverman, R. M., Esbaugh, A. J., Kenney, L., Chew, S. F., Ip, Y. K. and Perry, S. F. (2007b). Mechanisms of Acid-Base Regulation in the African Lungfish *Protopterus Annectens*. *Journal of Experimental Biology* **210**, 1944-1959.

Gilmour, K. M. and Perry, S. F. (2004). Branchial Membrane-Associated Carbonic Anhydrase Activity Maintains Co₂ Excretion in Severely Anemic Dogfish. *American Journal of Physiology-Regulatory Integrative and Comparative Physiology* **286**, R1138-R1148.

Gilmour, K. M. and Perry, S. F. (2007). Branchial Chemoreceptor Regulation of Cardiorespiratory Function. In *Sensory Systems Neuroscience*, vol. 25 eds. T. J. Hara and B. S. Zielinski, pp. 97-151. San Diego: Elsevier Academic Press Inc.

Gilmour, K. M. and Perry, S. F. (2009). Carbonic Anhydrase and Acid-Base Regulation in Fish. *Journal of Experimental Biology* **212**, 1647-1661.

Gilmour, K. M., Perry, S. F., Bernier, N. J., Henry, R. P. and Wood, C. M. (2001). Extracellular Carbonic Anhydrase in the Dogfish, *Squalus Acanthias*: A Role in Co₂ Excretion. *Physiological and Biochemical Zoology* **74**, 477-492.

Gilmour, K. M., Thomas, K., Esbaugh, A. J. and Perry, S. F. (2009). Carbonic Anhydrase Expression and Co₂ Excretion During Early Development in Zebrafish *Danio Rerio*. *J Exp Biol* **212**, 3837-45.

Gonzalez, A., Ronce, O., Ferriere, R. and Hochberg, M. E. (2013). Evolutionary Rescue: An Emerging Focus at the Intersection between Ecology and Evolution. *Philosophical Transactions of the Royal Society B-Biological Sciences* **368**, 8.

Goss, G. G. and Perry, S. F. (1994). Different Mechanisms of Acid-Base Regulation in Rainbow-Trout (*Oncorhynchus-Mykiss*) and American Eel (*Anguilla-Rostrata*) During NaHCO₃ Infusion. *Physiological Zoology* **67**, 381-406.

Goss, G. G., Perry, S. F., Fryer, J. N. and Laurent, P. (1998). Gill Morphology and Acid-Base Regulation in Freshwater Fishes. *Comparative Biochemistry and Physiology a-Molecular & Integrative Physiology* **119**, 107-115.

Goss, G. G., Perry, S. F., Wood, C. M. and Laurent, P. (1992). Mechanisms of Ion and Acid-Base Regulation at the Gills of Fresh-Water Fish. *Journal of Experimental Zoology* **263**, 143-159.

Green, J. A. (2011). The Heart Rate Method for Estimating Metabolic Rate: Review and Recommendations. *Comparative Biochemistry and Physiology a-Molecular & Integrative Physiology* **158**, 287-304.

Green, L. and Jutfelt, F. (2014). Elevated Carbon Dioxide Alters the Plasma Composition and Behaviour of a Shark. *Biology Letters* **10**, 4.

Grosell, M. and Wood, C. M. (2002). Copper Uptake across Rainbow Trout Gills: Mechanisms of Apical Entry. *Journal of Experimental Biology* **205**, 1179-1188.

Guffey, S., Esbaugh, A. and Grosell, M. (2011). Regulation of Apical H⁺-Atpase Activity and Intestinal HCO₃⁻ Secretion in Marine Fish Osmoregulation. *American Journal of Physiology-Regulatory Integrative and Comparative Physiology* **301**, R1682-R1691.

Guffey, S. C., Fliegel, L. and Goss, G. G. (2015). Cloning and Characterization of Na⁺/H⁺ Exchanger Isoforms Nhe2 and Nhe3 from the Gill of Pacific Dogfish *Squalus*

Suckleyi. *Comparative Biochemistry and Physiology B-Biochemistry & Molecular Biology* **188**, 46-53.

Hamilton, T. J., Holcombe, A. and Tresguerres, M. (2014). Co₂-Induced Ocean Acidification Increases Anxiety in Rockfish Via Alteration of Gabaa Receptor Functioning. *Proc Biol Sci* **281**, 20132509.

Hawkings, G. S., Galvez, F. and Goss, G. G. (2004). Seawater Acclimation Causes Independent Alterations in Na⁺/K⁺- and H⁺-Atpase Activity in Isolated Mitochondria-Rich Cell Subtypes of the Rainbow Trout Gill. *Journal of Experimental Biology* **207**, 905-912.

Heisler, N. (1986). Comparative Aspects of Acid-Base Regulation. In *Acid-Base Regulation in Animals*, (ed. N. Heisler), pp. 397-449. Amsterdam: Elsevier.

Henry, R. P. (1991). Techniques for Measuring Carbonic Anhydrase Activity in Vitro. In *The Carbonic Anhydrases*, pp. 119-125: Springer.

Henry, R. P., Tufts, B. L. and Boutilier, R. G. (1993). The Distribution of Carbonic Anhydrase Type I and II Isozymes in Lamprey and Trout: Possible Co-Evolution with Erythrocyte Chloride/Bicarbonate Exchange. *Journal of Comparative Physiology B* **163**, 380-388.

Heuer, R. M., Esbaugh, A. J. and Grosell, M. (2012). Ocean Acidification Leads to Counterproductive Intestinal Base Loss in the Gulf Toadfish (*Opsanus Beta*). *Physiological and Biochemical Zoology* **85**, 450-459.

Heuer, R. M. and Grosell, M. (2014). Physiological Impacts of Elevated Carbon Dioxide and Ocean Acidification on Fish. *Am J Physiol Regul Integr Comp Physiol* **307**, R1061-84.

Heuer, R. M. and Grosell, M. (2016). Elevated Co₂ Increases Energetic Cost and Ion Movement in the Marine Fish Intestine. *Scientific Reports* **6**, 8.

Heuer, R. M., Munley, K. M., Narsinghani, N., Wingar, J. A., Mackey, T. and Grosell, M. (2016a). Changes to Intestinal Transport Physiology and Carbonate Production at Various Co₂ Levels in a Marine Teleost, the Gulf Toadfish (*Opsanus Beta*). *Physiological and Biochemical Zoology* **89**, 402-416.

Heuer, R. M., Welch, M. J., Rummer, J. L., Munday, P. L. and Grosell, M. (2016b). Altered Brain Ion Gradients Following Compensation for Elevated Co₂ Are Linked to Behavioural Alterations in a Coral Reef Fish. *Scientific Reports* **6**, 10.

Hirata, T., Kaneko, T., Ono, T., Nakazato, T., Furukawa, N., Hasegawa, S., Wakabayashi, S., Shigekawa, M., Chang, M. H., Romero, M. F. et al. (2003). Mechanism of Acid Adaptation of a Fish Living in a Ph 3.5 Lake. *American Journal of Physiology-Regulatory Integrative and Comparative Physiology* **284**, R1199-R1212.

Hiroi, J., Kaneko, T. and Tanaka, M. (1999). In Vivo Sequential Changes in Chloride Cell Morphology in the Yolk-Sac Membrane of Mozambique Tilapia (*Oreochromis Mossambicus*) Embryos and Larvae During Seawater Adaptation. *Journal of Experimental Biology* **202**, 3485-3495.

Hiroi, J. and McCormick, S. D. (2007). Variation in Salinity Tolerance, Gill Na⁺/K⁺-Atpase, Na⁺/K⁺/2Cl⁻ Cotransporter and Mitochondria-Rich Cell Distribution

in Three Salmonids *Salvelinus Namaycush*, *Salvelinus Fontinalis* and *Salmo Salar*. *Journal of Experimental Biology* **210**, 1015-1024.

Hofmann, G. E., Smith, J. E., Johnson, K. S., Send, U., Levin, L. A., Micheli, F., Paytan, A., Price, N. N., Peterson, B., Takeshita, Y. et al. (2011). High-Frequency Dynamics of Ocean Ph: A Multi-Ecosystem Comparison. *Plos One* **6**, 11.

Hofmann, G. E. and Todgham, A. E. (2010). Living in the Now: Physiological Mechanisms to Tolerate a Rapidly Changing Environment. In *Annual Review of Physiology*, vol. 72, pp. 127-145. Palo Alto: Annual Reviews.

Holcombe, A., Howorko, A., Powell, R. A., Schalomon, M. and Hamilton, T. J. (2013). Reversed Scototaxis During Withdrawal after Daily-Moderate, but Not Weekly-Binge, Administration of Ethanol in Zebrafish. *Plos One* **8**, 7.

Holt, S. A., Kitting, C. L. and Arnold, C. R. (1983). Distribution of Young Red Drums among Different Sea-Grass Meadows. *Transactions of the American Fisheries Society* **112**, 267-271.

Huss, M. and Wieczorek, H. (2009). Inhibitors of V-Atpases: Old and New Players. *Journal of Experimental Biology* **212**, 341-346.

Hwang, P. P. (2009). Ion Uptake and Acid Secretion in Zebrafish (*Danio Rerio*). *Journal of Experimental Biology* **212**, 1745-1752.

Hwang, P. P., Lee, T. H. and Lin, L. Y. (2011). Ion Regulation in Fish Gills: Recent Progress in the Cellular and Molecular Mechanisms. *Am J Physiol Regul Integr Comp Physiol* **301**, R28-47.

Hwang, P. P., Sun, C. M. and Wu, S. M. (1989). Changes of Plasma Osmolality, Chloride Concentration and Gill Na-K-Atpase Activity in *Tilapia Oreochromis-Mossambicus* During Seawater Acclimation. *Marine Biology* **100**, 295-299.

Incardona, J. P., Gardner, L. D., Linbo, T. L., Brown, T. L., Esbaugh, A. J., Mager, E. M., Stieglitz, J. D., French, B. L., Labenia, J. S., Laetz, C. A. et al. (2014). Deepwater Horizon Crude Oil Impacts the Developing Hearts of Large Predatory Pelagic Fish. *Proc Natl Acad Sci U S A* **111**, E1510-8.

Jutfelt, F. and Hedgarde, M. (2013). Atlantic Cod Actively Avoid Co₂ and Predator Odour, Even after Long-Term Co₂ Exposure. *Frontiers in Zoology* **10**, 7.

Kellenberger, S. and Schild, L. (2002). Epithelial Sodium Channel/Degenerin Family of Ion Channels: A Variety of Functions for a Shared Structure. *Physiological Reviews* **82**, 735-767.

Kelly, M. W. and Hofmann, G. E. (2013). Adaptation and the Physiology of Ocean Acidification. *Functional Ecology* **27**, 980-990.

Kelly, M. W., Padilla-Gamino, J. L. and Hofmann, G. E. (2013). Natural Variation and the Capacity to Adapt to Ocean Acidification in the Keystone Sea Urchin *Strongylocentrotus Purpuratus*. *Global Change Biology* **19**, 2536-2546.

Kettner, C., Bertl, A., Obermeyer, G., Slayman, C. and Bihler, H. (2003). Electrophysiological Analysis of the Yeast V-Type Proton Pump: Variable Coupling Ratio and Proton Shunt. *Biophysical Journal* **85**, 3730-3738.

Killen, S. S., Costa, I., Brown, J. A. and Gamperl, A. K. (2007). Little Left in the Tank: Metabolic Scaling in Marine Teleosts and Its Implications for Aerobic Scope. *Proceedings of the Royal Society B-Biological Sciences* **274**, 431-438.

Kwan, G. T., Wexler, J. B., Wegner, N. C. and Tresguerres, M. (2019). Ontogenetic Changes in Cutaneous and Branchial Ionocytes and Morphology in Yellowfin Tuna (*Thunnus Albacares*) Larvae. *Journal of Comparative Physiology B-Biochemical Systems and Environmental Physiology* **189**, 81-95.

Laghmani, K., Borensztein, P., Ambuhl, P., Froissart, M., Bichara, M., Moe, O. W., Alpern, R. J. and Paillard, M. (1997). Chronic Metabolic Acidosis Enhances Nhe-3 Protein Abundance and Transport Activity in the Rat Thick Ascending Limb by Increasing Nhe-3 Mrna. *Journal of Clinical Investigation* **99**, 24-30.

Lee, T. H., Tsai, J. C., Fang, M. J., Yu, M. J. and Hwang, P. P. (1998). Isoform Expression of Na⁺-K⁺-Atpase Alpha-Subunit in Gills of the Teleost *Oreochromis Mossambicus*. *American Journal of Physiology-Regulatory Integrative and Comparative Physiology* **275**, R926-R932.

Lewis, E. and Wallace, D. (1998). Program Developed for Co2 System Calculations, (ed. C. D. I. A. C.-O. R. N. Laboratory).

Li, Z. J., Lui, E. Y., Wilson, J. M., Ip, Y. K., Lin, Q. S., Lam, T. J. and Lam, S. H. (2014). Expression of Key Ion Transporters in the Gill and Esophageal-Gastrointestinal Tract of Euryhaline Mozambique Tilapia *Oreochromis Mossambicus* Acclimated to Fresh Water, Seawater and Hypersaline Water. *Plos One* **9**, 11.

Lin, C. H., Huang, C. L., Yang, C. H., Lee, T. H. and Hwang, P. P. (2004). Time-Course Changes in the Expression of Na, K-Atpase and the Morphometry of Mitochondrion-Rich Cells in Gills of Euryhaline Tilapia (*Oreochromis Mossambicus*) During Freshwater Acclimation. *Journal of Experimental Zoology Part a-Comparative Experimental Biology* **301A**, 85-96.

Lin, H., Pfeiffer, D. C., Vogl, A. W., Pan, J. and Randall, D. J. (1994). Immunolocalization of H⁺-Atpase in the Gill Epithelia of Rainbow-Trout. *Journal of Experimental Biology* **195**, 169-183.

Lin, H. and Randall, D. (1995). Proton Pumps in Fish Gills. In *Cellular and Molecular Approaches to Fish Ionic Regulation*, eds. C. M. Wood and T. J. Shuttleworth), pp. 229-255. San Diego, CA: Academic.

Lin, H. and Randall, D. J. (1993). H⁺-Atpase Activity in Crude Homogenates of Fish Gill Tissue - Inhibitor Sensitivity and Environmental and Hormonal-Regulation. *Journal of Experimental Biology* **180**, 163-174.

Lin, L. Y., Horng, J. L., Kunkel, J. G. and Hwang, P. P. (2006). Proton Pump-Rich Cell Secretes Acid in Skin of Zebrafish Larvae. *Am J Physiol Cell Physiol* **290**, C371-8.

Lin, Y. M., Chen, C. N. and Lee, T. H. (2003). The Expression of Gill Na, K-Atpase in Milkfish, *Chanos Chanos*, Acclimated to Seawater, Brackish Water and Fresh Water. *Comparative Biochemistry and Physiology a-Molecular & Integrative Physiology* **135**, 489-497.

Liu, S. T., Horng, J. L., Chen, P. Y., Hwang, P. P. and Lin, L. Y. (2016). Salt Secretion Is Linked to Acid-Base Regulation of Ionocytes in Seawater-Acclimated Medaka: New Insights into the Salt-Secreting Mechanism. *Scientific Reports* **6**, 13.

Liu, S. T., Tsung, L., Horng, J. L. and Lin, L. Y. (2013). Proton-Facilitated Ammonia Excretion by Ionocytes of Medaka (*Oryzias Latipes*) Acclimated to Seawater. *American Journal of Physiology-Regulatory Integrative and Comparative Physiology* **305**, R242-R251.

Lonthair, J., Ern, R. and Esbaugh, A. (2017). The Early Life Stages of an Estuarine Fish, the Red Drum (*Sciaenops Ocellatus*), Are Tolerant to High Pco₂. *Ices Journal of Marine Science*.

Maier, T., Guell, M. and Serrano, L. (2009). Correlation of Mrna and Protein in Complex Biological Samples. *Febs Letters* **583**, 3966-3973.

Marshall, W. and Grosell, M. (2006). Ion Transport, Osmoregulation, and Acid-Base Balance. In *The Physiology of Fishes*, eds. D. H. Evans and J. B. Claiborne), pp. 177-230: CRC Press.

Marshall, W. S. (2002). Na⁺, Cl⁻, Ca²⁺ and Zn²⁺ Transport by Fish Gills: Retrospective Review and Prospective Synthesis. *Journal of Experimental Zoology* **293**, 264-283.

Marshall, W. S. and Bryson, S. E. (1998). Transport Mechanisms of Seawater Teleost Chloride Cells: An Inclusive Model of a Multifunctional Cell. *Comparative Biochemistry and Physiology a-Molecular and Integrative Physiology* **119**, 97-106.

Martin, L., Allmon, E. B. and Esbaugh, A. J. (In Review). Osmoregulatory Plasticity Facilitates Hypersalinity Acclimation in Red Drum, *Sciaenops Ocellatus*. *Journal of Experimental Biology*.

Masreel, B., Pochet, L. and Laeckmann, D. (2003). An Overview of Inhibitors of Na⁺/H⁺ Exchanger. *European Journal of Medicinal Chemistry* **38**, 547-554.

Maximino, C., de Brito, T. M., Dias, C., Gouveia, A. and Morato, S. (2010). Scototaxis as Anxiety-Like Behavior in Fish. *Nature Protocols* **5**, 209-216.

Maximino, C., Marques, T., Dias, F., Cortes, F. V., Taccolini, I. B., Pereira, P. M., Colmanetti, R., Gazolla, R. A., Tavares, R. I., Rodrigues, S. T. K. et al. (2007). A Comparative Analysis of the Preference for Dark Environments in Five Teleosts. *International Journal of Comparative Psychology* **20**, 351-367.

McCormick, S. D. (1993). Methods for Nonlethal Gill Biopsy and Measurement of Na⁺, K⁺ -Atpase Activity. *Canadian Journal of Fisheries and Aquatic Sciences* **50**, 656-658.

McCormick, S. D., Sundell, K., Bjornsson, B. T., Brown, C. L. and Hiroi, J. (2003). Influence of Salinity on the Localization of Na⁺/K⁺-Atpase, Na⁺/K⁺/2cl⁻) Cotransporter (Nkcc) and Cftr Anion Channel in Chloride Cells of the Hawaiian Goby (*Stenogobius Hawaiiensis*). *Journal of Experimental Biology* **206**, 4575-4583.

McMillan, O. J. L., Dichiera, A. M., Wilson, J. M., Esbaugh, A. J. and Brauner, C. J. (2019). Blood and Gill Carbonic Anhydrase in the Context of a Chondrichthyan Model of Co₂ Excretion. *Physiological and Biochemical Zoology*.

- McNeil, B. I. and Sasse, T. P.** (2016). Future Ocean Hypercapnia Driven by Anthropogenic Amplification of the Natural Co₂ Cycle. *Nature* **529**, 383-+.
- Melzner, F., Thomsen, J., Koeve, W., Oschlies, A., Gutowska, M. A., Bange, H. W., Hansen, H. P. and Kortzinger, A.** (2013). Future Ocean Acidification Will Be Amplified by Hypoxia in Coastal Habitats. *Marine Biology* **160**, 1875-1888.
- Michael, K., Kreiss, C. M., Hu, M. Y., Koschnick, N., Bickmeyer, U., Dupont, S., Portner, H. O. and Lucassen, M.** (2016). Adjustments of Molecular Key Components of Branchial Ion and Ph Regulation in Atlantic Cod (*Gadus Morhua*) in Response to Ocean Acidification and Warming. *Comparative Biochemistry and Physiology B-Biochemistry & Molecular Biology* **193**, 33-46.
- Miller, G. M., Watson, S. A., Donelson, J. M., McCormick, M. I. and Munday, P. L.** (2012). Parental Environment Mediates Impacts of Increased Carbon Dioxide on a Coral Reef Fish. *Nature Climate Change* **2**, 858-861.
- Miller, S., Pollack, J., Bradshaw, J., Kumai, Y. and Perry, S. F.** (2014). Cardiac Responses to Hypercapnia in Larval Zebrafish (*Danio Rerio*): The Links between Co₂ Chemoreception, Catecholamines and Carbonic Anhydrase. *Journal of Experimental Biology* **217**, 3569-3578.
- Miller, S. H., Breitburg, D. L., Burrell, R. B. and Keppel, A. G.** (2016). Acidification Increases Sensitivity to Hypoxia in Important Forage Fishes. *Marine Ecology Progress Series* **549**, 1-8.
- Mount, D. B. and Romero, M. F.** (2004). The Slc26 Gene Family of Multifunctional Anion Exchangers. *Pflugers Archiv-European Journal of Physiology* **447**, 710-721.
- Munday, P. L., Crawley, N. E. and Nilsson, G. E.** (2009a). Interacting Effects of Elevated Temperature and Ocean Acidification on the Aerobic Performance of Coral Reef Fishes. *Marine Ecology Progress Series* **388**, 235-242.
- Munday, P. L., Dixon, D. L., Donelson, J. M., Jones, G. P., Pratchett, M. S., Devitsina, G. V. and Doving, K. B.** (2009b). Ocean Acidification Impairs Olfactory Discrimination and Homing Ability of a Marine Fish. *PNAS* **106**, 1848-1852.
- Munday, P. L., Dixon, D. L., McCormick, M. I., Meekan, M., Ferrari, M. C. O. and Chivers, D. P.** (2010). Replenishment of Fish Populations Is Threatened by Ocean Acidification. *Proceedings of the National Academy of Sciences of the United States of America* **107**, 12930-12934.
- Munday, P. L., Watson, S. A., Parsons, D. M., King, A., Barr, N. G., McLeod, I. M., Allan, B. J. M. and Pether, S. M. J.** (2016). Effects of Elevated Co₂ on Early Life History Development of the Yellowtail Kingfish, *Seriola Lalandi*, a Large Pelagic Fish. *Ices Journal of Marine Science* **73**, 641-649.
- Murray, C. S. and Baumann, H.** (2018). You Better Repeat It: Complex Co₂ X Temperature Effects in Atlantic Silverside Offspring Revealed by Serial Experimentation. *Diversity-Basel* **10**, 19.
- Murray, C. S., Fuiman, L. A. and Baumann, H.** (2017). Consequences of Elevated Co₂ Exposure across Multiple Life Stages in a Coastal Forage Fish. *Ices Journal of Marine Science* **74**, 1051-1061.

Murray, C. S., Malvezzi, A., Gobler, C. J. and Baumann, H. (2014). Offspring Sensitivity to Ocean Acidification Changes Seasonally in a Coastal Marine Fish. *Marine Ecology Progress Series* **504**, 1-11.

Nilsson, G. E., Dixon, D. L., Domenici, P., McCormick, M. I., Sorensen, C., Watson, S. A. and Munday, P. L. (2012). Near-Future Carbon Dioxide Levels Alter Fish Behaviour by Interfering with Neurotransmitter Function. *Nature Climate Change* **2**, 201-204.

NOAA. System-Wide Monitoring Program. National Estuarine Research Reserve System (NERRS): NOAA Centralized Data Management Office.

Noel, J. and Pouyssegur, J. (1995). Hormonal-Regulation, Pharmacology, and Membrane Sorting of Vertebrate Na⁺/H⁺ Exchanger Isoforms. *American Journal of Physiology-Cell Physiology* **268**, C283-C296.

Oot, R. A., Couoh-Cardel, S., Sharma, S., Stam, N. J. and Wilkens, S. (2017). Breaking up and Making Up: The Secret Life of the Vacuolar H⁺-Atpase. *Protein Science* **26**, 896-909.

Orr, J. C., Fabry, V. J., Aumont, O., Bopp, L., Doney, S. C., Feely, R. A., Gnanadesikan, A., Gruber, N., Ishida, A., Joos, F. et al. (2005). Anthropogenic Ocean Acidification over the Twenty-First Century and Its Impact on Calcifying Organisms. *Nature* **437**, 681-6.

Ou, M., Hamilton, T. J., Eom, J., Lyall, E. M., Gallup, J., Jiang, A., Lee, J., Close, D. A., Yun, S. S. and Brauner, C. J. (2015). Responses of Pink Salmon to Co₂-Induced Aquatic Acidification. *Nature Climate Change* **5**, 950-+.

Paillard, M. (1997). Na⁺/H⁺ Exchanger Subtypes in the Renal Tubule: Function and Regulation in Physiology and Disease. *Experimental Nephrology* **5**, 277-284.

Pan, T. C. F., Applebaum, S. L. and Manahan, D. T. (2015). Experimental Ocean Acidification Alters the Allocation of Metabolic Energy. *Proceedings of the National Academy of Sciences of the United States of America* **112**, 4696-4701.

Perry, S. F. and Abdallah, S. (2012). Mechanisms and Consequences of Carbon Dioxide Sensing in Fish. *Respiratory Physiology & Neurobiology* **184**, 309-315.

Perry, S. F., Beyers, M. L. and Johnson, D. A. (2000). Cloning and Molecular Characterisation of the Trout (*Oncorhynchus Mykiss*) Vacuolar H⁺-Atpase B Subunit. *Journal of Experimental Biology* **203**, 459-470.

Perry, S. F., Braun, M. H., Genz, J., Vulesevic, B., Taylor, J., Grosell, M. and Gilmour, K. M. (2010). Acid-Base Regulation in the Plainfin Midshipman (*Porichthys Notatus*): An Agglomerular Marine Teleost. *Journal of Comparative Physiology B-Biochemical Systemic and Environmental Physiology* **180**, 1213-1225.

Perry, S. F., Esbaugh, A., Braun, M. and Gilmour, K. M. (2009). Gas Transport and Gill Function in Water-Breathing Fish. In *Cardio-Respiratory Control in Vertebrates: Comparative and Evolutionary Aspects*, eds. M. L. Glass and S. C. Wood), pp. 5-42. Berlin: Springer-Verlag Berlin.

Perry, S. F., Furimsky, M., Bayaa, M., Georgalis, T., Shahsavarani, A., Nickerson, J. G. and Moon, T. W. (2003a). Integrated Responses of Na⁺/Hco₃-

Cotransporters and V-Type H⁺-Atpases in the Fish Gill and Kidney During Respiratory Acidosis. *Biochimica Et Biophysica Acta-Biomembranes* **1618**, 175-184.

Perry, S. F. and Gilmour, K. M. (2002). Sensing and Transfer of Respiratory Gases at the Fish Gill. *Journal of Experimental Zoology* **293**, 249-263.

Perry, S. F. and Gilmour, K. M. (2006). Acid-Base Balance and Co₂ Excretion in Fish: Unanswered Questions and Emerging Models. *Respiratory Physiology & Neurobiology* **154**, 199-215.

Perry, S. F., Shahsavarani, A., Georgalis, T., Bayaa, M., Furimsky, M. and Thomas, S. L. Y. (2003b). Channels, Pumps, and Exchangers in the Gill and Kidney of Freshwater Fishes: Their Role in Ionic and Acid-Base Regulation. *Journal of Experimental Zoology Part a-Comparative Experimental Biology* **300A**, 53-62.

Pespeni, M. H., Sanford, E., Gaylord, B., Hill, T. M., Hosfelt, J. D., Jaris, H. K., LaVigne, M., Lenz, E. A., Russell, A. D., Young, M. K. et al. (2013). Evolutionary Change During Experimental Ocean Acidification. *Proceedings of the National Academy of Sciences of the United States of America* **110**, 6937-6942.

Pfaffl, M. W. (2001). A New Mathematical Model for Relative Quantification in Real-Time Rt-Pcr. *Nucleic Acids Research* **29**, 6.

Pfister, C. A., Esbaugh, A. J., Frieder, C. A., Baumann, H., Bockmon, E. E., White, M. M., Carter, B. R., Benway, H. M., Blanchette, C. A., Carrington, E. et al. (2014). Detecting the Unexpected: A Research Framework for Ocean Acidification. *Environmental Science & Technology* **48**, 9982-9994.

Piermarini, P. M. and Evans, D. H. (2000). Effects of Environmental Salinity on Na⁺/K⁺-Atpase in the Gills and Rectal Gland of a Euryhaline Elasmobranch (*Dasyatis Sabina*). *Journal of Experimental Biology* **203**, 2957-2966.

Pimentel, M., Pegado, M., Repolho, T. and Rosa, R. (2014). Impact of Ocean Acidification in the Metabolism and Swimming Behavior of the Dolphinfinch (*Coryphaena Hippurus*) Early Larvae. *Marine Biology* **161**, 725-729.

Portner, H. O. (2012). Integrating Climate-Related Stressor Effects on Marine Organisms: Unifying Principles Linking Molecule to Ecosystem-Level Changes. *Marine Ecology Progress Series* **470**, 273-290.

Riebesell, U., Fabry, V. J., Hansson, L. and Gattuso, J.-P. (2010). Guide to Best Practices for Ocean Acidification Research and Data Reporting: European Commission.

Rimoldi, S., Terova, G., Brambilla, F., Bernardini, G., Gornati, R. and Saroglia, M. (2009). Molecular Characterization and Expression Analysis of Na⁺/H⁺ Exchanger (Nhe)-1 and C-Fos Genes in Sea Bass (*Dicentrarchus Labrax*, L) Exposed to Acute and Chronic Hypercapnia. *Journal of Experimental Marine Biology and Ecology* **375**, 32-40.

Ritter, M., Fuerst, J., Woll, E., Chwatal, S., Gschwentner, M., Lang, F., Deetjen, P. and Paulmichl, M. (2001). Na⁺/H(+)Exchangers: Linking Osmotic Dysequilibrium to Modified Cell Function. *Cellular Physiology and Biochemistry* **11**, 1-18.

Roa, J. N., Munevar, C. L. and Tresguerres, M. (2014). Feeding Induces Translocation of Vacuolar Proton Atpase and Pendrin to the Membrane of Leopard Shark (Triakis Semifasciata) Mitochondrion-Rich Gill Cells. *Comparative Biochemistry and Physiology a-Molecular & Integrative Physiology* **174**, 29-37.

Roche, D. G., Careau, V. and Binning, S. A. (2016). Demystifying Animal 'Personality' (or Not): Why Individual Variation Matters to Experimental Biologists. *Journal of Experimental Biology* **219**, 3832-3843.

Rombough, P. (2002). Gills Are Needed for Ionoregulation before They Are Needed for O-2 Uptake in Developing Zebrafish, Danio Rerio. *Journal of Experimental Biology* **205**, 1787-1794.

Rombough, P. (2007). The Functional Ontogeny of the Teleost Gill: Which Comes First, Gas or Ion Exchange? *Comparative Biochemistry and Physiology a-Molecular & Integrative Physiology* **148**, 732-742.

Romero, M. F., Chen, A. P., Parker, M. D. and Boron, W. F. (2013). The Slc4 Family of Bicarbonate (Hco₃⁻) Transporters. *Molecular Aspects of Medicine* **34**, 159-182.

Ross, J. L., Stevens, T. M. and Vaughan, D. S. (1995). Age, Growth, Mortality, and Reproductive-Biology of Red Drums in North-Carolina Waters. *Transactions of the American Fisheries Society* **124**, 37-54.

Salin, K., Villasevil, E. M., Anderson, G. J., Lamarre, S. G., Melanson, C. A., McCarthy, I., Selman, C. and Metcalfe, N. B. (2019). Differences in Mitochondrial Efficiency Explain Individual Variation in Growth Performance. *Proceedings of the Royal Society B-Biological Sciences* **286**, 8.

Schade, F. M., Clemmesen, C. and Wegner, K. M. (2014). Within- and Transgenerational Effects of Ocean Acidification on Life History of Marine Three-Spined Stickleback (Gasterosteus Aculeatus). *Marine Biology* **161**, 1667-1676.

Seidelin, M., Brauner, C. J., Jensen, F. B. and Madsen, S. S. (2001). Vacuolar-Type H⁺-Atpase and Na⁺, K⁺-Atpase Expression in Gills of Atlantic Salmon (Salmo Salar) During Isolated and Combined Exposure to Hyperoxia and Hypercapnia in Fresh Water. *Zoological Science* **18**, 1199-1205.

Seidelin, M., Madsen, S. S., Blenstrup, H. and Tipsmark, C. K. (2000). Time-Course Changes in the Expression of Na⁺,K⁺-Atpase in Gills and Pyloric Caeca of Brown Trout (Salmo Trutta) During Acclimation to Seawater. *Physiological and Biochemical Zoology* **73**, 446-453.

Sheaves, M. J. (1993). Patterns of Movement of Some Fishes within an Estuary in Tropical Australia. *Australian Journal of Marine and Freshwater Research* **44**, 867-880.

Silva, P., Solomon, R., Spokes, K. and Epstein, F. H. (1977). Ouabain Inhibition of Gill Na-K-Atpase - Relationship to Active Chloride Transport. *Journal of Experimental Zoology* **199**, 419-426.

Simone, B. W., Martinez-Galvez, G., WareJoncas, Z. and Ekker, S. C. (2018). Fishing for Understanding: Unlocking the Zebrafish Gene Editor's Toolbox. *Methods* **150**, 3-10.

Solomon, S., Qin, D., Manning, M., Chen, Z. and Marquis, M. (2007). Climate Change 2007: The Physical Science Basis: Contribution of Working Group I to the Fourth Assessment Report of the Intergovernmental Panel on Climate Change. New York: Cambridge University Press.

Strobel, A., Bennecke, S., Leo, E., Mintenbeck, K., Portner, H. O. and Mark, F. C. (2012). Metabolic Shifts in the Antarctic Fish *Notothenia Rossii* in Response to Rising Temperature and Pco₂. *Frontiers in Zoology* **9**, 15.

Stumpp, M., Hu, M. Y., Melzner, F., Gutowska, M. A., Dorey, N., Himmerkus, N., Holtmann, W. C., Dupont, S. T., Thorndyke, M. C. and Bleich, M. (2012). Acidified Seawater Impacts Sea Urchin Larvae Ph Regulatory Systems Relevant for Calcification. *Proceedings of the National Academy of Sciences of the United States of America* **109**, 18192-18197.

Stumpp, M., Wren, J., Melzner, F., Thorndyke, M. C. and Dupont, S. T. (2011). Co₂ Induced Seawater Acidification Impacts Sea Urchin Larval Development I: Elevated Metabolic Rates Decrease Scope for Growth and Induce Developmental Delay. *Comparative Biochemistry and Physiology a-Molecular & Integrative Physiology* **160**, 331-340.

Sullivan, G. V., Fryer, J. N. and Perry, S. F. (1995). Immunolocalization of Proton Pumps (H⁺-Atpase) in Pavement Cells of Rainbow-Trout Gill. *Journal of Experimental Biology* **198**, 2619-2629.

Sullivan, G. V., Fryer, J. N. and Perry, S. F. (1996). Localization of Mrna for the Proton Pump (H⁺-Atpase) and Cl⁻/Hco₃⁻ Exchanger in the Rainbow Trout Gill. *Canadian Journal of Zoology-Revue Canadienne De Zoologie* **74**, 2095-2103.

Swenson, E. (2000). Respiratory and Renal Roles of Carbonic Anhydrase in Gas Exchange and Acid-Base Regulation. *EXS* **90**.

Takei, Y., Hiroi, J., Takahashi, H. and Sakamoto, T. (2014). Diverse Mechanisms for Body Fluid Regulation in Teleost Fishes. *American Journal of Physiology-Regulatory Integrative and Comparative Physiology* **307**, R778-R792.

Taylor, J. R., Cooper, C. A. and Mommsen, T. P. (2011). Implications of Gi Function for Gas Exchange, Acid-Base Balance and Nitrogen Metabolism. In *Multifunctional Gut of Fish*, vol. 30 eds. M. Grosell A. P. Farrell and C. J. Brauner), pp. 213-259. San Diego: Elsevier Academic Press Inc.

Taylor, J. R., Mager, E. M. and Grosell, M. (2010). Basolateral Nbc_{el} Plays a Rate-Limiting Role in Transepithelial Intestinal Hco₃⁻ Secretion, Contributing to Marine Fish Osmoregulation. *Journal of Experimental Biology* **213**, 459-468.

Taylor, J. R., Whittamore, J. M., Wilson, R. W. and Grosell, M. (2007). Postprandial Acid-Base Balance and Ion Regulation in Freshwater and Seawater-Acclimated European Flounder, *Platichthys Flesus*. *Journal of Comparative Physiology B-Biochemical Systemic and Environmental Physiology* **177**, 597-608.

Teplova, V. V., Tonshin, A. A., Grigoriev, P. A., Saris, N. E. L. and Salkinoja-Salonen, M. S. (2007). Bafilomycin A1 Is a Potassium Ionophore That Impairs Mitochondrial Functions. *Journal of Bioenergetics and Biomembranes* **39**, 321-329.

Tipsmark, C. K., Madsen, S. S. and Borski, R. J. (2004). Effect of Salinity on Expression of Branchial Ion Transporters in Striped Bass (*Morone Saxatilis*). *Journal of Experimental Zoology Part a-Comparative Experimental Biology* **301A**, 979-991.

Tresguerres, M., Katoh, F., Fenton, H., Jasinska, E. and Goss, G. G. (2005). Regulation of Branchial V-H⁺-Atpase Na⁺/K⁺-Atpase and Nhe2 in Response to Acid and Base Infusions in the Pacific Spiny Dogfish (*Squalus Acanthias*). *Journal of Experimental Biology* **208**, 345-354.

Tresguerres, M., Parks, S. K. and Goss, G. G. (2007a). Recovery from Blood Alkalosis in the Pacific Hagfish (*Eptatretus Stoutii*): Involvement of Gill V-H⁺-Atpase and Na⁺/K⁺-Atpase. *Comparative Biochemistry and Physiology a-Molecular & Integrative Physiology* **148**, 133-141.

Tresguerres, M., Parks, S. K., Katoh, F. and Goss, G. G. (2006). Microtubule-Dependent Relocation of Branchial V-H⁺-Atpase to the Basolateral Membrane in the Pacific Spiny Dogfish (*Squalus Acanthias*): A Role in Base Secretion. *Journal of Experimental Biology* **209**, 599-609.

Tresguerres, M., Parks, S. K., Wood, C. M. and Goss, G. G. (2007b). V-H⁺ -Atpase Translocation During Blood Alkalosis in Dogfish Gills: Interaction with Carbonic Anhydrase and Involvement in the Postfeeding Alkaline Tide. *Am J Physiol Regul Integr Comp Physiol* **292**, R2012-9.

Tseng, Y. C., Hu, M. Y., Stumpp, M., Lin, L. Y., Melzner, F. and Hwang, P. P. (2013). Co₂-Driven Seawater Acidification Differentially Affects Development and Molecular Plasticity Along Life History of Fish (*Oryzias Latipes*). *Comparative Biochemistry and Physiology a-Molecular & Integrative Physiology* **165**, 119-130.

Varsamos, S., Diaz, J. P., Charmantier, G., Blasco, C., Connes, R. and Flik, G. (2002). Location and Morphology of Chloride Cells During the Post-Embryonic Development of the European Sea Bass, *Dicentrarchus Labrax*. *Anatomy and Embryology* **205**, 203-213.

Verdouw, H., Vanechteld, C. J. A. and Dekkers, E. M. J. (1978). Ammonia Determination Based on Indophenol Formation with Sodium Salicylate. *Water Research* **12**, 399-402.

Vogel, C. and Marcotte, E. M. (2012). Insights into the Regulation of Protein Abundance from Proteomic and Transcriptomic Analyses. *Nature Reviews Genetics* **13**, 227-232.

Vulesevic, B. and Perry, S. F. (2006). Developmental Plasticity of Ventilatory Control in Zebrafish, *Danio Rerio*. *Respiratory Physiology & Neurobiology* **154**, 396-405.

Wallace, R. B., Baumann, H., Grear, J. S., Aller, R. C. and Gobler, C. J. (2014). Coastal Ocean Acidification: The Other Eutrophication Problem. *Estuarine Coastal and Shelf Science* **148**, 1-13.

Watson, C. J., Nordi, W. M. and Esbaugh, A. J. (2014). Osmoregulation and Branchial Plasticity after Acute Freshwater Transfer in Red Drum, *Sciaenops Ocellatus*. *Comparative Biochemistry and Physiology a-Molecular & Integrative Physiology* **178**, 82-89.

- Weinstein, M. P.** (1979). Shallow Marsh Habitats as Primary Nurseries for Fishes and Shellfish, Cape Fear River, North-Carolina. *Fishery Bulletin* **77**, 339-357.
- Wells, P. R. and Pinder, A. W.** (1996). The Respiratory Development of Atlantic Salmon .2. Partitioning of Oxygen Uptake among Gills, Yolk Sac and Body Surfaces. *Journal of Experimental Biology* **199**, 2737-2744.
- Williams, C. R., Dittman, A. H., McElhany, P., Busch, D. S., Maher, M. T., Bammler, T. K., MacDonald, J. W. and Gallagher, E. P.** (2019). Elevated Co₂ Impairs Olfactory-Mediated Neural and Behavioral Responses and Gene Expression in Ocean-Phase Coho Salmon (*Oncorhynchus Kisutch*). *Global Change Biology* **25**, 963-977.
- Wilson, J. M., Randall, D. J., Donowitz, M., Vogl, A. W. and Ip, A. K. Y.** (2000). Immunolocalization of Ion-Transport Proteins to Branchial Epithelium Mitochondria-Rich Cells in the Mudskipper (*Periophthalmodon Schlosseri*). *Journal of Experimental Biology* **203**, 2297-2310.
- Wilson, J. M., Whiteley, N. M. and Randall, D. J.** (2002). Ionoregulatory Changes in the Gill Epithelia of Coho Salmon During Seawater Acclimation. *Physiological and Biochemical Zoology* **75**, 237-249.
- Wilson, R. W., Millero, F. J., Taylor, J. R., Walsh, P. J., Christensen, V., Jennings, S. and Grosell, M.** (2009). Contribution of Fish to the Marine Inorganic Carbon Cycle. *Science* **323**, 359-362.
- Xie, W. H., Shiu, W. Y. and Mackay, D.** (1997). A Review of the Effect of Salts on the Solubility of Organic Compounds in Seawater. *Marine Environmental Research* **44**, 429-444.
- Yan, J. J., Chou, M. Y., Kaneko, T. and Hwang, P. P.** (2007). Gene Expression of Na⁺/H⁺ Exchanger in Zebrafish H⁺-ATPase-Rich Cells During Acclimation to Low-Na⁺ and Acidic Environments. *American Journal of Physiology-Cell Physiology* **293**, C1814-C1823.
- Yoshimori, T., Yamamoto, A., Moriyama, Y., Futai, M. and Tashiro, Y.** (1991). Bafilomycin-A1, a Specific Inhibitor of Vacuolar-Type H⁺-ATPase, Inhibits Acidification and Protein-Degradation in Lysosomes of Cultured-Cells. *Journal of Biological Chemistry* **266**, 17707-17712.
- Zimmer, A. M., Pan, Y. K., Chandrapalan, T., Kwong, R. W. M. and Perry, S. F.** (2019). Loss-of-Function Approaches in Comparative Physiology: Is There a Future for Knockdown Experiments in the Era of Genome Editing? *Journal of Experimental Biology* **222**, 13.